University of Alberta

A Study of Peridotite Xenoliths from Voyageur Kimberlite, Slave Craton, Canada

by

Eliza Daniela Verigeanu

A thesis submitted to the Faculty of Graduate Studies and Research in partial fulfillment of the requirements for the degree of *Master of Science*

Department of *Earth and Atmospheric Sciences*

Edmonton, Alberta

Fall 2006

Library and Archives Canada

Published Heritage Branch

395 Wellington Street
Ottawa ON K1A 0N4
Canada

Bibliothèque et Archives Canada

Direction du Patrimoine de l'édition

395, rue Wellington
Ottawa ON K1A 0N4
Canada

Your file Votre référence
ISBN: 978-0-494-22396-3
Our file Notre référence
ISBN: 978-0-494-22396-3

NOTICE:
The author has granted a non-exclusive license allowing Library and Archives Canada to reproduce, publish, archive, preserve, conserve, communicate to the public by telecommunication or on the Internet, loan, distribute and sell theses worldwide, for commercial or non-commercial purposes, in microform, paper, electronic and/or any other formats.

The author retains copyright ownership and moral rights in this thesis. Neither the thesis nor substantial extracts from it may be printed or otherwise reproduced without the author's permission.

AVIS:
L'auteur a accordé une licence non exclusive permettant à la Bibliothèque et Archives Canada de reproduire, publier, archiver, sauvegarder, conserver, transmettre au public par télécommunication ou par l'Internet, prêter, distribuer et vendre des thèses partout dans le monde, à des fins commerciales ou autres, sur support microforme, papier, électronique et/ou autres formats.

L'auteur conserve la propriété du droit d'auteur et des droits moraux qui protège cette thèse. Ni la thèse ni des extraits substantiels de celle-ci ne doivent être imprimés ou autrement reproduits sans son autorisation.

In compliance with the Canadian Privacy Act some supporting forms may have been removed from this thesis.

While these forms may be included in the document page count, their removal does not represent any loss of content from the thesis.

Conformément à la loi canadienne sur la protection de la vie privée, quelques formulaires secondaires ont été enlevés de cette thèse.

Bien que ces formulaires aient inclus dans la pagination, il n'y aura aucun contenu manquant.

Canada

ABSTRACT

Twenty two peridotite xenoliths from the Voyageur kimberlite were studied to characterize the mantle rocks from the northern part of the Slave Province and to provide information regarding their conditions of origin. Major and minor element compositions of the constituent mineral phases were determined using electron microprobe techniques (EPMA) and selected garnet and clinopyroxene grains were analyzed for trace and ultra-trace elements by laser-ablation inductively coupled plasma mass spectroscopy (LA-ICPMS).

The study showed that "depleted" garnets are completely absent. Trace element data suggest pervasive metasomatic enrichment beneath Voyageur and different stages of equilibration of an initial harzburgitic composition with low volume percolating melts. Geothermobarometry results define an array representing equilibration of the Voyageur peridotite xenoliths along a 40mW/m^2 geotherm and a thickness of at least 170km of the subcratonic lithospheric mantle at the time of kimberlite emplacement.

AKNOWLEDGEMENTS

I would like to especially thank my supervisor, Dr. Thomas Stachel, without whom this thesis would not exist. He gave me the opportunity to work in the very stimulating intellectual environment provided by the faculty and graduate students of the Earth and Atmospheric Sciences Department (University of Alberta, Edmonton) and particularly of the Diamond Research Group. Thank you for your guidance, patience, financial support, favors and for the time you spent reading the various drafts of this thesis. It has been my honor to be your student and a member of your research team.

A special word of gratitude goes to my other committee member as well. To Dr. Larry Heaman, for his valuable commentaries on my work, my sincere appreciation.

Many thanks to Dr. Jeff Gu, who was so kind to participate as an external to my thesis defence.

I would like to thank Casey Hetman and DeBeers Canada (Exploration Division) for sharing their samples. I am also very grateful to Dante Canil (University of Victoria, BC) for his help with the LA-ICPMS work and to Sergei Matveev (University of Alberta, Edmonton) for his guidance with the microprobe analysis. Without their assistance I would not have had any data.

Sincere thanks must also go to Ralf Tappert, Anetta Banas, Steven Creighton and Cara Donnelly (DRG members) for their friendship.

I would also like to acknowledge the financial support provided by the Earth and Atmospheric Sciences Department (University of Alberta, Edmonton) in the form of teaching and research assistantships.

Finally, and by no means the least, I would like to express my profound appreciation to my family for their support.

To each of the above, I extend my deepest appreciation.

DEDICATION

With all my love, to my beautiful daughter

Diana Maria

TABLE OF CONTENTS

TITLE

ABSTRACT

ACKNOWLEDGEMENTS

TABLE OF CONTENTS

LIST OF TABLES

LIST OF FIGURES

LIST OF APPENDICES

CHAPTER 1 - INTRODUCTION, BACKGROUND AND RATIONALE FOR STUDY **1**

1.1. INTRODUCTION **1**

1.2. PETROLOGICAL BACKGROUND **3**

1.2.1. Petrographic features of mantle-derived xenoliths in kimberlites **3**

1.2.2. Peridotite geothermobarometry **8**

1.2.3. Mantle metasomatism **10**

1.3. OBJECTIVES OF THIS STUDY **11**

CHAPTER 2 - REGIONAL SETTING/LOCAL GEOLOGY **21**

2.1. GENERAL GEOLOGY OF THE SLAVE PROVINCE **21**

2.2. DISTRIBUTION OF KIMBERLITES IN THE SLAVE PROVINCE **26**

2.3. THE SUBCRATONIC LITHOSPHERIC MANTLE **29**

2.4. HOST KIMBERLITE **33**

CHAPTER 3 – PETROGRAPHY AND MINERAL CHEMISTRY **43**

3.1. SAMPLES AND ANALYTICAL TECHNIQUES **43**

3.2. PETROGRAPHY **46**

3.3. MINERAL CHEMISTRY (MAJOR AND MINOR ELEMENTS) **57**

3.4. TRACE ELEMENTS GEOCHEMISTRY **66**

CHAPTER 4 – GEOTHERMOBAROMETRY **78**

CHAPTER 5 – DISCUSSION **90**

CONCLUSIONS **101**

LIST OF TABLES

Table 1.2.1.1 Summary of the textural classification of peridotite-pyroxenite suite rocks (from Harte, 1977) **6**

Table 3.2.1 Petrographic summary of peridotite xenoliths from the Voyageur kimberlite **47**

Table 4.1 Averaged equilibration pressures and temperatures for the mineral cores of peridotite xenoliths from the Voyageur kimberlite **80**

LIST OF FIGURES

Fig. 1.2.1.1 Classification and nomenclature of ultramafic peridotites and pyroxenites based on the modal proportion of olivine, orthopyroxene and clinopyroxene (after Streckeisen, 1973) **4**

Fig. 1.2.1.2 Major types of mantle-derived peridotite xenoliths **7**

Fig. 2.1.1 Geological map of the Slave Province, Canada (modified after Davis & Bleeker, 1999) **22**

Fig. 2.2.1 Distribution of kimberlites in the Slave Province (locations and domains after Heaman et al., 2003, 2004) **27**

Fig. 2.3.1 Distribution of kimberlites in the Slave Province **31**

Fig. 2.3.2 The layered structure of the Slave lithospheric mantle shown by key geochemical indicators (from O'Reilly et al., 2001) **32**

Fig. 3.1.1 Comparison of LA-ICP-MS measurements on mantle garnet PN2 obtained at the University of Victoria with SIMS measurements on the same garnet obtained at Heilderberg, Pavia and Edinburgh University and Woods Hole Oceanographic Insitution laboratories **45**

Fig. 3.2.1 Core samples from the Voyageur kimberlite pipe **50**

Fig. 3.2.2 Thin section images of garnet lherzolites from the Voyageur kimberlite pipe **51**

Fig. 3.2.3 Thin section images of spinel lherzolites from the Voyageur kimberlite pipe **52**

Fig. 3.2.4 Thin section images of harzburgites from the Voyageur kimberlite pipe **53**

Fig. 3.2.5 Thin section images of wehrlites from the Voyageur kimberlite pipe **54**

Fig. 3.2.6 Thin section images of spinel-garnet lherzolites from the Voyageur kimberlite pipe **55**

Fig. 3.2.7 Thin section images of heterogeneous samples from the Voyageur kimberlite pipe **56**

Fig. 3.3.1 Mg-numbers of olivines and orthopyroxenes from the Voyageur peridotite xenoliths **58**

Fig. 3.3.2 Composition of orthopyroxenes from the Voyageur peridotite xenoliths **59**

Fig. 3.3.3 Composition of clinopyroxenes from the Voyageur peridotite xenoliths **61**

Fig. 3.3.4 Composition of garnets from the Voyageur peridotite xenoliths **63**

Fig. 3.3.5 Composition of spinels from the Voyageur peridotite xenoliths **65**

Fig. 3.4.1 Averaged trace elements abundances in lherzolitic garnets from Voyageur normalized to the C1 chondrite of McDonough & Sun (1995) **67**

Fig. 3.4.2 Averaged REE abundances in lherzolitic clinopyroxenes from Voyageur peridotite xenoliths normalized to the C1 chondrite composition of McDonough & Sun (1995) **68**

Fig. 3.4.3 Averaged REE abundances in lherzolitic garnets and clinopyroxenes from the Voyageur peridotite xenoliths normalized to the composition of the primitive garnet/clinopyroxene J4 (Jagoutz & Spettel) **69**

Fig. 3.4.4 Origin of t lherzolitic garnets through metasomatic enrichment of former harzburgites **71**

Fig. 3.4.5 Averaged REE abundances in lherzolitic garnets from Voyageur peridotite xenoliths normalized to the composition of the primitive garnet J4 (Jagoutz & Spettel) **72**

Fig. 3.4.6 Zr (ppm) and Y (ppm) concentrations in lherzolitic garnets from the Voyageur peridotite xenoliths **73**

Fig. 4.1 Averaged P-T estimates of peridotite xenoliths from the Voyageur kimberlite calculated iteratively using T_{BKN}-P_{BKN} **82**

Fig. 4.2 Averaged P-T estimates of peridotite xenoliths from the Voyageur kimberlite calculated iteratively using **a)** $T_{O'Neill}$-P_{BKN} and **b)** T_{Harley}-P_{BKN} **83**

Fig. 4.3 Averaged P-T estimates of peridotite xenoliths from the Voyageur kimberlite calculated iteratively using T_{NTcpx}-P_{NTcpx} **84**

Fig. 4.4 Comparison of garnet equilibration temperatures calculated using $T_{Ni\text{-}in\text{-}garnet}$ (version of Canil, 1999) and T_{BKN}-P_{BKN} geothermometers **85**

Fig. 5.1 Mg-number of olivines from peridotite xenoliths worldwide **91**

Fig. 5.2 Comparison of the CCGE trend in garnets from Voyageur and Jericho kimberlites **93**

Fig. 5.3 Equilibrium pressure and temperature estimates calculated using the T_{BKN}-P_{BKN} geothermobarometer for Voyageur garnet peridotite xenoliths in comparison with data from cratonic mantle worldwide **95**

LIST OF APPENDICES

APPENDIX I EPMA analyses of olivines from the Voyageur peridotite xenoliths **104**

APPENDIX II EPMA analyses of orthopyroxenes from the Voyageur peridotite xenoliths **114**

APPENDIX III EPMA analyses of clinopyroxenes from the Voyageur peridotite xenoliths **121**

APPENDIX IV EPMA analyses of garnets from the Voyageur peridotite xenoliths **127**

APPENDIX V EPMA analyses of spinels from the Voyageur peridotite xenoliths **134**

APPENDIX VI LA-ICPMS analyses of lherzolitic garnets from the Voyageur peridotite xenoliths **137**

APPENDIX VII LA-ICPMS analyses of lherzolitic clinopyroxenes from the Voyageur peridotite xenoliths **138**

CHAPTER 1

INTRODUCTION, BACKGROUND AND RATIONALE FOR STUDY

1.1. INTRODUCTION

The subcontinental lithospheric mantle is that part of the upper mantle that is stable for long periods of time. It is considered by some to be the refractory residue produced by partial melting at considerable depths (Boyd, 1989; McDonough, 1990; Griffin et al., 1999) and can be defined as "a chemical, thermal and mechanical boundary layer insulating the continental crust from the hotter and more dynamic interior of the Earth" (Griffin et al., 1999).

Although it is generally thought to be the same age and modified broadly at the same time as the crust to which it is linked (Griffin et al., 1999), SCLM is less understood due to the difficulty of direct sampling. There is generally a consensus that subcontinental lithospheric mantle is overall lherzolitic in composition, depleted in major element composition but enriched in incompatible elements and has developed through a series of tectono-magmatic events; details like the degree of enrichment or the models that explain its growth are subject of a continuous debate.

Constraints on the nature of subcontinental lithospheric mantle are provided mainly by geophysical and xenolith/xenocryst studies. Ultramafic xenoliths and xenocrysts (individual crystals such as garnets, pyroxenes and spinels representing disaggregated mantle material) are fragments of the wall rock

conduits entrained accidentally in the magmas traveling to the Earth's surface (mainly alkali basalts and kimberlites).

The mineralogy of the xenoliths suggests their formation under pressure and temperature conditions characteristic of the upper mantle. They can be brought up from great depths (up to 250km in the case of kimberlitic magmas that sample stable cratonic regions) and, thus, are the only direct source of information we have on the composition, structure, thermal state and temporal evolution of the subcontinental lithosphere.

Studies based on large xenolith databases have shown that subcontinental lithospheric mantle is made up of domains that are compositionally distinct depending on their tectonic setting and stabilization age, "old" (cratonic) lithosphere being relatively thick, depleted and cold whereas "young" (more recent) lithosphere is relatively thin, fertile and hot (Boyd, 1987; Ionov et al., 1993; Boyd et al., 1997; Griffin et al., 1999). A secular variation was also recognized: starting from the Archean, subcontinental lithospheric mantle becomes progressively less depleted in terms of Al and Ca contents as well as in Mg numbers and Fe/Al ratios (O'Reilly & Griffin, 1996; Griffin et al., 1999; O'Reilly et al., 2001).

Since there is a demonstrated coupling between the subcontinental mantle and its overlying crust (Zhao & McCulloch, 1993; Chen et al., 1994; Grütter et al., 1999), knowledge of subcontinental lithospheric mantle architecture and evolution is important for understanding the large-scale tectonic events in the crust.

The 4D lithosphere mapping methodology developed in the last decade (O'Reilly & Griffin, 1996) combines petrological, geochemical and petrophysical data provided by mantle-derived xenoliths/xenocrysts with geophysical information (that helps mapping the lateral extent of known mantle domains) allowing a detailed investigation of the deep structure of the Earth and providing a picture (time and space) not only of the composition, structure and thermal state of the subcontinental lithospheric mantle but also of the processes that affected it (such as metasomatism).

1.2. PETROLOGICAL BACKGROUND

1.2.1. Petrographic features of mantle-derived xenoliths in kimberlites

Mantle-derived inclusions in kimberlites are generally rounded or ovoid in shape and commonly less than 30cm in size. They may be cut by fractures and veining, and cross cutting dikelets as well as banding can be observed in large specimens.

Five broad groups of mantle-derived xenoliths were recognized in kimberlitic magmas: 1) peridotites and pyroxenites; 2) eclogites and grospydites; 3) metasomatized peridotites; 4) glimmerites and MARID-suite (mica-amphibole-rutile-ilmenite-diopside) rocks; 5) miscellaneous xenoliths (Dawson et al., 1980). Each group varies considerably in relative abundance from one intrusion to another, generally representing together only few percents of the volcanic host rock. Peridotite is the most common xenolith type present in kimberlites, although pyroxenites or eclogites may predominate sometimes.

Peridotite classification is based on its content of the mafic minerals olivine, orthopyroxene and clinopyroxene. In the IUGS scheme (Fig.1.2.1.1) peridotites are subdivided into dunites (mainly olivine), harzburgites (olivine and orthopyroxene), lherzolites (olivine, orthopyroxene and clinopyroxene) and wehrlites (olivine and clinopyroxene). For xenolith studies, small sample size hampers statistically valid assessment of modal abundances. The harzburgite-lherzolite division in this and many other studies is thus based on the subcalcic Ca-saturated composition of garnet, rather than the 5% cpx division of the IUGS nomenclature.

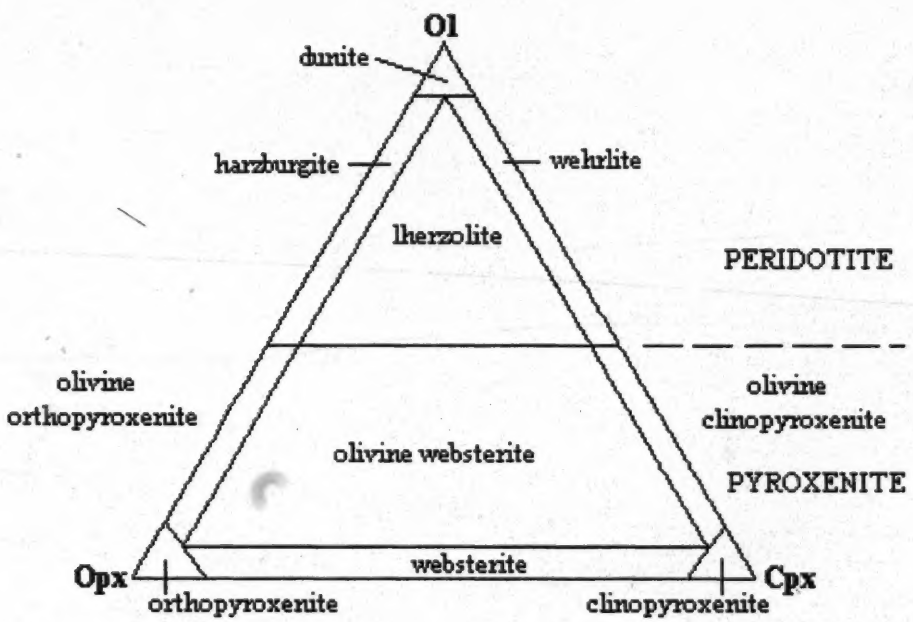

Fig.1.2.1.1 Classification and nomenclature of ultramafic peridotites and pyroxenites based on the modal proportion of olivine, orthopyroxene and clinopyroxene (after Streckeisen, 1973)

Depending on the aluminous phase present, peridotites can be assigned to different facies: plagioclase peridotites, spinel peridotites, garnet peridotites or spinel-garnet peridotites. Diamond, graphite, sulphides, phlogopite, ilmenite and zircon can also be present as accessory minerals.

Many of the textural characteristics of peridotite xenoliths in kimberlites must have originated in the upper mantle. They reflect a diversity of deformation and recrystallization processes and can be described as coarse, porpyroclastic and granuloblastic based on the presence/absence of porphyroclasts and grain size characteristics (Harte, 1977; Table 1.2.1.1; Fig. 1.2.1.2). Essentially, porphyroclastic textures are the result of deformation and recrystallization of coarse, equigranular precursors (Cox et al., 1973; Boullier & Nicholas, 1975; Harte et al., 1975) whereas granuloblastic textures are indicative of "extensive recrystallization of all minerals with variable amounts of grain growth (annealing) and little subsequent deformation" (Harte, 1977; p. 283).

Different terms have been used in the scientific literature to describe those textures: relatively little deformed peridotites have been called "granular" (Boyd, 1973; Nixon & Boyd, 1973; Boyd & Nixon, 1975; Boyd, 1975) whereas the strongly deformed ones are often known as "sheared" (Boyd & Nixon, 1975) or as "flaser" textured (Cox et al., 1973; Harte et al., 1975). Harte et al. (1975) used the term "even-textured" to describe granuloblastic xenoliths from Matsoku.

A special peridotite group is comprised of xenoliths with textural characteristics derived from subsolidus reactions between constituent minerals.

Table 1.2.1.1 Summary of the textural classification of peridotite-pyroxenite suite rocks (from Harte, 1977)

Rock type	Porphyroclasts	Grain size	Grain boundaries	Subtypes
Coarse	Absent	Average grain size greater than 2.0mm	Variable. Often largely straight or smoothly curving but may be less regular	Equant Tabular
Porphyroclastic	Present. More than 10% of olivine occurs as porphyroclasts	Two major populations, one represented by porphyroclasts (1-2mm), the other by finer-grained matrix (<0.5mm)	Irregular in porphyroclasts, straight in neoblasts. Some neoblasts equant, others tabular	Neither disrupted nor laminated Disrupted Fluidal Laminated and disrupted
Mosaic-porphyroclastic	Present. Less than 10% of olivine occurs as porphyroclasts	Usually two populations, one represented by porphyroclasts, the other by finer-grained matrix. One fine-grained population in porphyroclast-free rocks	Irregular in porphyroclasts, straight in neoblasts. Some neoblasts equant, others tabular	Neither disrupted nor laminated Fluidal Laminated and disrupted
Granuloblastic	Absent or rare for all mineral species	Small size range for each mineral species (excepting rare porphyroclasts). Grain size generally less than 2.0mm	Straight or smoothly curving, bounding grains of polygonal tabular shape	Equant Tabular

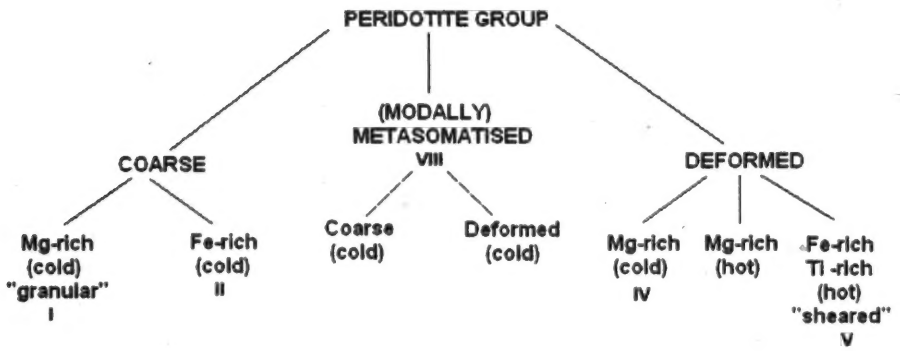

Fig. 1.2.1.2 Major types of mantle-derived peridotite xenoliths. "Cold" and "hot" correspond to "low-T" and "high-T" peridotite xenoliths, respectively; the Roman numbers indicate the corresponding types in the classification of Gurney & Harte, 1980. From Harte, 1983 (Fig.2; p.53)

Those reactions are generally either the result of metasomatic addition of alkalies and volatiles from the host kimberlite or due to changing of pressure and temperature conditions from garnet to spinel facies. The final reaction products are present in the form of kelyphitic rims (aggregates of spinel, mica, orthopyroxene, clinopyroxene and amphibole) surrounding or replacing the garnets.

The composition of mineral phases of mantle-derived xenoliths in kimberlites shows not only small differences between different localities but also inter-grain differences within single specimens. *Olivine* is forsteritic (Fo_{88-94}) and has the simplest chemistry. The commonest *orthopyroxene* is enstatite (En_{87-95}) and the *clinopyroxene* is often a Cr-diopside with considerable variation in both chemistry and modal abundance. *Garnet* has higher modal abundance in high-pressure

lherzolites than in harzburgites. It is usually a Cr-pyrope and generally has a homogeneous composition, although small inter-grain and intra-grain variations can be noticed in its CaO, TiO_2 and Cr_2O_3 content. *Spinel* usually occurs as discrete grains with a fairly constant Mg/Fe ratio but different Cr/Al ratios depending on the rock type and pressure of origin (the Cr content of spinel in equilibrium with garnet is a geothermobarometer).

1.2.2. Peridotite geothermobarometry

Pressure and temperature are fundamental parameters for understanding the processes that occur in the Earth's mantle. Equilibrium mineral assemblages in mantle xenoliths can be used to establish the P-T conditions under which rocks equilibrate in the part of the lithosphere sampled by kimberlite magmas. Various combinations of published geothermometers and geobarometers can be used to accomplish this, with each combination requiring the presence of certain mineralogies in the mantle xenoliths (e.g. Brey & Köhler, 1990).

For peridotite xenoliths in kimberlites pressure estimates can be obtained by "Al-in-Opx" geobarometry that utilizes the pressure-dependent exchange of a tschermakitic component ($MgAl_2SiO_6$ or $MgCrAlSiO_6$) between garnet and orthopyroxene (Brey & Köhler, 1990) and can be combined with geothermometers that utilize the partitioning of Fe and Mg between garnet and orthopyroxene (Harley, 1984) or garnet and olivine (O'Neill & Wood, 1979). An alternative method for temperature estimates that is widely used for lherzolitic xenoliths is the two-pyroxene thermometer of Brey & Köhler (1990).

The enstatite-in-clinopyroxene geothermobarometer of Nimis & Taylor, 2000 can provide temperature and pressure estimates from the composition of clinopyroxene alone (if equilibrium with orthopyroxene and garnet is assumed). Also, the concentration of trace element Ni in garnet can be used to obtain T_{Ni} for each garnet in mantle-derived xenoliths, assuming equilibrium with coexisting olivine of uniform Ni content (Ryan et al., 1996; Canil, 1999).

Based on equilibration temperature, peridotite xenoliths in kimberlites can be assigned to a low-temperature group (T<1100-1200°C) and a high-temperature group (>1100-1200°C) (Boyd, 1987).

Some modal, textural and compositional features are characteristic for each group:

- low-temperature peridotite xenoliths are the most abundant and commonly contain chromite, phlogopite and, occasionally, diamond and graphite as accessory minerals. Generally they show minimal or no deformation and are depleted in basaltic components (especially Fe and Ti) as the result of partial-melting events that preceded the eruption of kimberlites and the formation of subcontinental lithospheric mantle.
- high-temperature lherzolites are fertile with respect to basaltic components and often are derived from greater depths. Their textures are typically deformed.

When the two groups are found together there is usually a gap in P-T space between their conditions of equilibration.

1.2.3. Mantle metasomatism

Metasomatism is a process of alteration that involves introduction of components from an external source and changes the chemical and/or mineralogical composition of the affected rock through a multitude of chemical reactions (Goldschmidt, 1922; Wilshire, 1987; Harte et al., 1987). It has an important role in the geochemical evolution of the mantle (McKenzie et al., 1985; Smith & Boyd, 1987; Menzies & Hawkesworth, 1987; Harte & Hawkesworth, 1989; Griffin et al., 1989, 1999b).

The movement of fluids through the mantle causes metasomatism and numerous studies have suggested that metasomatic fluids are usually melts ("fluids incorporating a major proportion of dissolved silicate constituents") derived from the astenosphere and/or subduction-related processes (Harte, 1987). They penetrate the solid rocks by two main processes: infiltration (components are carried by intergranular fluids) and diffusion (components are introduced as individual atoms, ions or molecules).

Various types of metasomatism have been recognized in peridotite xenoliths: "modal metasomatism" (Harte et al., 1987) or "patent metasomatism" (Dawson, 1980) involves the introduction of mineral species not previously present in the rock whereas "cryptic metasomatism" is invoked for the enrichment in incompatible elements (particularly LREE) seen in many coarse xenoliths (Dawson, 1980; Menzies et al., 1985).

Common minerals documenting metasomatism in peridotite rocks include phlogopite, K-richterite, diopside, ilmenite, rutile, apatite and calcite.

Replacement textures and dykes/veins cutting the mantle xenoliths also provide evidence for rock alteration. Chemical zoning in mineral grains (common in certain high-temperature deformed peridotites) may be used to establish relationships between chemically unmodified and modified rocks and thus may document an enrichment in major, minor and trace element composition even in the absence of modal metasomatism (Wilshire & Shervais, 1975; Harte et al., 1987; Irving, 1980).

Finally, trace element geochemistry can also help understanding depletion and enrichment processes in the source region of xenoliths. Different trace element patterns (which are associated with different types of enrichment) and combined petrographical and chemical data (which put some limits on the composition of the fluids) can provide information about the metasomatic agent.

1.3. OBJECTIVES OF THIS STUDY

Until quite recently much of the information we had on Archean lithospheric mantle was provided by studies of xenoliths from South Africa (Kaapvaal craton) and Yakutia (Siberian craton), well known as diamond producing areas.

Since 1991 numerous kimberlite fields have been discovered on the Slave craton (Pell, 1997) and a wealth of xenoliths have become available for study.

A comparison with other cratonic mantle sections in the world revealed many common features: the presence of two distinct suites of low-temperature and high-temperature peridotites, overall comparable degrees of depletion, common presence of Ca-saturated (G9) garnets in modally cpx-free harzburgites etc.

(Boyd, 1987; Boyd & Canil, 1997; Pearson et al., 1999; Kopylova et al., 1999; Kopylova & Caro, 2004; Menzies et al., 2004). Some unique characteristics of the Slave craton are the chemical stratification of the subcontinental lithospheric mantle and a spinel-controlled compositional trend of peridotitic garnet into the wehrlitic field (Griffin et al., 1999; Kopylova et al., 1999; O'Reilly et al., 2001).

This study focuses on peridotite xenoliths derived from the northern part of the Slave craton. The purpose of this thesis is to characterize the mantle rocks sampled by the Voyageur kimberlite and to provide information regarding their conditions of origin.

To accomplish this, the study will complete:

(1) A detailed description of the petrography and mineral chemistry of the peridotite xenoliths recovered from the Voyageur kimberlite

(2) An estimation of pressure-temperature conditions at the time of kimberlite emplacement

(3) A documentation of metasomatic processes in the section of the Slave lithosphere sampled by Voyageur kimberlite

By integrating information regarding the composition, structure, thermal state and metasomatic effects a more detailed picture of the mantle lithosphere from the northern part of the Slave Province will be obtained.

Comparison of the results with similar studies conducted on cratonic areas elsewhere will help understanding the nature of the lithospheric mantle underlying the Slave province.

LITERATURE CITED

- **Boullier, A.M. and Nicholas, A., 1975** – *Classification of textures and fabrics of peridotite xenoliths from South African kimberlites*. Phys. Chem. Earth 9: 467-476
- **Boyd, 1973** – *A pyroxene geotherm*. Geochim. Cosmochim. Acta 37: 2533-2546
- **Boyd, F.R. and Nixon, P.H., 1975** – *Origins of the ultramafic nodules from some kimberlites of Northern Lesotho and the Monastery Mine, South Africa*. Phys. Chem. Earth 9:431-454
- **Boyd, F.R., 1987** – *High- and low-temperature garnet peridotite xenoliths and their possible relation to the lithosphere-astenosphere boundary beneath South Africa*. In: P.H. Nixon (Ed.) Mantle xenoliths, John Wiley, New York, pp: 403-412
- **Boyd, F.R., 1989** – *Compositional distinction between oceanic and cratonic lithosphere*. Earth and Planetary Science Letters 96: 15-26
- **Boyd, F. R. and Canil, D., 1997** - *Peridotite xenoliths from the Slave craton, NWT. Lunar and Planetary Institute Contribution* 921: 34
- **Boyd, F.R.; Pokhilenko, N.P.; Pearson, D.G.; Mertzman, S.A. and Finger, L.W., 1997** – *Composition of the Siberian cratonic mantle: evidence from Udachnaya peridotite xenoliths*. Contrib. Mineral. Petrol. 128: 228-246

- **Brey, G.P. and Köhler, T. and Nickel, K.G., 1990** – Geothermobarometry of four-phase lherzolites: I. Experimental results from 10 to 60kb. Journal of Petrology 6: 1313-1352
- **Brey, G.P. and Köhler, T., 1990** – *Geothermobarometry in four-phase lherzolites: II. New thermometers and practical assessement of existing thermobarometers*. Journal of Petrology 31: 1353-1378
- **Canil D., 1999** - The Ni-in-garnet geothermometer: calibration at natural abundances. Contrib. Mineral. Petrol. 136: 240-246
- **Chen, Y.D.; O'Reilly, S.Y.; Kinny, P.D. and Griffin, W.L., 1994** – *Dating lower crust and mantle events: an ion microprobe study of xenoliths from kimberlite pipes, South Australia*. Lithos 32: 77-94
- **Cox, K.G.; Gurney, J.J. and Harte, B., 1973** – *Xenoliths from the Matsoku pipe*. In: P.H. Nixon (Ed.) Lesotho Kimberlites p: 76-100 Maseru, Lesotho
- **Dawson, J. B.; Smith, J. V. and Hervig, R. L., 1980** – *Heterogeneity in upper-mantle lherzolites and harzburgites*. Phil. Trans. R. Soc. Lond., A 297:323-331
- **Dawson, J.B., 1980** – *Kimberlites and their xenoliths*. Springer Verlag
- **Goldschmidt, V.M., 1922** – On *the metasomatic processes in silicate* rocks. Economic Geology 17: 105-123
- **Griffin, W.L.; Smith, D.; Boyd, F.R.; Cousens, D.R.; Ryan, C.G.; Sie, S.H. and Suter, G.F., 1989** – *Trace element zoning in garnets from sheared mantle xenoliths*. Geochim. Cosmochim. Acta 53 (2): 561-567

- **Griffin, W.L.; Fisher, N.I.; Friedman, J.; Ryan, C.G.; and O'Reilly, S.Y., 1999** – *Cr-pyrope garnets in the lithospheric mantle. I. Compositional systematics and relations to tectonic setting.* Journal of Petrology 40: 679-704
- **Griffin, W.L.; O'Reilly, Y. and Ryan, C.G., 1999** – *The composition and origin of sub-continental lithospheric mantle.* In: Fei, Y.; Bertka, C.M. and Mysen, B.O. (Eds.), Mantle Petrology: Field observations and High Pressure Experimentation: A tribute to Francis R. (Joe) Boyd. Geochemical Society Special Publication, vol. 6: 13-45
- **Griffin, Wl.L., Doyle, B.J., Ryan, C.G., Perason, N.J., O'Reilly, S.Y., Davies, R., Kivi, K., van Actenberg, E. and Natapov, L.M., 1999** – *Layered mantle lithosphere in the Lac de Gras area, Slave craton: composition, structure and origin.* Journal of Petrology 40: 705-727
- **Griffin, Wl.L., Doyle, B.J., Ryan, C.G., Perason, N.J., O'Reilly, S.Y., Natapov, L.M., Kivi, K., Kretschmar, U and Ward, J., 1999** – *Lithosphere structure and mantle terranes: Slave Craton, Canada.* In: Gurney, J.J.; Gurney, J.L.; Pascoe; M.D., Richardson, S.R. (Eds.) Proceedings to the 7th international Kimberlite Conference, J.B. Dawson volume, Red Roof Designs, Cape Town pp: 307-313
- **Griffin, W.L.; Fisher, N.I.; Friedman, J.; Ryan, C.G.; and O'Reilly, S.Y., 2002** – *Cr-pyrope garnets in the lithospheric mantle 2. Compositional populations and their distribution in time and space.* Geochem. Geophys. Geosystema 3 (12): 1073

- **Grütter, H.S.; Apter, D.B.; Kong, J., 1999** – *Crust-mantle coupling: evidence from mantle-derived xenocrystic garnets.* In: Gurney, J.J.; Gurney, J.L., Pascoe, M.D., Richardson, S.R. (Eds.) Proceedings to the 7th international Kimberlite Conference, J.B. Dawson volume, Red Roof Designs, Cape Town pp: 299-306
- **Harley, S.L., 1984** – *An experimental study of the partitioning of Fe and Mg between garnet and orthopyroxene.* Contrib Mineral Petrol 86: 359-373
- **Harte, B.; Cox, K.G. and Gurney, J.J., 1975** – *Petrography and geological history of upper mantle xenoliths from the Matsoku kimberlite pipe.* Phys. Chem. Earth. 9:447-506
- **Harte, B., 1977** – *Rock nomenclature with particular relation to deformation and crystallization textures in olivine-bearing xenoliths.* Journal of Geology 85: 279-288
- **Harte, B., 1983** - *Mantle peridotites and processes–the kimberlite sample.* In: Hawkesworth, C.J. and Norry, M.J. (Eds.) Continental basalts and mantle pp: 46-91
- **Harte, B.; Winterburn, P.A. and Gurney, J.J., 1987** – *Metasomatic phenomena in garnet peridotite facies mantle xenoliths from the Matsoku kimberlite pipe, Lesotho.* In: Menzies, M.A. and Hawkesworth, C.J., (Eds) *Mantle metasomatism.* London: Academic Press, p: 145-200

- **Harte, B. and Hawkesworth, C.J., 1989** – *Mantle domains and mantle xenoliths*. In: Ross, J.; Jaques, A.L.; Ferguson. J.; Green, D.H.; O'Reilly, S.Y.; Danchin, R.V. and Janse, A.J.A. – Kimberlites and related rocks, volume 2. Geological Society of Australia, Special Publication 14: 649-686
- **Ionov, D.A.; Askhepkov, I.V.; Stosch, H.G.; Witt-Eickschen, G. and Seck, H.A., 1993** – *Garnet peridotite xenoliths from the Vitim volcanic field, Baikal region: the nature of the garnet-spinel peridotite transition zone in the continental mantle*. Journal of Petrology 34: 1141-1175
- **Irving, A, J., 1980** - *Petrology and geochemistry of composite ultramafic xenoliths in alkalic basalts and implications for magmatic processes within the mantle*. American Journal of Science, 280-A: 389-426.
- **Kopylova, M.G.; Russell, J.K. and Cookenboo, H., 1999a** – *Petrology of peridotite and pyroxenite xenoliths from Jericho kimberlite: Implications for the thermal state of the mantle beneath the Slave craton, Northern Canada*. Journal of Petrology 40: 79-104
- **Kopylova, M.G.; Russell, J.K. and Cookenboo, H., 1999b** – *Mapping the lithosphere beneath the North Central Slave Craton*. In: Gurney, J.J.; Richardson, S.R. (Eds.) Proceedings to the 7th international Kimberlite Conference, Red Roof Designs, Cape Town pp: 468-479
- **Kopylova, M.G. and Caro, G., 2004** – *Mantle Xenoliths from Southeastern Slave Craton: Evidence for a Chemical Zonation in a Thick, Cold Lithosphere*. Journal of Petrology 45: 1045-1067

- **McDonough, W.F., 1990** – *Constraints on the composition of the continental lithospheric mantle*. Earth and Planetary Science Letters 101: 1-18
- **McKenzie, D., 1985** – *The extraction of magma from the crust and mantle*. Earth and Planetary Science Letters 74 (1): 81-91
- **Menzies, M, Kempton, P. and Dungan, M. 1985** - *Interaction of continental lithosphere and asthenospheric melts below the Geronimo Volcanic Field, Arizona, U.S.A*. Journal of Petrology 26: 663-693
- **Menzies, M.A. and Hawkesworth, C.J., 1987** – (Eds) *Mantle metasomatism*, London: Academic Press
- **Menzies, M.A.; Westerlund, K.; Grutter, H., Gurney, J., Carlson, J., Fung, A. and Nowicki, T., 2004** – *Peridotitic mantle xenoliths from kimberlites on the Ekati Diamond Mine property, N.W.T., Canada: major element compositions and implications for the lithosphere beneath the central Slave craton*
- **Nixon, P.H. and Boyd, F.R., 1973** - *The discrete nodule association in kimberlitesfrom Northern Lesotho*. In P.H. Nixon, Ed., Lesotho Kimberlites, LesothoNational Development Corp., Maseru, Lesotho, 67–75.
- **O'Neill, H.St.C. and Wood, B.J., 1979** – *An experimental study of Fe-Mg partitioning between garnet and olivine, and its calibration as a geothermometer*. Contrib Mineral Petrol 70: 59-70

- **O'Neill H.St.C. and Wood, B.J., 1980** - *An experimental study of Fe-Mg partitioning between garnet and olivine, and its calibration as a geothermometers*: corrections. Contrib Mineral Petrol 72: 337
- **O'Reilly, S.Y. and Griffin, W.L., 1996** – *4-D lithosphere mapping: methodology and examples*. Tectonophysics 262: 3-18
- **O'Reilly, S.Y.; Griffin, W.L.; Djomani, Y.H.P. and Morgan, P., 2001** – *Are lithospheres forever? Tracking changes in subcontinental lithospheric mantle through time*. GSA Today, April: 4-10
- **Pearson, N.J.; Griffin, W.L.; Doyle, B.J.; O'Reilly, S.Y; van Achterbergh, E. and Kiwi, K., 1999** – *Xenoliths from kimberlite pipes of the Lac de Gras area, Slave Craton, Canada*. In: Gurney, J.J.; Gurney, J.L.; Pascoe, M.D.; Richardson, S.H. (Eds.) Proceedings to the 7th international Kimberlite Conference P.H. Nixon volume, Red Roof Designs, Cape Town pp: 644-658
- **Pell, 1997** – *Kimberlites in the Slave Craton, Northwest Territories, Canada*. Geoscience Canada 24 (2): 77-90
- **Ryan, C.G.; Griffin, W.L. and Pearson, N.J., 1996** – *Garnet geotherms: pressure-temperature data from Cr-pyrope garnet xenocrysts in volcanic rocks*. Journal of Geophysical Research 101 (B3): 5611-5625
- **Smith, D. and Boyd, F.R., 1987** – *Compositional heterogeneities in a high-temperature lherzolite nodule and implications for mantle processes*. In: Nixon, P.H. (Ed) Mantle Xenoliths. Chichester: John Wiley, pp: 551-561

- **Zhao, J. and McCulloch, M.T., 1993** – *Melting of a subduction-modified continental lithospheric mantle; evidence from late Proterozoic mafic dyke swarms in central Australia*. Geology 21 (5): 463-466
- **Wilshire, H.G and Shervais, J. W., 1975** – Physics and Chemistry of the Earth 9:257-272
- **Wilshire, H.G., 1987** – *A model of metasomatism*; Geological Society of America, Special Publication 215:47-60

CHAPTER 2

REGIONAL SETTING/LOCAL GEOLOGY

2.1. GENERAL GEOLOGY OF THE SLAVE PROVINCE

The Slave Province (Fig. 2.1.1.) is a small (~200000 km^2) but well exposed cratonic area located in the northwestern part of the Canadian Shield (Northwest Territories and Nunavut, Canada) and bounded on three sides by Paleoproterozoic belts: Thelon Tectonic Zone (2.02-1.91Ga) on the East, Wopmay Orogen (1.91-1.84Ga) to the West, Great Slave Lake Shear Zone (1.98-1.93Ga) and Taltson Magmatic Zone (1.99-1.91Ga) to South and Southeast, respectively. Its northern boundary is covered by the Proterozoic and younger sediments of the Bear Province and the Arctic Platform, which extend along the Bathurst Fault Zone on the north-eastern side and into the Kilohigok Basin (Goulborn Group) across the craton (Padgham & Fyson, 1992; Card & King, 1992; Isachsen & Bowring, 1994; Bleeker & Davis, 1999; Griffin et al., 1999; Armstrong & Kjarsgaard, 2003; Davis et al., 2003).

The general character of the Slave Province is that of a granite-greenstone terrane (a typical suite for Archean domains) with a rock record that goes back to the world's oldest known rocks, the Acasta gneisses (3.96-4.02Ga), located in the western part of the craton (Bowring et al., 1989; Padgham & Fyson, 1992; Isachsen & Bowring, 1994; Stern & Bleeker, 1998; Bowring & Williams, 1999).

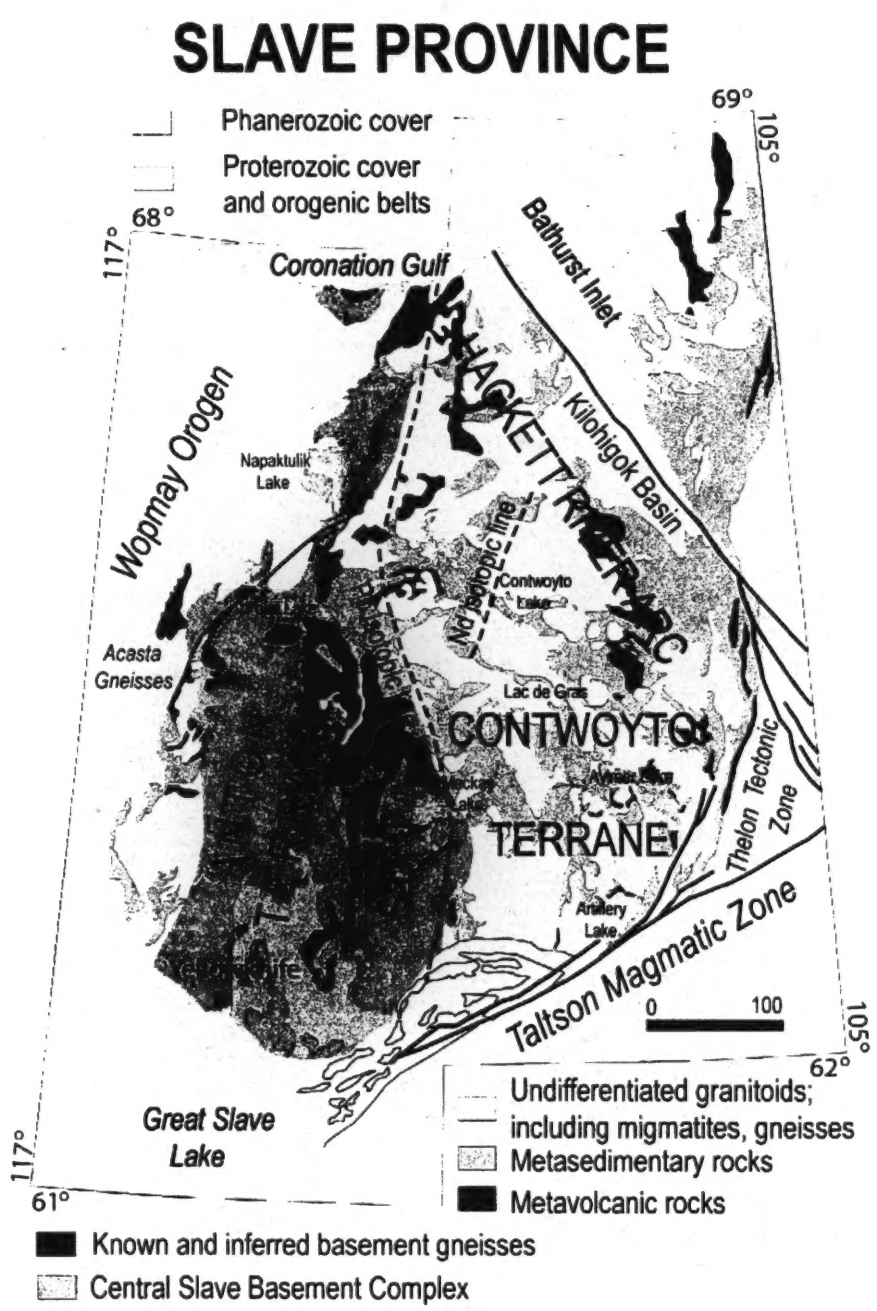

Fig. 2.1.1 Geological map of the Slave Province, Canada (modified after Davis & Bleeker, 1999). Lithotectonic terrains after Kusky (1990). Pb isotopic line from Thorpe et al. (1992), Nd isotopic line from Davis and Hegner (1992).

Details regarding the regional geology and tectonic evolution of the Slave Province have been given by numerous authors and reveal some unique features (see below) that distinguish its evolution from other Archean cratons (Kusky, 1989; Padgham, 1990; Card & King, 1992; Isachsen & Bowring, 1994; Davis et al., 1994, 1996; Griffin et al., 1999; Bleeker et al., 1999; Yamashita et al., 2000; Bleeker, 2003; Ketchum et al., 2004).

In summary, the Neoarchean (2.7-2.6Ga) metasedimentary rocks and syn-volcanic plutons of the Yellowknife Supergroup supracrustals dominate the surface geology of the Slave Province, overlaying a Hadean to Mesoarchean (4.0-2.9Ga) sialic basement terrane documented in the central and western parts of the craton and being intruded by extensive, Neoarchean (2.6-2.5Ga), syn- and post-deformational granitoid plutons.

The **sialic basement terrane** appears as scattered outcrops of old (>2.9Ga) granitoid rocks (including the Acasta gneisses) from the northern to the southern Slave Province but is only present in the western and central parts of the craton. Its absence from the eastern Slave imposes a separation of the craton into different geological domains and is supported by isotopic studies: the western Slave is characterized by more evolved Pb isotopic signatures (high $^{207}Pb/^{204}Pb$ ratios derived from an ancient upper crustal source) in comparison with the eastern Slave, which is isotopically more juvenile (low $^{207}Pb/^{204}Pb$ ratios derived from mantle and juvenile crustal sources). The Nd isotopic signatures reveal a similar pattern, with negative ε_{Nd} values (suggesting derivation from older crust) in the western domain and positive ε_{Nd} values (consistent with derivation from

juvenile sources) in the eastern domain (Thorpe et al., 1992; Davis & Hegner, 1992; Davis et al., 1996). The two distinct isotopic boundaries trending roughly N-S are referred to as the Pb and Nd isotopic lines and show changes in the isotopic composition of Pb and Nd in large granitoid bodies intruded throughout the Slave Province and of Pb in galena from volcanogenic massive sulfides, syn-volcanic veins and breccias.

Kusky (1990) viewed the basement outcrops as part of a single block (Anton Terrane) to which the Contwoyto Terrane (westward-verging folds and thrusts of graywake-mudstone turbidites) and the Hackett River Arc Terrane (northwest-striking volcanic rocks) were accreted along the Sleepy Dragon Terrane (viewed as a deformed continental margin setting) in the Neoarchean (2.8-2.5Ga). Bleeker et al. (1999) acknowledged the apparent absence of similar basement rocks in the southwestern Slave, noted strong indications that they occur farther to the east and named that block the "Central Slave Basement Complex".

A thin, discontinuous **cover sequence** (dated at ca 2.85Ga) of quartzite, conglomerate, banded iron formation and minor volcanic rocks unconformably overlie the basement gneisses (Bleeker et al., 1999; Sircombe et al., 2001). Given the diagnostic lithology and the association with the basement rocks, Bleeker et al. (1999) grouped it in a single unit named the "Central Slave Cover Group" which was interpreted to represent initial rifting and subsidence of the underlying crust.

The **Yellowknife Supergroup** supracrustal series (2.73-2.6Ga) dominate the exposed crust of the Slave craton. Tholeiitic basalts (2.73-2.70Ga) structurally overlie the basement and its diagnostic cover in the western Slave (Padgham, 1992; van Breemen et al., 1992; Isachsen & Bowring, 1994) whereas calc-alkaline volcanic rocks (ca. 2.70-2.66Ga) can be correlated across the entire craton (van Breemen et al., 1992) and are roofed by 2.66-2.63Ga thick turbidite sequences (Bleeker & Villeneuve, 1995; Pehrsson & Villeneuve, 1999). Unlike other cratons, the metasedimentary rocks of the Slave are present in higher proportion relative to metavolcanic rocks, making up ~80% of the supracrustal package (Padgham & Fyson, 1992; Isachsen & Bowring, 1994).

Between 2.63 and 2.58 Ga, the Slave Province saw a widespread **emplacement of granitoid plutons** and, simultaneously, has been subjected to **regional compressional deformation** and **high-T/low-P metamorphism**.

The granitoid plutons are typically subdivided into syn-deformation granodiorites to tonalities (2.62-2.60Ga) and post-deformation monzogranites (2.60-2.58Ga) covering approximately 50% of the Slave craton (Davis et al., 1994; Davis & Bleeker, 1999).

Deformation was characterized by multiple phases of folding (at least three events) resulting in significant horizontal shortening.

All supracrustal rocks have been metamorphosed at greenshist to granulite facies (Pehrsson et al., 2000; Davis & Bleeker, 1999; Davis et al., 2003).

2.2. DISTRIBUTION OF KIMBERLITES IN THE SLAVE PROVINCE

The Slave craton is part of the western North American region (Heaman et al., 2004) containing kimberlite fields with different emplacement ages from Precambrian to Eocene (a type 3 kimberlite province; Mitchell, 1986). The first diamondiferous kimberlitic occurrence was reported at Point Lake in 1991 and, since then, more than 350 kimberlites have been found throughout the Slave Province (Pell, 1997; Carlson et al., 1999; Armstrong & Kjarsgaard, 2003 and references therein). Most of the pipes are fairly small and do not crop out at surface but are covered by lakes or glacial till.

The main diamond-bearing kimberlite cluster is Cretaceous-Tertiary in age (74-45Ma; Davis & Kjarsgaard, 1997; Carlson et al., 1999; Graham et al., 1999; Heaman et al., 2003, 2004; Creaser et al., 2004 and references therein) and is located in Lac de Gras region, east-central Slave (Fig. 2.2.1). Being a part of Domain III of Heaman et al. (2003), the Lac de Gras kimberlite field hosts more than 250 kimberlites, including the producing diamond mines Diavik and Ekati. Crater and hypabyssal-facies kimberlites are common, but diatreme or incipient diatreme-facies kimberlites are also present (Pell, 1997; Carlson et al., 1999; Graham et al., 1999).

Outside the Lac de Gras area the clusters are smaller and relatively isolated. In the SE Slave (Domain II of Heaman et al., 2003) the Gahcho Kué cluster comprises diamondiferous kimberlite bodies with Cambrian ages: 5034 (542Ma; Heaman et al., 2003), Tesla, Tuzo and Hearne (542-531Ma; Hetman et al., 2004). Further to the west, the Snap Lake Dyke has been dated at

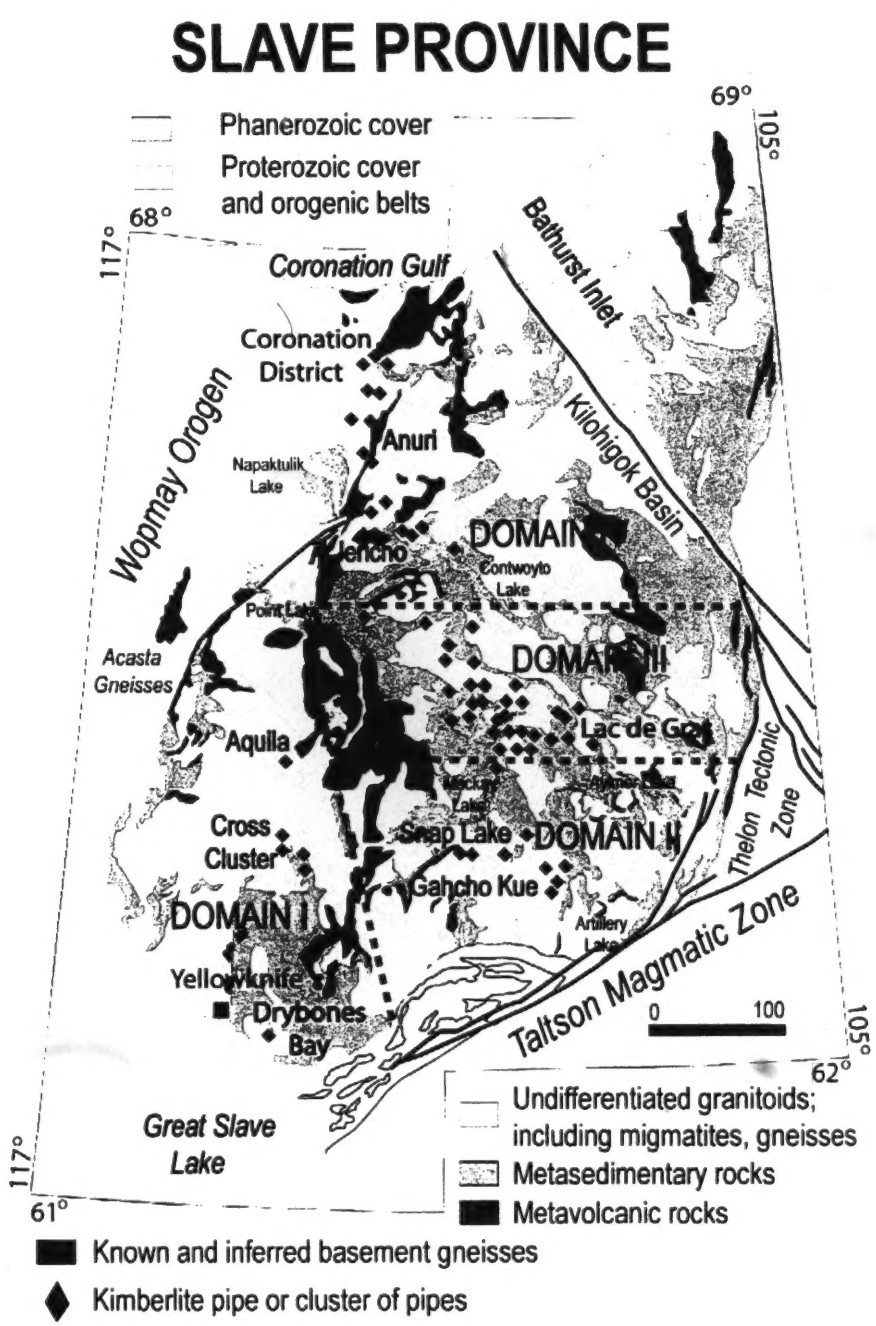

Fig. 2.2.1 Distribution of kimberlites in the Slave Province. Geology modified after Davis & Bleeker (1999). Locations and domains after Heaman et al. (2003, 2004).

535-523Ma (Agashev et al., 2001; Heaman et al., 2003). The SE Slave kimberlite field is dominated by hypabyssal-facies kimberlites, with subordinate diatreme-facies kimberlites. Gahcho Kué is a transitional hypabyssal to diatreme-facies kimberlite (Hetman et al., 2004; Caro & Kopylova, 2004).

The SW Slave kimberlite field (Domain I of Heaman et al., 2004) is Siluro-Ordovician in age (ca 465-435Ma; Carlson et al., 1999; Heaman et al., 2003) and includes the Snare Lake, Cross Lake, Carp Lake and Drybones Bay clusters (Pell, 1997; Carlson et al., 1999). Drybones Bay is located on the north shore of Great Slave Lake, 50km SE of Yellowknife. The pipe has a U-Pb zircon age of 441Ma (Heaman et al., 2003) and includes crater and diatreme facies kimberlite. At the Carp Lake cluster, Ursa and Orion (459Ma and 435Ma, respectively; Carlson et al., 1999; Heaman et al., 2003) are dominated by hypabyssal kimberlites. The Cross pipe (a possible crater facies kimberlite located 120km NNE of Yellowknife) has been dated at 450Ma (Heaman et al., 2003). No emplacement age has been reported for Aquila (a weakly diamondiferous pipe placed 90km N of the Cross cluster).

Finally, the northern Slave kimberlite field (Domain IV of Heaman et al., 2003) comprises the Jurassic Contwoyto cluster (including Jericho, Muskox, Rush, Peregrine, Nazareth) together with few isolated kimberlites: Anuri, Potentilla, Artemisa, Knife. Jericho is a diamondiferous pipe located ~150km NW of Lac de Gras, at the northwestern tip of Contwoyto Lake and characterized by hypabyssal and diatreme facies kimberlite (Cookenboo, 1999). Its emplacement age was reported at 172Ma (Middle Jurassic) based on Rb-Sr on phlogopite

(Heaman et al., 2002 and references therein). W and NW of Jericho, Muskox is dominated by hypabyssal kimberlite or kimberlite breccia (Pell, 1997) and Anuri is infilled with two contrasting phases: volcaniclastic kimberlite and, much less common, hypabyssal kimberlite (Masun et al., 2004). Both pipes are significantly diamodiferous. Anuri is the only kimberlite with Precambrian emplacement age (613Ma) reported so far for the Slave craton (Masun et al., 2004).

2.3. THE SUBCRATONIC LITHOSPHERIC MANTLE

The structure, composition and thermal state of the subcontinental lithosphere in cratonic areas can be established by direct study of mantle xenoliths hosted in kimberlites. Over the past two decades many petrological and geophysical investigations were conducted with the purpose to determine the nature of the mantle underlying the Slave Province. It is a classical setting for the occurrence of diamondiferous kimberlites (stable Archean craton with a cool mantle root) and, following the discovery of diamonds, has become a major focus for the scientific community.

Geophysical and xenolith/xenocryst studies documented a heterogeneous Slave mantle lithosphere consisting of distinct domains that appear to transect the roughly N-S oriented crustal asymmetry (Grutter et al., 1999; Griffin et al., 1999; Kopylova and Russell, 2000; Jones et al., 2001; Carbno and Canil, 2002; Davis et al., 2003a; Kopylova and Caro, 2004). There is evidence for a ~200km thick lithospheric root in the Slave Province, petrological and mineralogical data suggest an increase in thickness from ~160-190km in the

northern part to ~200km in the central part and >230km in the southern part (Grütter et al., 1999; Griffin et al., 1999;Kopylova et al., 1999; Kopylova and Russell, 2000). Using a large database of garnet xenocrysts, Grütter et al. (1999) proposed three WSW-ENE trending lithospheric domains characterized by distinct garnet chemistry (Fig. 2.2.1). A lherzolitic mantle with a high proportion of eclogitic garnet xenocrysts distinguishes the Northern Slave from the Central (harzburgitic) and Southern Slave (lherzolitic and subordinate eclogitic) domains. Based on the contrasting garnet compositions (high-Cr harzburgitic garnets are only present in the SW Slave), Carbno & Canil (2002) further divided the Southern Slave into western and eastern parts that could be delimited by the Pb isotopic line. The existence of the lithospheric domains described above is also supported by geophysical studies: magnetotelluric data revealed a layer of anomalously conductive mantle that is only present in the Central Slave (Jones et al., 2001) and S-wave (seismic shear wave) polarization suggests similar directions of mantle anisotropy for both Northern and Southern Slave but slightly different directions for the Central Slave domain (Bank et al., 2000).

All lithospheric domains are characterized by a pronounced chemical stratification that was first observed in the Lac de Gras area. Using xenoliths and heavy mineral concentrates, Griffin et al. (1999) discovered in the Central Slave a unique mantle stratigraphy: a two-layered lithospheric mantle comprising a shallow ultra-depleted, predominantly harzburgitic layer that is sharply separated at ~150km depth from a deeper, less depleted, predominantly lherzolitic layer (Fig. 2.2.2).

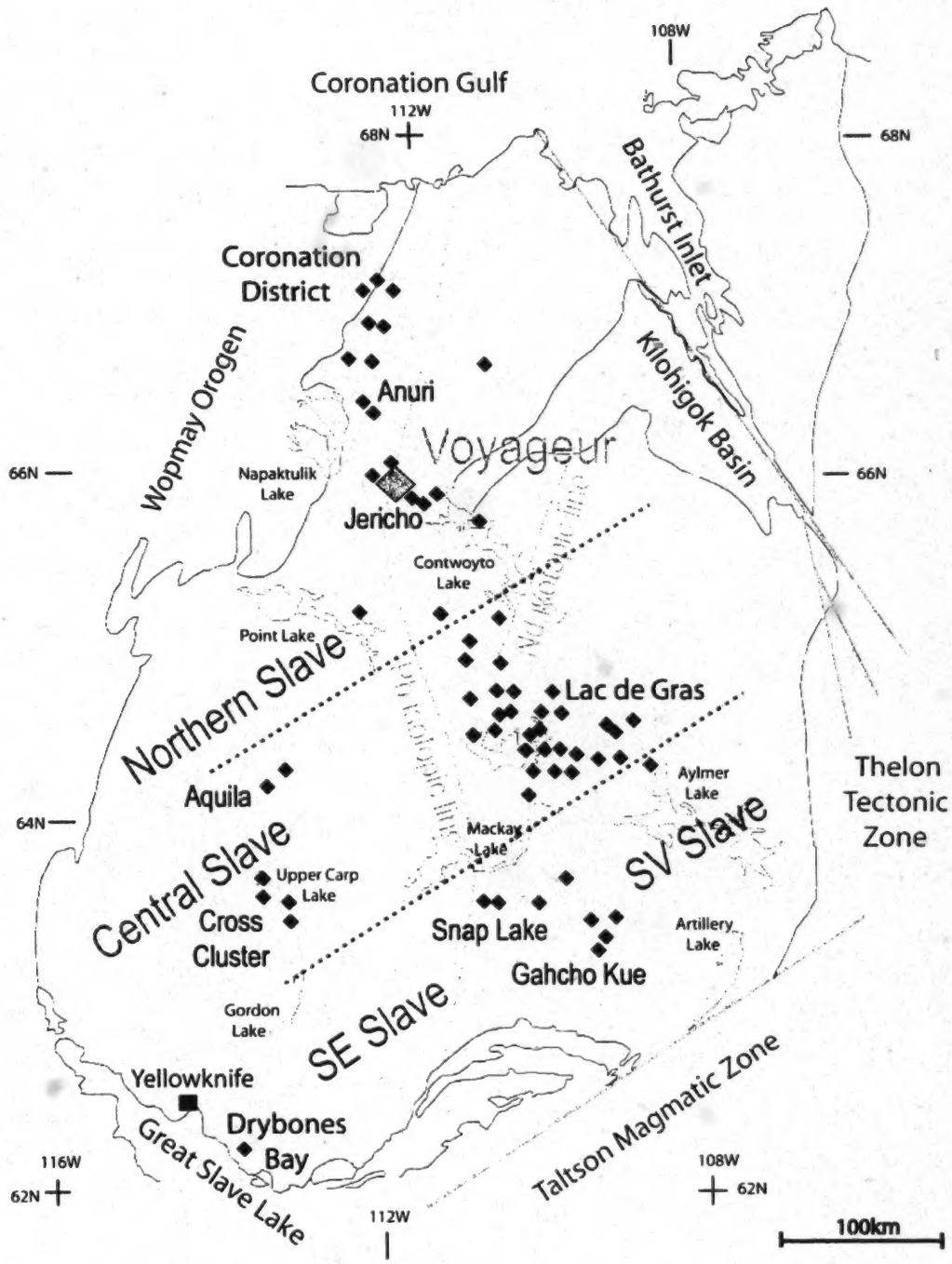

Fig. 2.3.1 Distribution of kimberlites in the Slave Province. Pb isotopic line from Thorpe et al., 1992. Nd isotopic line from Davis and Hegner, 1992. Geochemical boundaries from Grutter et al., 1999.

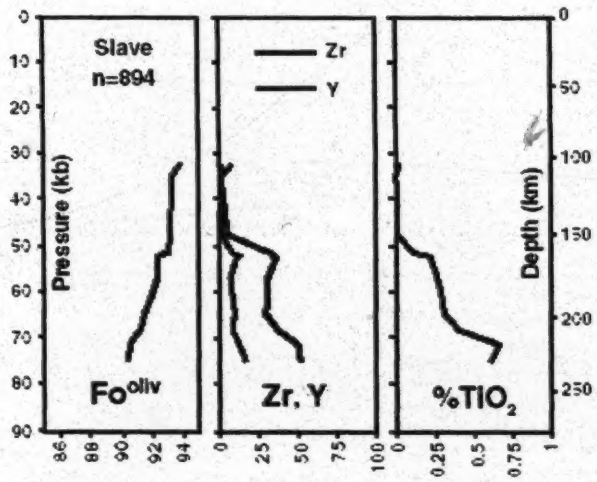

Fig. 2.3.2 The layered structure of the Slave lithospheric mantle shown by key geochemical indicators

(from O'Reilly et al., 2001)

The ultra-depleted harzburgitic layer is thinned in the southern, northern and western parts of the craton (Griffin et al., 1999; O'Reilly et al., 2001), so the chemical boundary appears at distinct depths in each lithospheric domain.

Geophysical results agree well with these petrological findings. The area of anomalous mantle conductivity determined by magnetotelluric studies coincides with the areal extent of the ultra-depleted harzburgitic layer (~9000km^2). Gravity data also show long wave negative Bouguer anomalies in the same (central) part of the Slave craton, across the diamond fields.

Although it has many characteristics common to cratonic mantle elsewhere, the subcratonic lithosphere of the Slave Province also shows some unique features that may point to a different evolution. There is no agreement yet regarding the processes responsible for the existence on distinct chemical layering in the mantle column, with more data on the geometry of the distinct domains being required.

2.4. HOST KIMBERLITE

The Voyageur kimberlite is located in the northern Slave kimberlite field, ~20km W of Jericho ($66^0$03'45"N and $111^0$52'30"W) (Fig. 2.3.1). No information has been reported in the scientific literature regarding this pipe so far. As part of the Contwoyto cluster and considering the spatial correlation of the certain periods of kimberlite magmatism documented in the Slave Province (Heaman et al., 2003), it can be assumed that the emplacement age of Voyageur kimberlite is Jurassic.

The pipe infill at Voyageur consists of "a number of texturally complex rocks which range from magmatic to magmaclastic. In general, the rocks can be classified as medium grained, olivine macrocrystic, monticellite kimberlites of the crater facies" (Casey Hetman 2005 - written communication).

LITERATURE CITED

- **Agashev, A.M.; Pokhilenko, N.P.; McDonald, J.A.; Takazawa, E.; Vavilov, M.A.; Sobolev, N.V. and Watanabe, T., 2001** – *A unique kimberlite-carbonatite primary association in the Snap Lake dyke system, Slave craton: evidence from geochemical and isotopic studies.* The Slave-Kaapvaal Workshop, Program with Abstract pp. 42-44
- **Armstrong, J.P. and Kjarsgaard, B.A., 2003** – *Geological setting of kimberlites in the Archean Slave Province.* In: Kjarsgaard, B. (Ed.) VIIth International Kimberlite Conference, Slave Province and Northern Alberta Field Trip Gudebook p.31-38
- **Bank, C.G.; Bostock, M.G.; Ellis and R.M.Cassidy, J.F., 2000** – *A reconnaissance teleseismic study of the upper mantle and transition zone beneath the Archean Slave Craton in NW Canada.* Tectonophysics 319:151-166
- **Bleeker, W and Villeneuve, M., 1995** – *Structural studies along the Slave portion of the SNORCLE transect.* In: Cook, F and Erdmer, P. Slave-Northern Cordillera Lithospheric Evolution, Report of 1995 Transect Meeting April 8-9; University of Calgary. LITHOPROBE report 44: 8-14
- **Bleeker, W. and Davis, W.J., 1999** – *The 1991-1996 NATMAP Slave Province Project: introduction.* Canadian Journal of Earth Sciences 36: 1033-1042

- **Bleeker, W; Ketchum, J.W.F.; Jackson, V.A. and Villeneuve, M.E., 1999a** – *The Central Slave Basement Complex: Part I. Its structural topology and autochtonous cover.* Canadian Journal of Earth Sciences 36: 1083-1109
- **Bleeker, W; Ketchum, J.W.F. and Davis, W.J., 1999b** – *The Central Slave Basement Complex: Part II. Age and tectonic significance of high-strain zones along basement-cover contact.* Canadian Journal of Earth Sciences 36: 1111-1130
- **Bleeker, 2003** – *The late Archean record: a puzzle in ca. 35 pieces.* Lithos 71: 99-134
- **Bowring, S.A. and Williams, 1999** – *Priscoan (4.00-4.03Ga) orthogenesis from northwestern Canada.* Contrib Mineral Petrol 134: 3-16
- **Carbno, G.B. and Canil, D., 2002**– *Mantle Structure beneath SW Slave Craton, Canada: Constraints from Garnet Geochemistry in Drybones Bay Kimberlite.* Journal of Petrology 43: 129-142
- **Card, K.D. and King, J.E., 1992** – *The tectonic evolution of the Superior and Slave provinces of the Canadian Shield: introduction.* Canadian Journal of Earth Sciences 29: 2059-2065
- **Carlson J.A.; Kirkley, M.B., Thomas, E.M. and Hiller, W.D., 1999**- *Recent Canadian Kimberlite Discoveries.* In: Gurney, J.J.; Gurney, J.L.; Pascoe, M.D and Richardson, S.H. (Eds) J.B Dawson Volume- Proceedings of the VIIth International Kimberlite Conference Red Roof Design, Cape Town v.1 pp. 81-89

- **Caro, G. and Kopylova, M.G., 2004** – *The hypabyssal 5034 kimberlite of the Gahcho Kue cluster, southwestern Slave Craton, Northwestern Territories, Canada: a granite-contaminated Group-I kimberlite*. The Canadian Mineralogist 42: 183-207
- **Cookenboo, H.O. 1999** – *History and process of emplacement of the Jericho (JD-1) kimberlite pipe, Northern Canada.* In: Gurney, J.J.; Richardson, S.R. (Eds.) Proceedings to the 7th international Kimberlite Conference, Red Roof Designs, Cape Town pp: 125-133
- **Creaser, R.A.; Grutter, H.; Carlson, J. and Crawford, B., 2004** – *Macrocrystal phlogopite Rb-Sr dates for the Ekati property kimberlites, Slave province, Canada: evidence for multiple intrusive episodesin the Paleocene and Eocene.* Lithos 76: 399-414
- **Davis, W.J. and Hegner, E., 1992** – *Neodymium isotopic evidence for the accretionary development of the Late Archean Slave Province*. Contrib. Mineral. Petrol. 111: 493-503
- **Davis, W.J.; Fryer, B.J. and King, J.E., 1994** - *Geochemistry and evolution of late Archean plutonism and its significance to the tectonic development of the Slave craton*. Precambrian research 67: 207-241
- **Davis, W.J., Gariepy, C. and van Breemen, O., 1996** – *Pb isotopic composition of late Archean granites and the extent of recycling early Archean crust in the Slave Province, northwest Canada*. Chem. Geol. 130: 255-269

- **Davis, W.J. and Kjarsgaard, B.A., 1997** - *A Rb-Sr isochron age for a kimberlite from the recently discovered Lac de Gras field, Slave Province, Northwest Canada*. Journal of Geology 105: 503-509
- **Davis, W.J. and Bleeker, W., 1999** – *Timing of plutonism, deformation and metamorphism in the Yellowknife Domain, Slave Province, Canada*. Canadian Journal of Earth Sciences 36: 1169-1187
- **Davis, W., Jones, A.G., Bleeker, W. and Grutter, H.S., 2003a** – *Lithosphere development in the Slave Craton: a linked crustal and mantle perspective*. Lithos 71: 575-589
- **Davis, W., Canil, D., MacKenzie, J.M. and Carbno, G.B., 2003b** – *Petrology and U-Pb geochronology of lower crustal xenoliths and the development of a craton, Slave Province, Canada*. Lithos 71: 541-573
- **Graham, I.; Burgess, J.L.; Bryan, D.; Ravenscroft, P.J.; Thomas, E.; Doyle, B.J.; Hopkins, R. and Armstrong, K.A., 1999** – *Exploration History & Geology of the Diavik Kimberlites, Lac de Gras, Northwestern Territories, Canada.* In: Gurney, J.J.; Gurney, J.L., Pascoe, M.D and Richardson, S.H. (Eds) J.B Dawson Volume- Proceedings of the VIIth International Kimberlite Conference Red Roof Design, Cape Town v.1 pp. 262-279
- **Griffin, W.L.; Fisher, N.I.; Friedman, J.; Ryan, C.G.; and O'Reilly, S.Y., 1999** - *Cr-pyrope garnets in the lithospheric mantle. I. Compositional systematics and relations to tectonic setting*. Journal of Petrology Journal of Petrology 40: 679-704

- **Griffin, W.L.; O'Reilly, Y. and Ryan, C.G., 1999** – *The composition and origin of sub-continental lithospheric mantle.* In: Fei, Y.; Bertka, C.M. and Mysen, B.O. (Eds.), Mantle Petrology: Field observations and High Pressure Experimentation: A tribute to Francis R. (Joe) Boyd. Geochemical Society Special Publication, vol. 6: 13-45
- **Griffin, Wl.L., Doyle, B.J., Ryan, C.G., Perason, N.J., O'Reilly, S.Y., Davies, R., Kivi, K., van Actenberg, E. and Natapov, L.M., 1999a** – *Layered mantle lithosphere in the Lac de Gras area, Slave craton: composition, structure and origin.* Journal of Petrology 40: 705-727
- **Griffin, Wl.L., Doyle, B.J., Ryan, C.G., Perason, N.J., O'Reilly, S.Y., Natapov, L.M., Kivi, K., Kretschmar, U and Ward, J., 1999b** – *Lithosphere structure and mantle terranes: Slave Craton, Canada.* In: Gurney, J.J.; Gurney, J.L.; Pascoe; M.D., Richardson, S.R. (Eds.) Proceedings to the 7th international Kimberlite Conference, J.B. Dawson volume, Red Roof Designs, Cape Town pp: 307-313
- **Griffin, W.L.; Shee, S.R.; Ryan, C.G.; Win, T.T. and Wyatt, B.A., 1999c** – *Harzburgite to lherzolite and back again: metasomatic processes in ultramafic xenoliths from Wesselton kimberlite, Kimberley, South Africa.* Contrib. Mineral. Petrol. 134: 232-250

- **Grütter, H.S.; Apter, D.B.; Kong, J., 1999** – *Crust-mantle coupling: evidence from mantle-derived xenocrystic garnets.* In: Gurney, J.J.; Gurney, J.L., Pascoe, M.D., Richardson, S.R. (Eds.) Proceedings to the 7th international Kimberlite Conference, J.B. Dawson volume, Red Roof Designs, Cape Town pp: 299-306
- **Heaman, L.M., Creaser, R.A. and Cookenboo, H.O., 2002** – *Extreme enrichment in high field strength elements in Jericho eclogites xenoliths: A cryptic record of Paleoproterozoic subduction, partial melting and metasomatism beneath Slave craton, Canada.* Geology 30 (6): 507-510
- **Heaman, L.M.; Kjarsgaard, B. and Creaser, R.A., 2003** – *The timing of kimberlite magmatism and implications of diamond exploration; a global perspective.* Lithos 71: 153-184
- **Heaman, L.M.; Kjarsgaard, B.A. and Creaser, R.A., 2004** – *The temporal evolution of North American kimberlites.* Lithos 76: 377-397
- **Hetman, C.M.; Scott Smith, B.H.; Paul, J.L. and Winter, F., 2004** – *Geology of the Gahcho Kue kimberlite pipes, NWT, Canada: root to diatreme magmatic transition zones.* Lithos: 51-74
- **Isachsen, C. and Bowring, C.A., 1994** – *Evolution of the Slave craton.* Geology 22: 917-920
- **Jones, A.G.; Ferguson, I.J.; Chave, A.D.; Evans, R.L. andMcNeice, G.W., 2001**– *Electric lithosphere of the Slave Craton.* Geology 29 (5): 423-426

- **Ketchum, J.W.F.; Bleeker, W. and Stern, R., 2004** – *Evolution of Archean basement complex and its autochtonous cover, southern Slave Province, Canada*. Precambrian Research 135: 149-176
- **Kopylova, M.G.; Russell, J.K. and Cookenboo, H., 1999a** – *Petrology of peridotite and pyroxenite xenoliths from Jericho kimberlite: Implications for the thermal state of the mantle beneath the Slave craton, Northern Canada*. Journal of Petrology 40: 79-104
- **Kopylova, M.G.; Russell, J.K. and Cookenboo, H., 1999b** – *Mapping the lithosphere beneath the North Central Slave Craton*. In: Gurney, J.J.; Richardson, S.R. (Eds.) Proceedings to the 7th international Kimberlite Conference, Red Roof Designs, Cape Town pp: 468-479
- **Kopylova, M.G. and Russell, J.K., 2000** – *Chemical stratification of cratonic lithosphere: Constraints from the Northern Slave craton, Canada*. Earth and Planetary Science Letters 181: 71-87
- **Kopylova, M.G. and Caro, G., 2004** – *Mantle Xenoliths from Southeastern Slave Craton: Evidence for a Chemical Zonation in a Thick, Cold Lithosphere*. Journal of Petrology 45: 1045-1067
- **Kusky, T.M., 1989**- *Accretion of the Archean Slave Province*. Geology 17 (1): 63-67
- **Masun, K.M.; Doyle, B.J.; Ball, S.A. and Walker, S.**, 2004 – *The geology and mineralogy of the Anuri kimberlite, Nunavut, Canada*. Lithos 76: 75-97

- **Mitchell, R.H., 1986** – *Kimberlites: mineralogy, geochemistry and petrology*. New York, Plennum Press
- **O'Reilly, S.Y.; Griffin, W.L.; Djomani, Y.H.P. and Morgan, P., 2001** – Are lithospheres forever? Tracking changes in subcontinental lithospheric mantle through time. GSA Today, April: 4-10
- **Padgham, W.A 1990** – *The Slave Province, an overview.* In Padgham, W.A. and Atkinson, D. (Eds) Mineral deposits of the Slave Province, Northwest Territories. Geological Survey of Canada Open file 2168, p.1-40
- **Padgham, W.A., 1992** – *Mineral deposits in the Archean Slave Structural Province; lithological and tectonic setting*. Precambrian Research 58: 1-24
- **Padgham, W.A. and Fyson, W.K., 1992** – *The Slave province: a distinct craton*. Canadian Journal of Earth Sciences 29: 2072-2086
- **Pehrsson, S.J. and Villeneuve, M.E., 1999** – *Deposition and imbrication of a 2670-2692Ma supracrustal sequence in the Indin Lake area, southwestern Slave Province, Canada.* Canadian Journal of Earth Sciences 36: 1149-1168
- **Pehrson, S.J.; Chacko, T.; Pilkington, M.; Villeneuve, M.E. and Bethune, K., 2000** – *Anton terrane revisited: Late Archean exhumation of a moderate-pressure granulite terrane in the western Slave Province.* Geology 28 (12): 1075-1078
- **Pell, 1997** – *Kimberlites in the Slave Craton, Northwest Territories, Canada*. Geoscience Canada 24 (2): 77-90

- **Sircombe, K.N.; Bleeker, W. and Stern, R.A., 2001** – *Detrital zircon geochronology and grain-size analysis of a ~2800Ma Mesoarchean proto-cratonic cover succession, Slave Province, Canada*. Earth and Planetary Science Letters 189: 207-220
- **Stern, R.A. and Bleeker, W., 1998** – *Age of the world's oldest rocks refined using Canada's SHRIMP. The Acasta gneiss complex, Northwest Territories, Canada*. Geoscience Canada 25: 27-31
- **Thorpe, R.I., Cumming, G.L., Mortensen, J.K., 1992** – *A significant Pb isotope boundary in the Slave Province and its probable relation to ancient basement in the western Slave Province*. Project Summaries, Canada Northwest Territories Mineral Development Subsidiary Agreement. Geological Survey of Canada Open File Report 2484, p. 279-284
- **Van Bremen, O; Davis, W.J. and King, J.E., 1992** – *Temporal distribution of granitoid plutonic rocks in the Archean Slave Province, northwest Canadian Shield*. Canadian Journal of Earth Sciences 29: 2186-2199
- **Yamashita, K.; Creaser, R.A.; Jensen, J.E. and Heaman, L.M., 2000** – *Origin and evolution of mid- to late-Archean crust in the Hanikahimajuk Lake area, Slave province, Canada; evidence from U-Pb geochronological, geochemical and Nd-Pb isotopic data*. Precambrian Research 99: 197-224

CHAPTER 3

PETROGRAPHY AND MINERAL CHEMISTRY

3.1. SAMPLES AND ANALYTICAL TECHNIQUES

About 40% of the available mantle xenoliths from Voyageur are eclogites, currently studied by Stephanie Schmidberger (post doctoral fellow at the University of Alberta). A total of 22 peridotite xenoliths were selected for this study (Table 3.2.1). The samples are fresh or show only minor alteration and generally are less than 11cm (5-6cm on average) in their long axes, with rare specimens being as large as 20cm (Fig. 3.2.1 a-h).

Standard polished thin sections were prepared to allow both a detailed description of the petrography and chemical analysis of minerals in the peridotite xenoliths. Individual garnet and clinopyroxene grains (small fragments of each phase) were extracted from six xenoliths, mounted in epoxy resin and polished for chemical analysis with laser ablation inductively coupled plasma mass spectrometry (LA-ICPMS).

Major and minor element compositions for minerals in Voyageur peridotite xenoliths were determined with the JEOL JXA 8900 electron microprobe located in the Department of Earth and Atmospheric Sciences at the University of Alberta using standard techniques. Mineral grains were analyzed at an accelerating voltage of 20kV and a 15-20nA beam current, with peak-counting times of 20s for Mg, Al, Si, Ca and K in all phases present.

At the same operating conditions Ni in olivine and chromite was counted for 15s, Na in pyroxenes, olivine and spinel for 10s and Fe in garnet for 30s. Ti, Cr and Mn were counted for 20s with 20kV accelerating voltage and 20nA beam current for all phases present. Instrument calibration was performed generally on natural standards with an attempt to closely match the matrix of mineral samples: kaersutite (CaO; Al2O3; Na2O; K2O; SiO2), Fo93 (SiO2; MgO), fayalite (FeO), rutile, ilmenite (TiO2), willemite (MnO), chromite (Cr2O3; Al2O3, FeO, MgO), orthoclase (K2O), rvgar1 (CaO), pyrope (Al2O3) and diopside (SiO2). Pure Ni-metal was used to calibrate Ni in all phases analysed. Minimum detection limits (3σ over background) were calculated as follows: SiO2 (0·04wt%), Na2O (0·03wt%), MgO (0·03wt%); Al2O3 (0.03wt%), NiO (0·05wt%); CaO (0·02wt%); TiO2 (0·05wt%); Cr2O3 (0·02wt%); MnO (0·02wt%); FeO (0·02wt%).

In order to evaluate any intra-grain and/or inter-grain homogeneity (important for geothermobarometry), at least two to three grains of each phase per xenolith were analyzed at three points in the core and three more points near the rims.

Selected garnet and clinopyroxene grains were analyzed for trace and ultra-trace elements by laser-ablation ICP-MS using a Merchantek Minilaze II UV laser ablation microprobe coupled with an ultra-high sensitivity VG PQIIS and ICP mass spectrometer software in the School of Earth and Ocean Sciences at the University of Victoria (Victoria, British Columbia, Canada). Norman et al. (1996, 1998) and Chen (1999) have given detailed descriptions of LA-ICPMS instrumentation and methods. Acurracy (better than 10% for all elements except

Ti and Sc for which it is 10% and 20%, respectively) and precision (5% or better for all elements) for this instrument have been tested on BCR-2 glass standard. Also, comparisons of trace elements compositions determined on mantle garnets at University of Victoria using different methods (laser ablation, secondary mass ion spectrometry, proton microprobe) were within 20% for Zr, Ti, Y and REE and better than 10% for Ni (Carbno & Canil, 2002). A comparison made over a period of 13 months at the University of Victoria of garnet PN2 previously analysed with INAA (instrumental neutron activation) and SIMS revealed that the LA-ICPMS results are generally elevated for La but within 20% (relative) of the results obtained by the other methods for most elements except Sc, Ti and Yb (Canil et al., 2003).

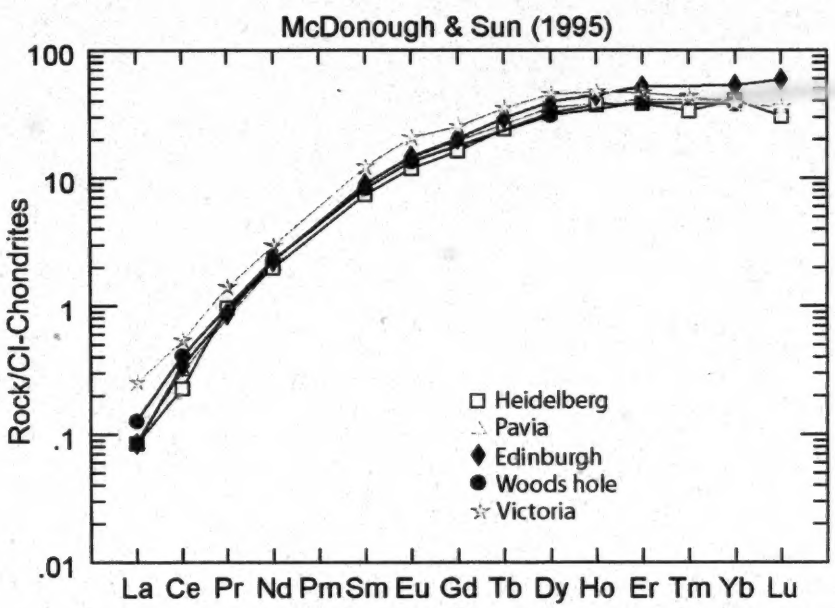

Fig. 3.1.1 Comparison of LA-ICPMS measurements on mantle garnet PN2 obtained at University of Victoria with SIMS measurements on the same garnet obtained at University of Edinburgh (Stachel), University of Heidelberg (Tappert), University of Pavia (Ottoloni) and Woods Hole Oceanographic Institution (Banas) laboratories.

A comparison of the results obtained from measurements of PN2 garnet with LA-ICPMS at the University of Victoria and SIMS (secondary mass ion spectrometry) in four different laboratories are presented in Fig. 3.1.1. Except for the slightly higher La concentrations, La-ICP-MS trace element contents match well the SIMS results obtained at Edinburgh, Heidelberg, Pavia and Woods Hole.

3.2. PETROGRAPHY

Based on modal mineralogy, three lithologies have been recognized in the peridotite xenolith suite from Voyageur: lherzolites (ol+opx+cpx±grt±sp), harzburgites (ol+opx±grt±sp) and wehrlites (ol+cpx±grt). They developed in spinel, spinel-garnet and/or garnet facies and have a variety of textures ranging from coarse to porphyroclastic and granuloblastic types (Table 3.2.1).

The majority of the **lherzolitic xenoliths** are coarse grained but porphyroclastic and granuloblastic varieties are also present (Fig. 3.2.2; 3.2.3). Olivine shape and size ranges from small, polygonal grains (1-2mm) in spinel lherzolites to large (up to 6mm), subanhedral to anhedral grains in spinel-free samples. Small (<1mm) neoblasts are mantling the larger porphyroclasts in deformed xenoliths. Strain-induced undulatory extinction is characteristic for olivine in the spinel and spinel-garnet facies, along with kink bands and, sometimes, a strong preferred orientation of the grains long axes.

Table 3.2.1. Petrographic summary of peridotite xenoliths from the Voyageur kimberlite pipe

Sample	Lithology	Parageneses	Texture
VYG343	garnet lherzolite	ol+opx+cpx+grt	coarse
VYG359	garnet lherzolite	ol+opx+cpx+grt	coarse
VYG372	garnet lherzolite	ol+opx+cpx+grt	coarse
VYG373	garnet lherzolite	ol+opx+cpx+grt	coarse
VYG347	garnet lherzolite	ol+opx+cpx+grt	transitional
VYG382	garnet lherzolite	ol+opx+cpx+grt	porphyroclastic
VYG355	spinel lherzolite	ol+opx+cpx+sp	coarse
VYG369	spinel lherzolite	ol+opx+(cpx)+sp	coarse
VYG371	spinel lherzolite	ol+opx+cpx+sp	coarse
VYG411	spinel lherzolite	ol+opx+cpx+sp	coarse
VYG356	spinel lherzolite	ol+opx+cpx+sp	granuloblastic
VYG375	spinel harzburgite	ol+opx+sp	coarse
VYG403	garnet harzburgite	ol+opx+grt	coarse
VYG368	sp-grt lherzolite	ol+opx+cpx+grt+sp	coarse
VYG402	sp-grt lherzolite	ol+opx+cpx+grt+sp	coarse
VYG345	wehrlite	ol+cpx	porphyroclastic
VYG354	wehrlite	ol+cpx	porphyroclastic
VYG358	wehrlite	ol+cpx	porphyroclastic laminated
VYG363	garnet wehrlite	ol+cpx+grt	porphyroclastic
VYG398	garnet wehrlite	ol+cpx+grt	porphyroclastic
VYG351	heterogeneous (grt harzburgite +sp harzburgite)	ol+opx+grt+sp	coarse
VYG394	heterogeneous (grt lherzolite + sp lherzolite)	ol+opx+cpx+grt+sp	coarse

In comparison with olivine, orthopyroxene has a markedly smaller size (~2mm on average). In thin sections it may occur in small clusters of colourless, anhedral to subhedral grains and accounts for less than 20-25% of the bulk rock in the spinel-free facies. Occasionally, orthopyroxenes show exsolution lamellae. Like olivine, orthopyroxene has a strong preferred orientation in the granuloblastic (sheared) spinel lherzolite VYG356. Larger orthopyroxene may poikilitically include olivine, clinopyroxene or garnet. Sometimes clouded rims are noticed, indicating minor alteration along the grain boundaries.

Clinopyroxene generally has an emerald-green colour and has a variety of shapes: tabular to elongated, rounded or, most commonly, irregular. Sometimes it is highly altered and represented by only a few grains per thin section. In the garnet facies, clinopyroxene is generally mantling olivine or garnet. In the spinel facies it appears either as large grains, emerald-green colored and/or as small, colorless grains between olivine and orthopyroxene.

Garnet has a pink color in thin section and appears as discrete, large (up to 7mm), rounded grains in spinel-free samples but is finer (2-3mm), subhedral and has a tendency to form clusters in the transitional facies. Commonly, garnet grains have kelyphitic rims.

Brown to dark-red spinel occurs as irregular, anhedral grains ranging in size from 0.1 to 2mm. In the spinel-garnet facies secondary spinel appears as rhombic, zoned crystals within the kelyphitic rims. In addition to the main phases noted above, phlogopite is present in the kelyphite rims or as interstitial grains.

Harzburgites (in the mineralogical sense, i.e. not based on garnet chemistry) were classified based on the apparent absence of clinopyroxene both in thin section and hand specimen. With the exception of VYG375 (spinel harzburgite), they contain garnets that plot within the lherzolitic field, suggesting equilibrium with clinopyroxene that may not be seen because of the small sample size. Apart from the absence of clinopyroxene, the appearance of these rocks in thin section is similar to that of coarse-grained lherzolites (Fig. 3.2.4).

All **wehrlites** are deformed, displaying features commonly associated with porphyroclastic peridotites: strained porphyroclasts (average size ≥2mm) in a finer grained matrix of recrystallized neoblasts (Fig. 3.2.5). Olivine occurs both as porphyroclasts with irregular outlines and equant or tabular neoblasts, emerald-green clinopyroxene commonly forms patchy zones in thin section and garnet displays its typical pink color, rounded shape and irregular grain boundaries. Large garnet grains can reach up to 7mm and may poikilitically include olivine. In the laminated sample VYG358, olivine and clinopyroxene form almost monomineralic bands, the grains being generally aligned with their long axes parallel to the strong foliation.

Two **heterogeneous peridotites** are present in the Voyageur xenolith suite (Fig. 3.2.6). VYG351 (modally harzburgitic with a pronounced foliation) and VYG394 (lherzolitic) have about 1/3 of the thin section developed in garnet facies and 2/3 developed in spinel facies. In both cases the textural appearance of the samples does not change across the spinel/garnet peridotite transition.

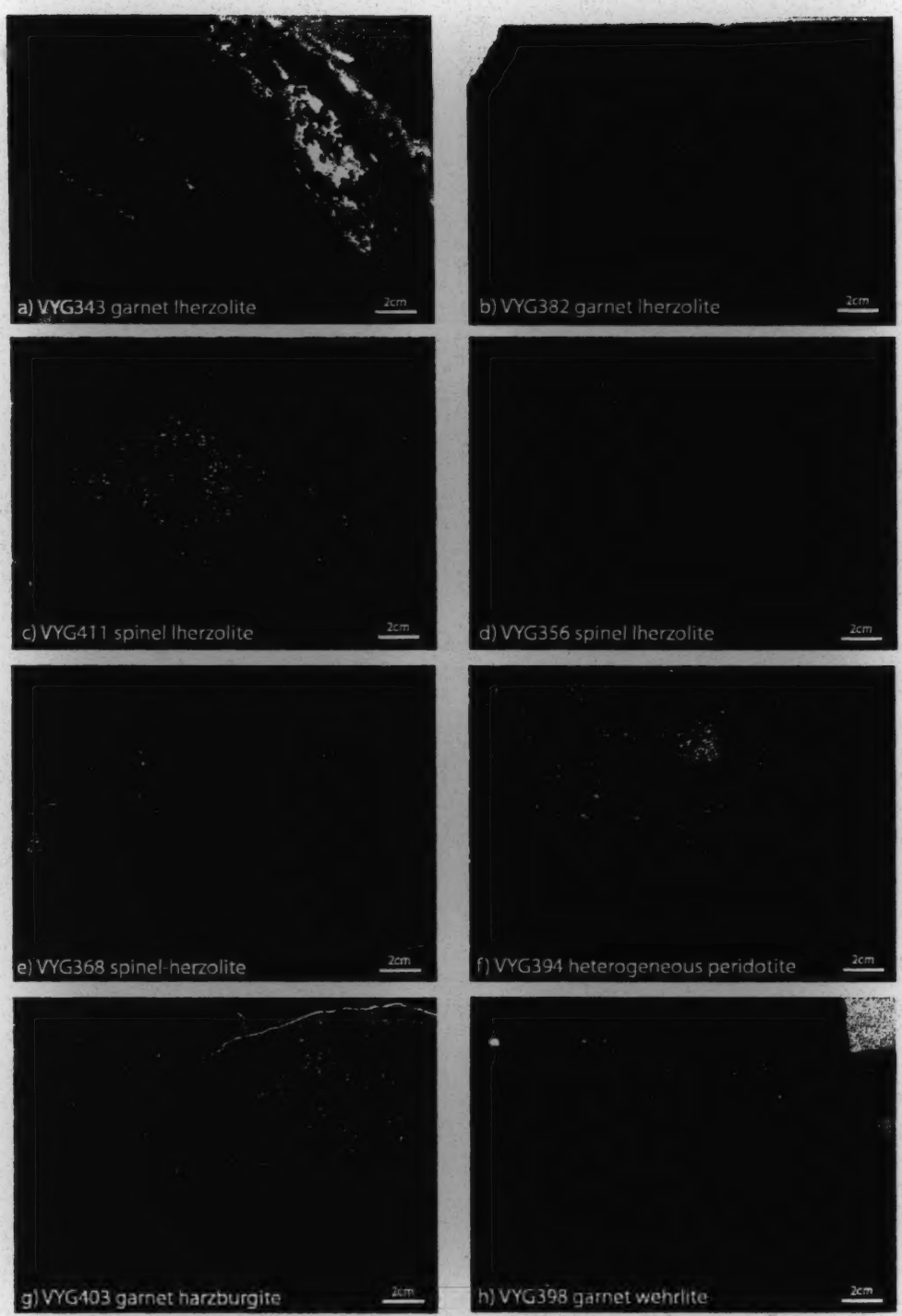

Fig. 3.2.1 Core samples from the Voyageur kimberlite pipe

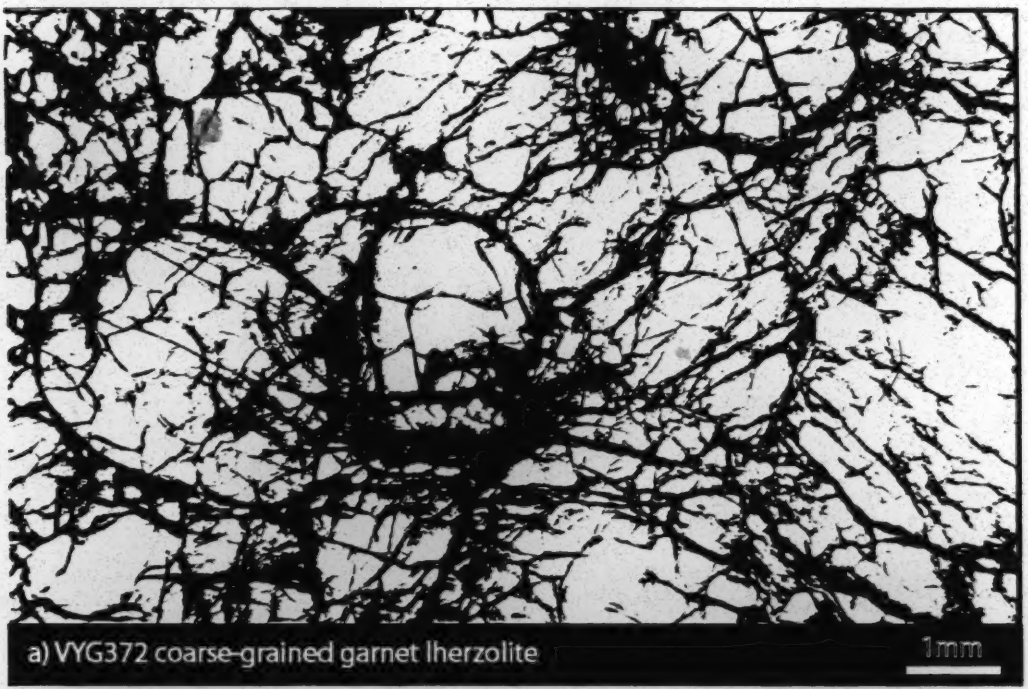

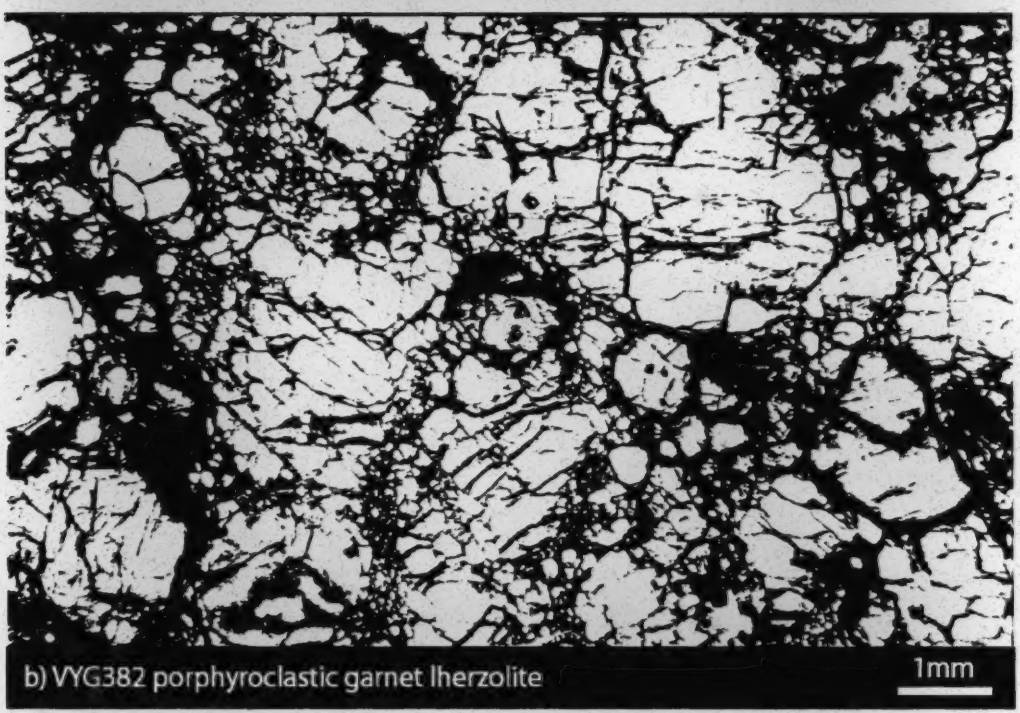

Fig. 3.2.2 Thin section images of garnet lherzolites from the Voyageur kimberlite pipe

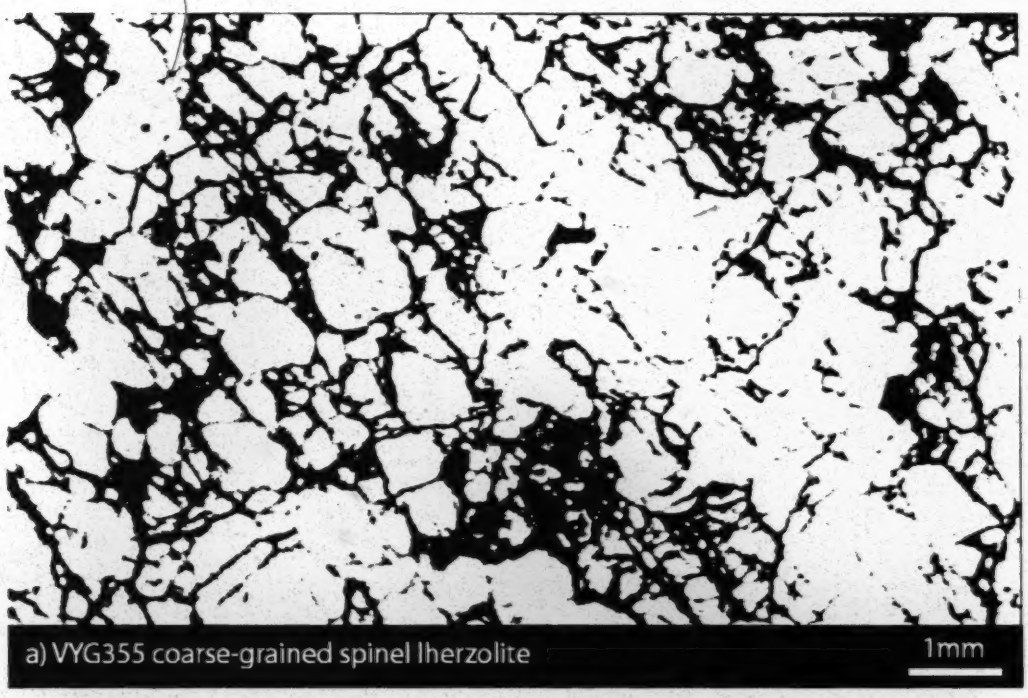

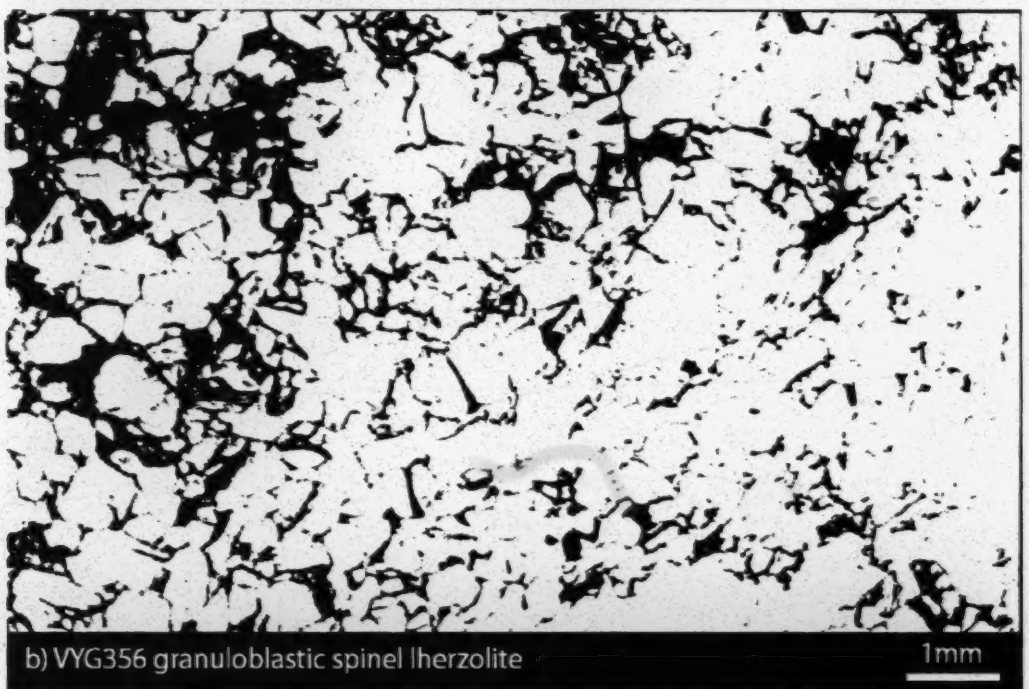

Fig. 3.2.3 Thin section images of spinel lherzolites from the Voyageur kimberlite pipe

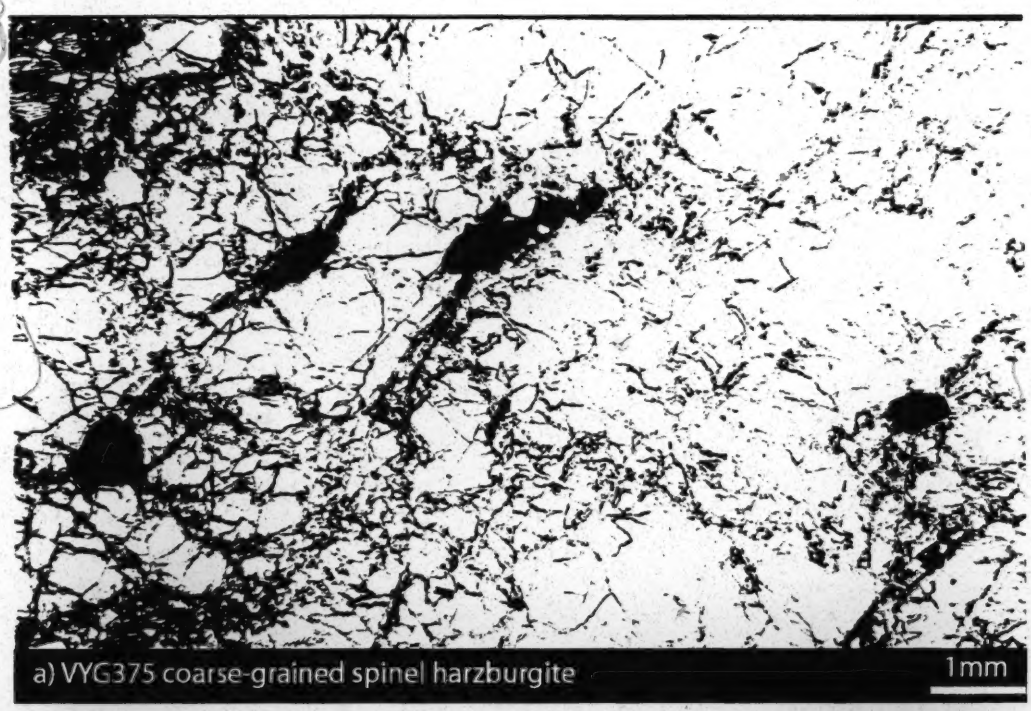

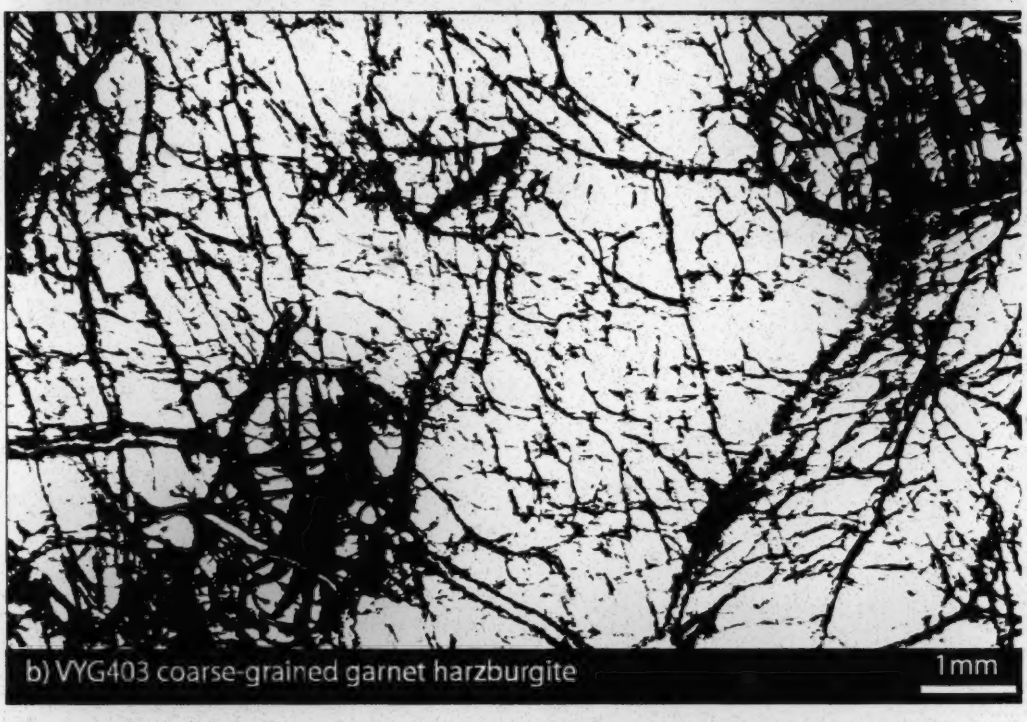

Fig. 3.2.4 Thin section images of harzburgites from the Voyageur kimberlite pipe

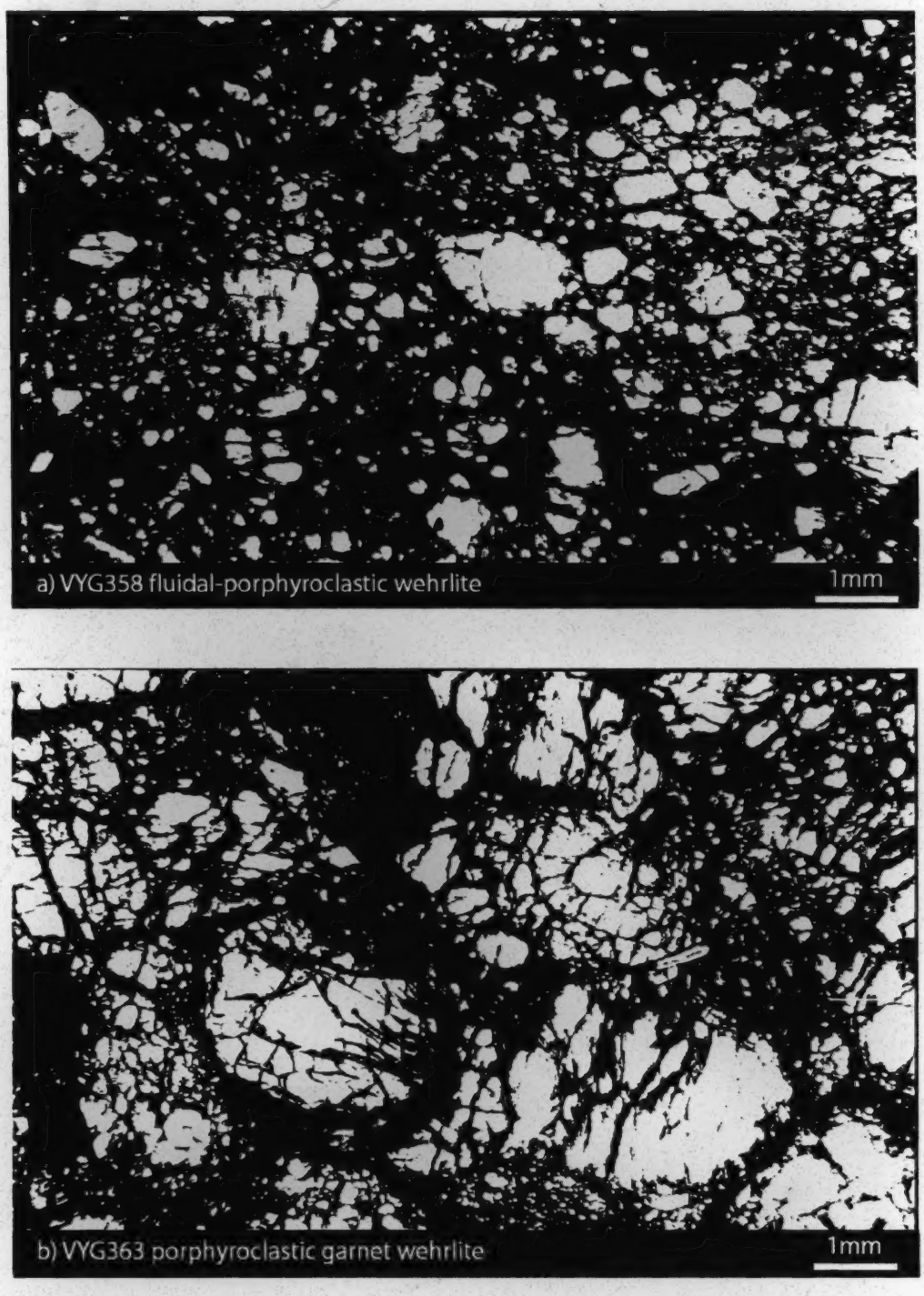

Fig. 3.2.5 Thin section images of wehrlites from the Voyageur kimberlite pipe

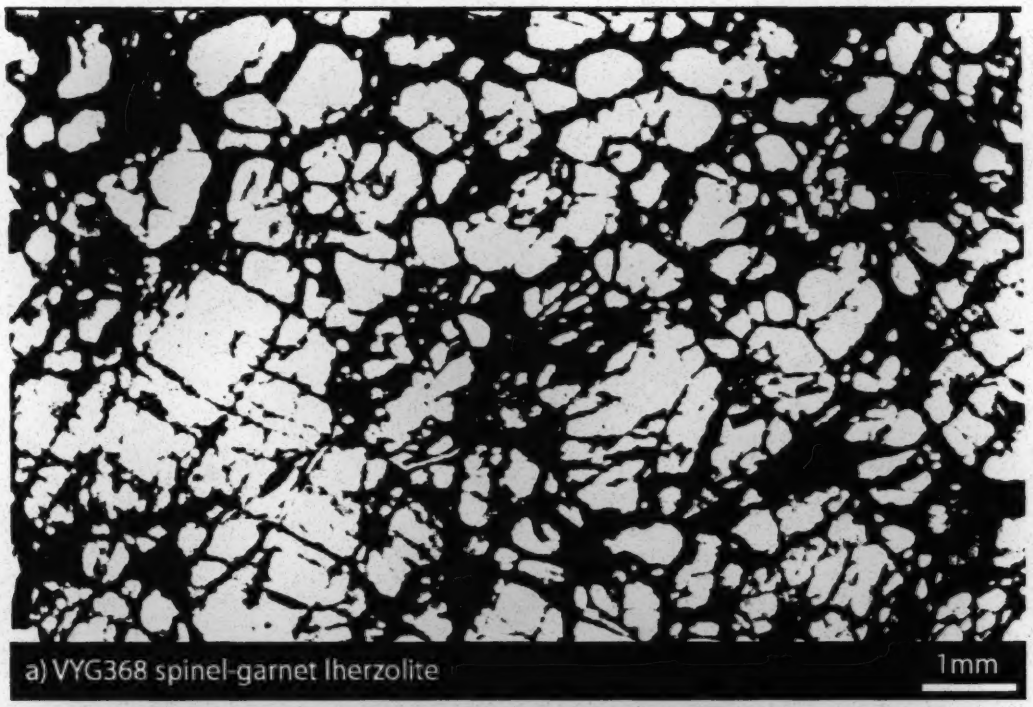

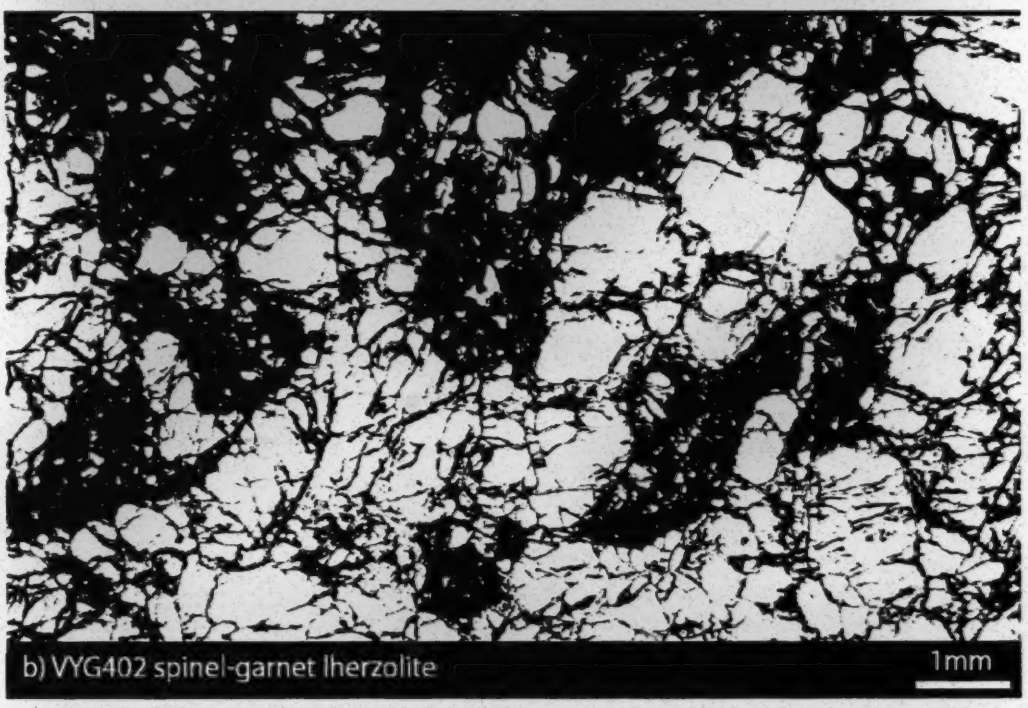

Fig. 3.2.6 Thin section images of spinel-garnet lherzolites from the Voyageur kimberlite pipe

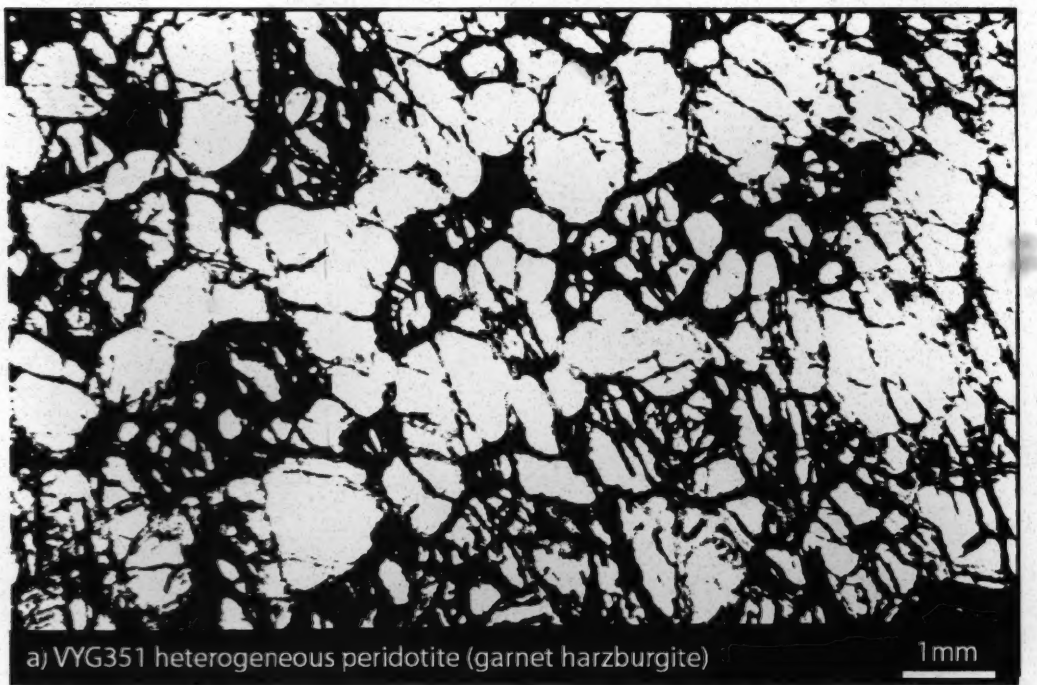

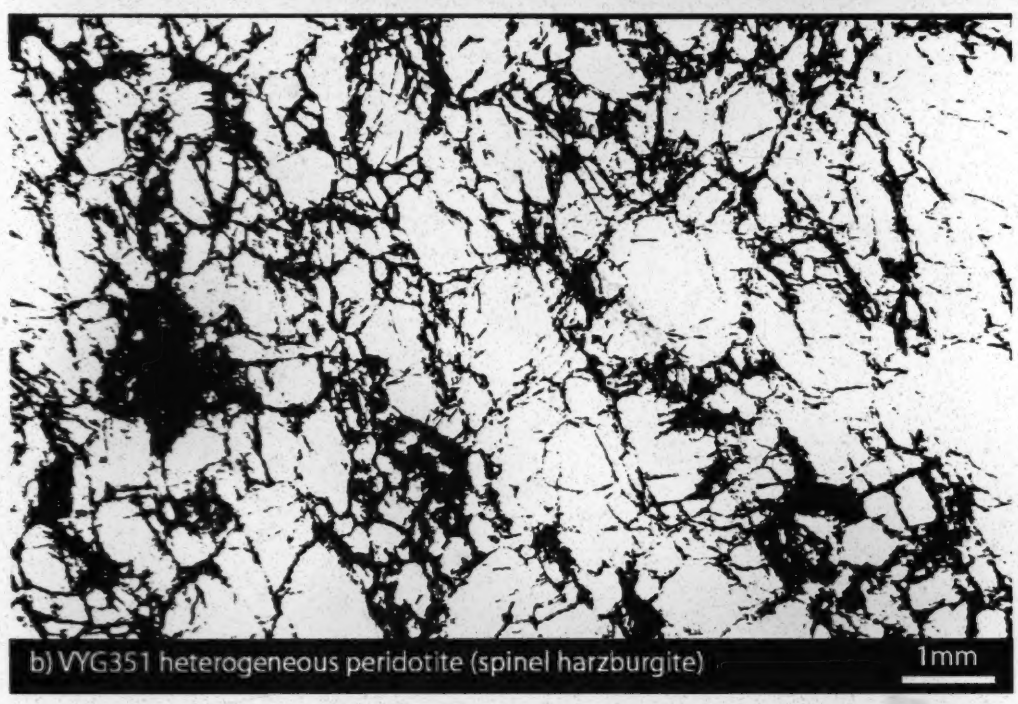

Fig. 3.2.7 Thin section images of heterogeneous samples from the Voyageur kimberlite pipe

3.3. MINERAL CHEMISTRY (MAJOR AND MINOR ELEMENTS)

Electron microprobe core analyses of minerals in Voyageur peridotite xenoliths are listed in Appendix I to V.

Olivine is forsteritic and shows a range in mg-number (molar Mg / Mg + Fe) for the whole peridotite xenolith suite of 0.879-0.933. The most magnesian olivines occur in spinel lherzolites (mg# = 0.927-0.933) (Fig.3.3.1a-b). There is a distinct compositional difference between porphyroclastic (mg# = 0.883-0.887) and coarse (mg# = 0.908-0.921) garnet lherzolites. Olivines from wehrlites (garnet-free and/or garnet facies) fall into the Mg-poor portion of the peridotite range (mg# = 0.879-0.898). The lowest Ni content in olivines was observed for garnet-free wehrlites (0.18-0.27wt% NiO) whereas spinel lherzolites show the highest concentrations (0.34-0.43wt% NiO). Similar to mg#, Ni concentration is lower in olivines from porphyroclastic garnet lherzolites (0.26-0.34wt% NiO) in comparison with those from coarse garnet lherzolites (0.32-0.42wt% NiO, respectively). Olivine included in other minerals is not compositionally distinct. Porphyroclasts are unzoned and identical in composition to neoblasts.

Orthopyroxene is classified as enstatite and has a range in mg-number from 0.900 to 0.937 (Fig. 3.3.1). Its composition varies between different xenoliths types, being more magnesian in spinel peridotites (mg#=0.931-0.937) than in garnet peridotites (mg#=0.900-0.931). Like in the case of olivine, there is a marked difference between the orthopyroxene from coarse garnet lherzolites and that from porphyroclastic garnet lherzolites (mg# = 0.922-0.932 vs. mg#= 0.900-0.905, respectively).

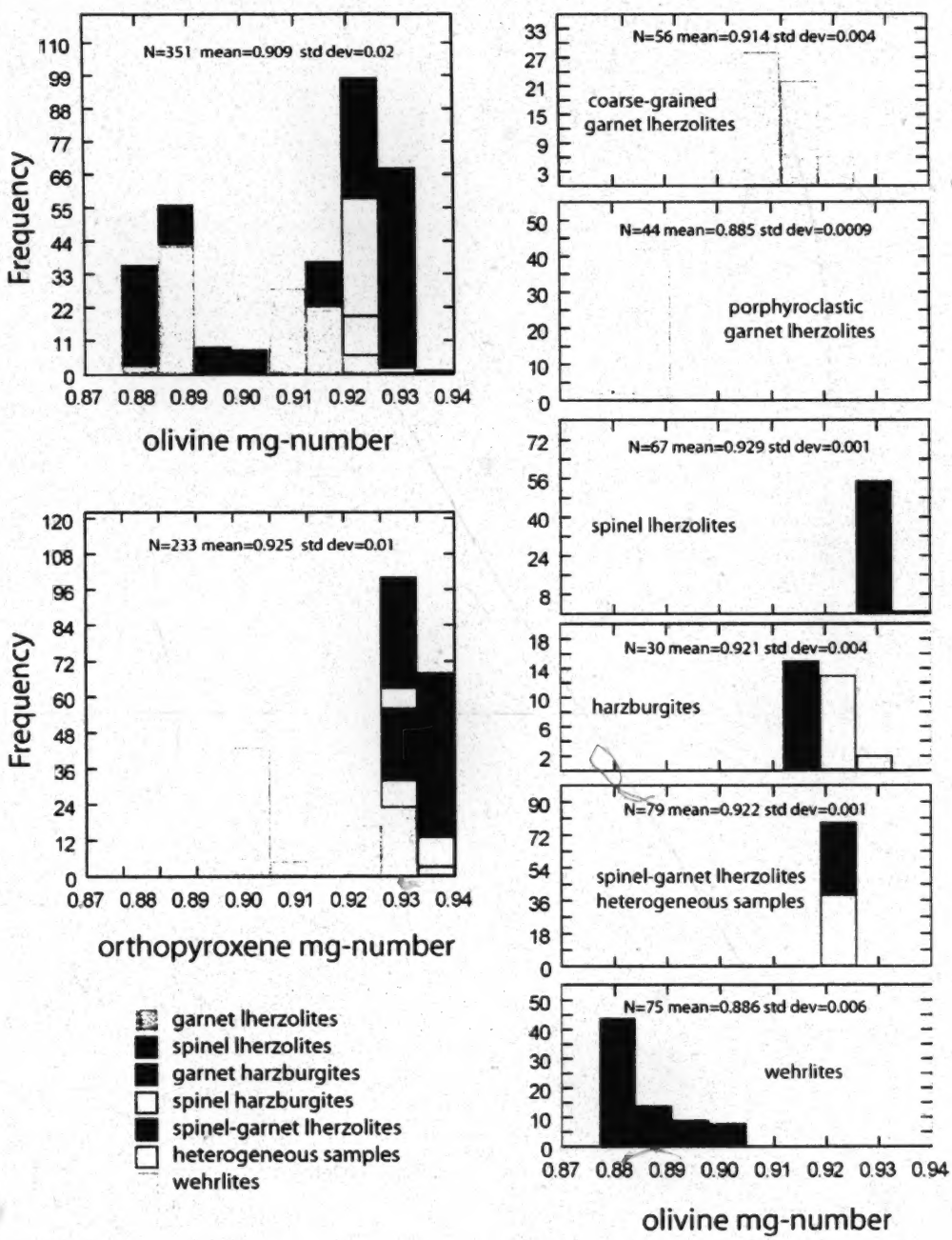

Fig. 3.3.1 Mg number of olivines and orthopyroxenes from the Voyageur peridotite xenoliths:

Left: Mg numbers of olivine and orthopyroxene

Right: Variation of olivine Mg number with texture and composition

The mg-number of orthopyroxenes is generally slightly higher than the mg-number of olivine, suggesting that the parageneses are equilibrated (Gurney et al., 1979). The exception is VYG356 (granuloblastic sample), where the orthopyroxenes and olivines have similar mg-numbers. Gregoire et al. (2005) assumed a metasomatic origin for samples showing this characteristic.

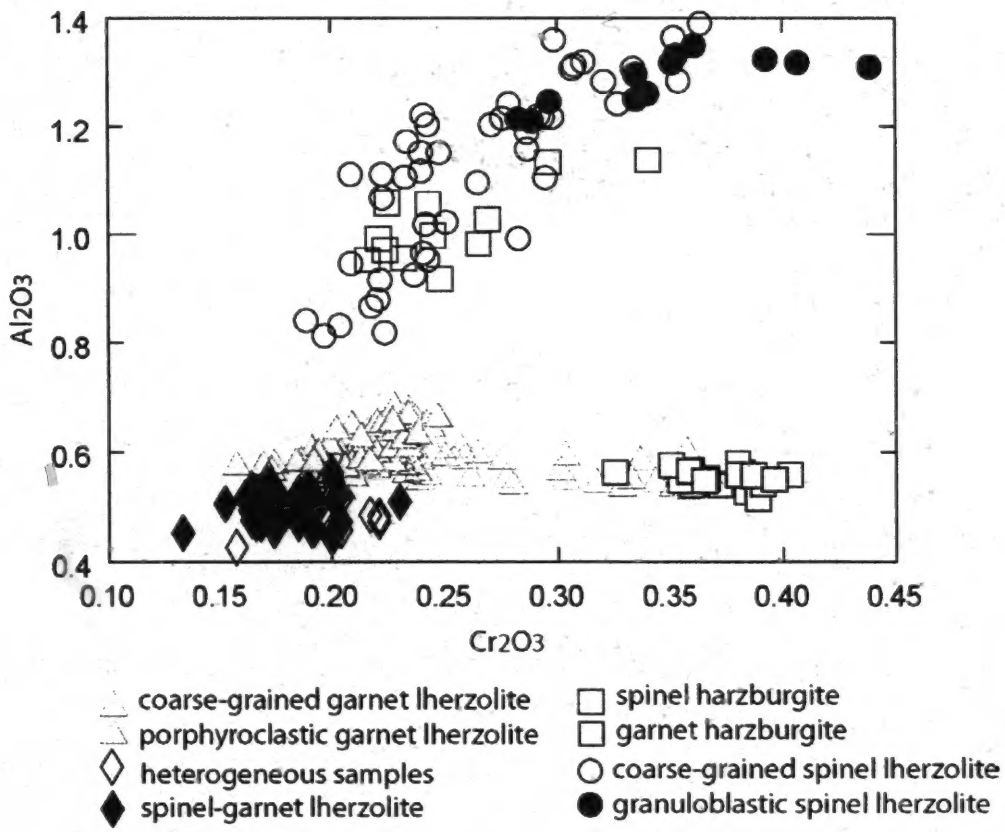

Fig. 3.3.2 Composition of orthopyroxenes from the Voyageur peridotite xenoliths

Orthopyroxenes in garnet harzburgites have the highest chromium content (0.32-0.40wt% Cr_2O_3) and, generally, coarse-grained garnet lherzolites are more chromium-rich than porphyroclastic garnet lherzolites (Fig.3.3.2) (0.14-0.38wt%

vs. 0.18-0.25wt% Cr_2O_3, respectively). Enstatites from spinel peridotites (lherzolites and harzburgite) are markedly more aluminous than the ones in garnet peridotites (0.81-1.35wt% vs. 0.14-0.40wt% Al_2O_3, respectively) and show a positive correlation between Al_2O_3 and Cr_2O_3.

Clinopyroxenes present in garnet lherzolites are mainly augitic ($Wo_{40-46}En_{48-54}Fs_{4-5}$) whereas the ones in spinel lherzolites are mainly diopsidic ($Wo_{48-50}En_{47-49}Fs_{1.9-2.2}$). All clinopyroxenes have significant Cr_2O_3 contents (0.36-2.46wt%) and, as such, they are generally termed chrome-diopsides (Fig. 3.3.3). Their Mg-numbers range from 0.897 to 0.962 and many of them have Na_2O contents higher than 1.5wt%, a limit established as being characteristic for clinopyroxenes of likely metasomatic origin (Van Achternberg et al., 2001; Gregoire et al., 2003). There is a marked compositional difference between clinopyroxenes in granuloblastic spinel lherzolite, which are poorer in Cr_2O_3 (0.55-0.75wt%), Al_2O_3 (1.07-1.25wt%) and Na_2O (0.32-0.48wt%) and clinopyroxenes in coarse-grained spinel lherzolites (1.04-1.67wt% Cr_2O_3, 2.09-2.85wt% Al_2O_3 and 1.23-1.73wt% Na_2O). Also, a third type of chrome-diopside can be observed in VYG411 (coarse-grained spinel lherzolite). In comparison with the large grains with an emerald-green color that generally appear in spinel lherzolites, this type of clinopyroxene is colorless and much finer, present in the interstices of olivine and orthopyroxene. Compositionally it is less aluminous (0.69-0.72wt% Al_2O_3), chromiferous (0.36-0.44wt% Cr_2O_3), sodium rich (0.81-0.88wt%Na_2O) and markedly more titaniferous (0.90-0.93wt% TiO_2) than the clinopyroxene generally present in the coarse-grained spinel lherzolites.

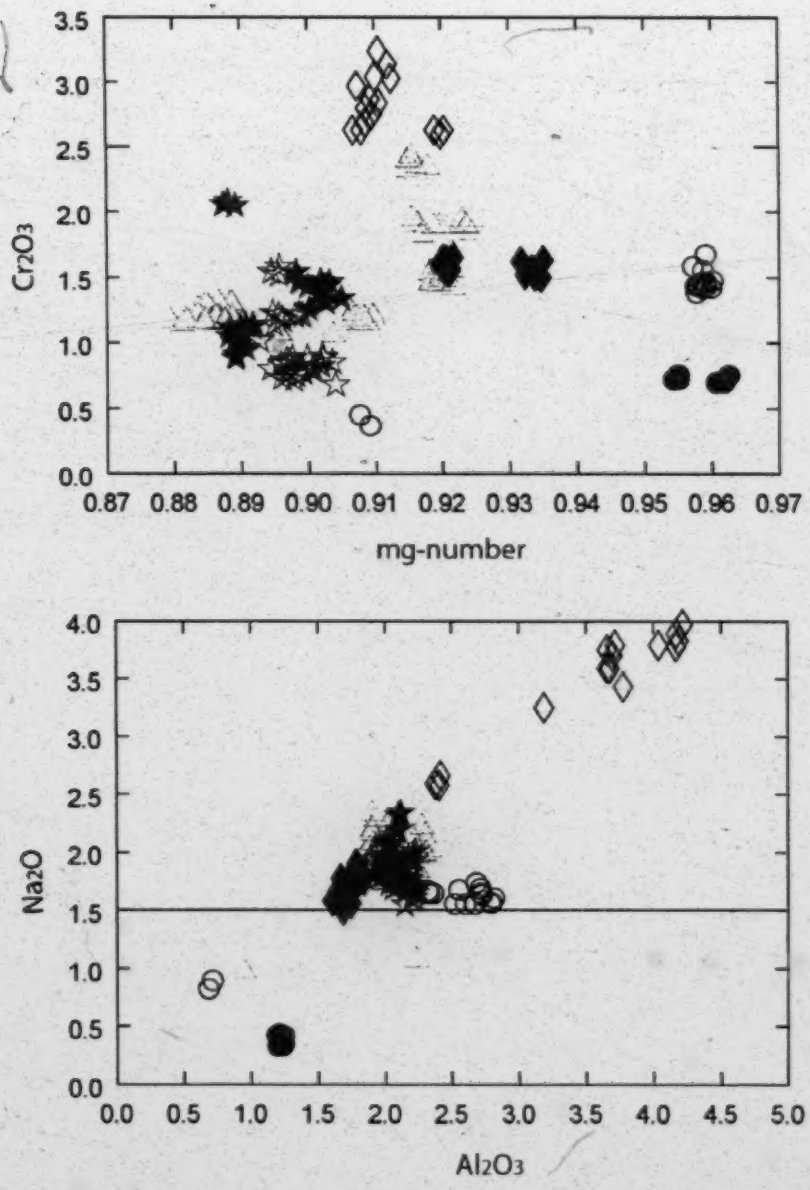

Fig. 3.3.3 Composition of clinopyroxenes from the Voyageur peridotite xenoliths

The heterogeneous sample VYG394 is characterized by the unusual presence of Cr-rich omphacitic clinopyroxene (3.25-4.20wt%Na_2O; 3.19-4.40wt%Al_2O_3; 17.07-19.02wt%CaO; 13.09-14.05wt%MgO; 2.51-3.84wt%Cr_2O_3) in addition to a Na- enriched chrome-diopside.

Core-rim variations within clinopyroxene grains are generally small and irregular.

Garnets from the Voyageur peridotite xenoliths are classified as pyropes. All of them plot within the G9 (lherzolitic) field in Cr_2O_3 -CaO diagram reflecting the likely presence of trace clinopyroxene even in the modally harzburgite samples (Fig. 3.3.4). Two trends that show a positive correlation between Cr_2O_3 and CaO can be distinguished on the CaO-Cr_2O_3 diagram. The "normal" lherzolitic trend, common in kimberlites (Sobolev et al., 1973), extends to Cr_2O_3 contents of up to 8.5wt% whereas the second, parallel trend develops at higher CaO for a given Cr_2O_3 content. This last mentioned trend is rarely observed in garnet xenocrysts and kimberlite-hosted xenoliths and is referred to as the "chromite-clinopyroxene-garnet equilibrium" (CCGE) trend (Kopylova et al., 1999; Kopylova et al., 2000).

The garnet compositions defining the CCGE trend at Voyageur derive from the spinel-garnet lherzolites and from the modally cpx-free heterogeneous sample VYG351. Garnets from VYG394 (which is a cpx-bearing heterogeneous sample) plot on the lherzolitic trend.

In the CaO-Cr_2O_3 diagram (Fig. 3.3.4a), the "harzburgitic" (modally cpx-free samples) garnets plot close to the G9/G10 boundary and show the most Cr-enriched compositions (7.53-8.63wt% Cr_2O_3).

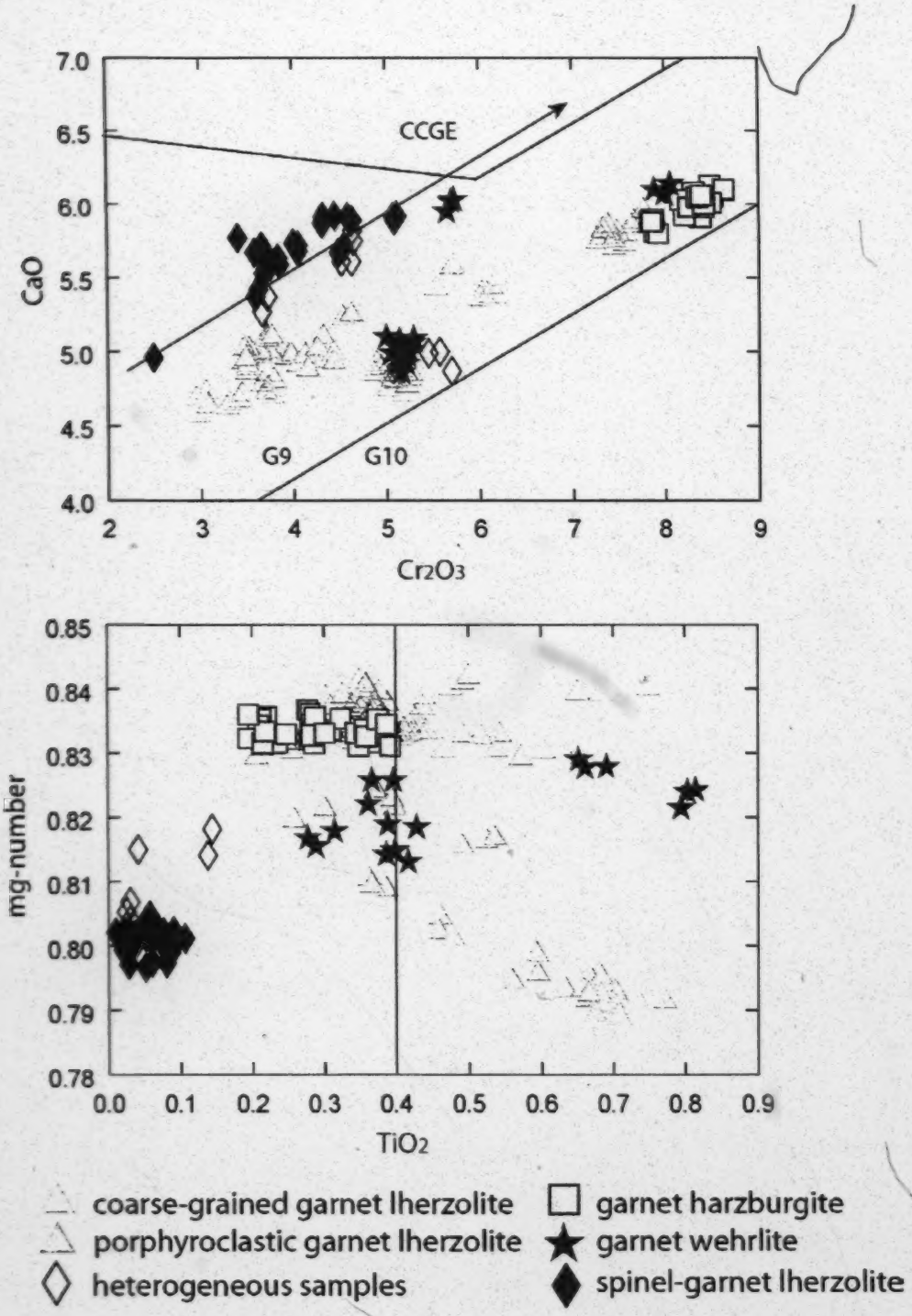

Fig. 3.3.4 Composition of garnets from the Voyageur peridotite xenoliths.

CCGE trend after Kopylova et al., 1999

As for orthopyroxenes, pyropes from coarse lherzolites have generally higher Cr_2O_3 contents (4.48-7.77wt %) than the ones in porphyroclastic lherzolites (3.45-4.43wt%).

The range in mg-numbers of the garnets from Voyageur peridotite xenoliths is relatively limited (0.788 to 0.841). In contrast, there is a wide range of TiO_2 concentration (0.01-0.81wt%): the majority of lherzolites and wehrlites exceed 0.4wt% TiO_2, with concentrations above this value pointing to possible metasomatic activity in the mantle (Fig. 3.3.4b; Menzies et al., 2004).

Garnets from VYG347 (lherzolite with a transitional texture) display a crude negative correlation between TiO_2 content and Mg-number (Fig. 3.3.4b).

Small variations in major element compositions can be observed among and within grains from the same sample. Generally, the rims are more Ti-, Al- and Ca-enriched and Cr-poor in comparison with the cores.

Mg-chromite in lherzolites and harzburgite has the following composition: 43.9-50.8wt% Cr_2O_3; 12.0-15.1wt% MgO; 12.8-17.6wt% FeO; <0.13wt% TiO_2. Mg-chromite is also present in spinel-garnet lherzolites (49.2-54.2wt% Cr_2O_3; 11.0-11.8wt% MgO; 0.50-3.2wt% TiO_2) and the heterogeneous samples (52.3-53.4wt% Cr_2O_3; 11.8-12.2wt% MgO; 0.2-0.3wt% TiO_2).

All spinels show low levels of SiO_2 (<0.1wt%) and MnO (<0.2wt%). A marked difference can be noticed in the Fe^{3+} contents of spinel-garnet lherzolites and heterogeneous samples (24.8-27.5 vs 30.6-37.9). Spinel in the keliphytic rims is zoned, extending from core to rim to lower Cr_2O_3 and higher MgO contents (Fig. 3.3.5).

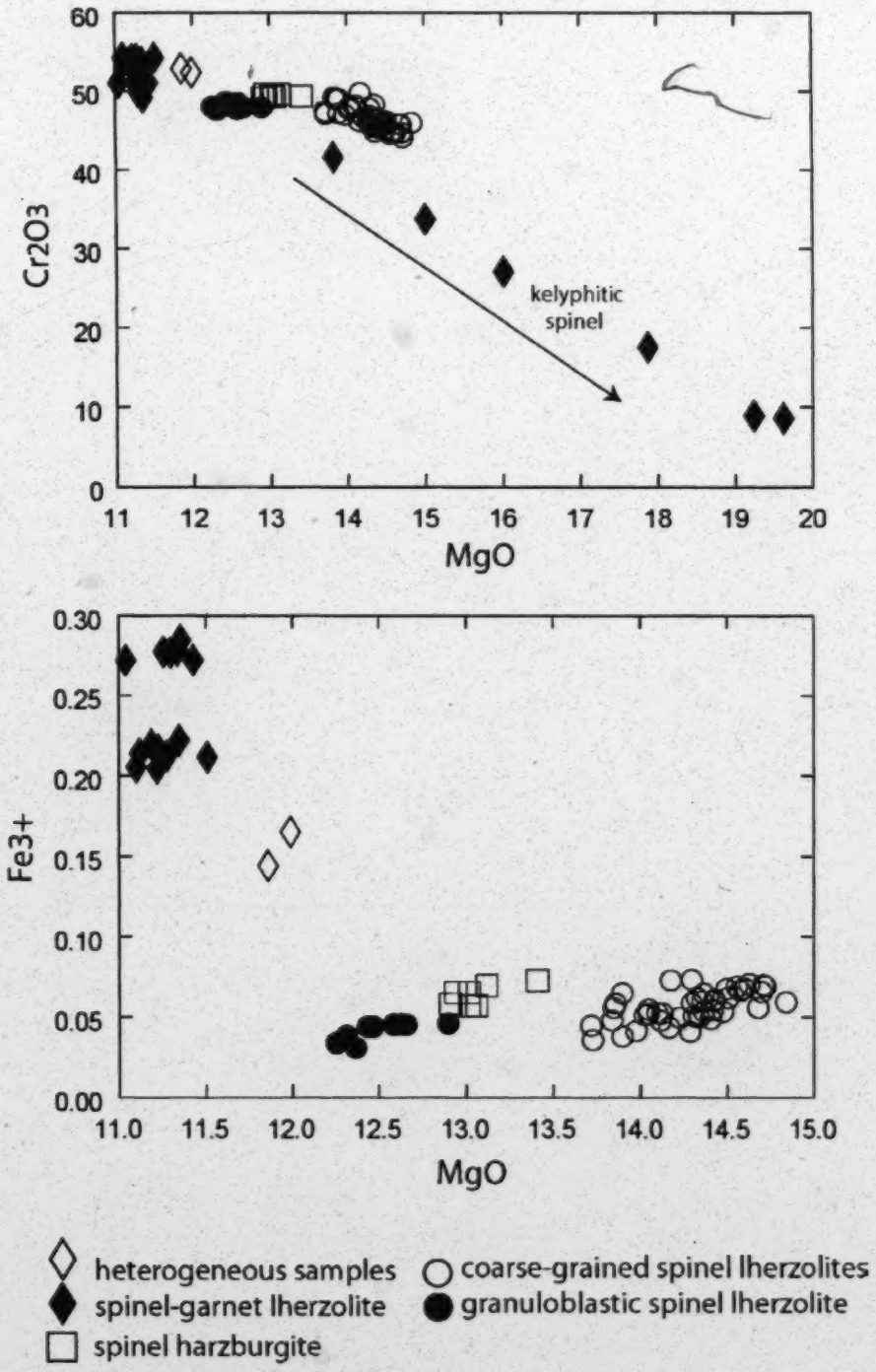

Fig. 3.3.5 Composition of spinels from the Voyageur peridotite xenoliths

Fe3+ calculated from Fe^{total} using stoichiometry

3.4. TRACE ELEMENTS GEOCHEMISTRY

Laser-ablation ICPMS analyses of garnet and clinopyroxene grains from Voyageur lherzolite xenoliths are listed in Appendix VI to VII.

Garnets from porphyroclastic lherzolites have higher overall trace elements abundances relative to garnets from coarse-grained lherzolites (Fig. 3.4.1).

When normalized to C1 chondrite, garnets from Voyageur lherzolite xenoliths have generally "normal" REE_N patterns ("N" stands for chondrite normalized), typical for lherzolitic garnets observed elsewhere (Shimizu, 1975; Stachel et al., 1998; 2004). $LREE_N$ concentrations increase steeply from La_N to Sm_N and become almost flat at $HREE_N$ concentrations of about 10 to 20 times chondritic abundances (Fig. 3.4.1a). VYG372 (coarse-grained lherzolite) makes an exception from the $HREE_N$-enrichment described above. Garnets from this sample show a moderately sinusoidal REE_N pattern with a maximum at Sm-Eu at about 10 times chondritic abundances and a decline towards Tm_N. The higher degree of sinuosity (Nd_N/Y_N >1) is also reflected in higher La_N/Yb_N ratios (0.02-0.04) relative to garnets from the other garnet lherzolite samples (<0.01).

Chondrite-normalized concentrations for trace elements other than REE generally increase in a similar fashion with increasing distribution coefficient showing enrichment in $HFSE_N$ (high field strength elements) for all garnets (Fig. 3.4.1b).

The porphyroclastic lherzolites host garnets enriched in Sr (1.0-3.5ppm) in comparison with the ones from coarse-grained lherzolites (<0.9ppm).

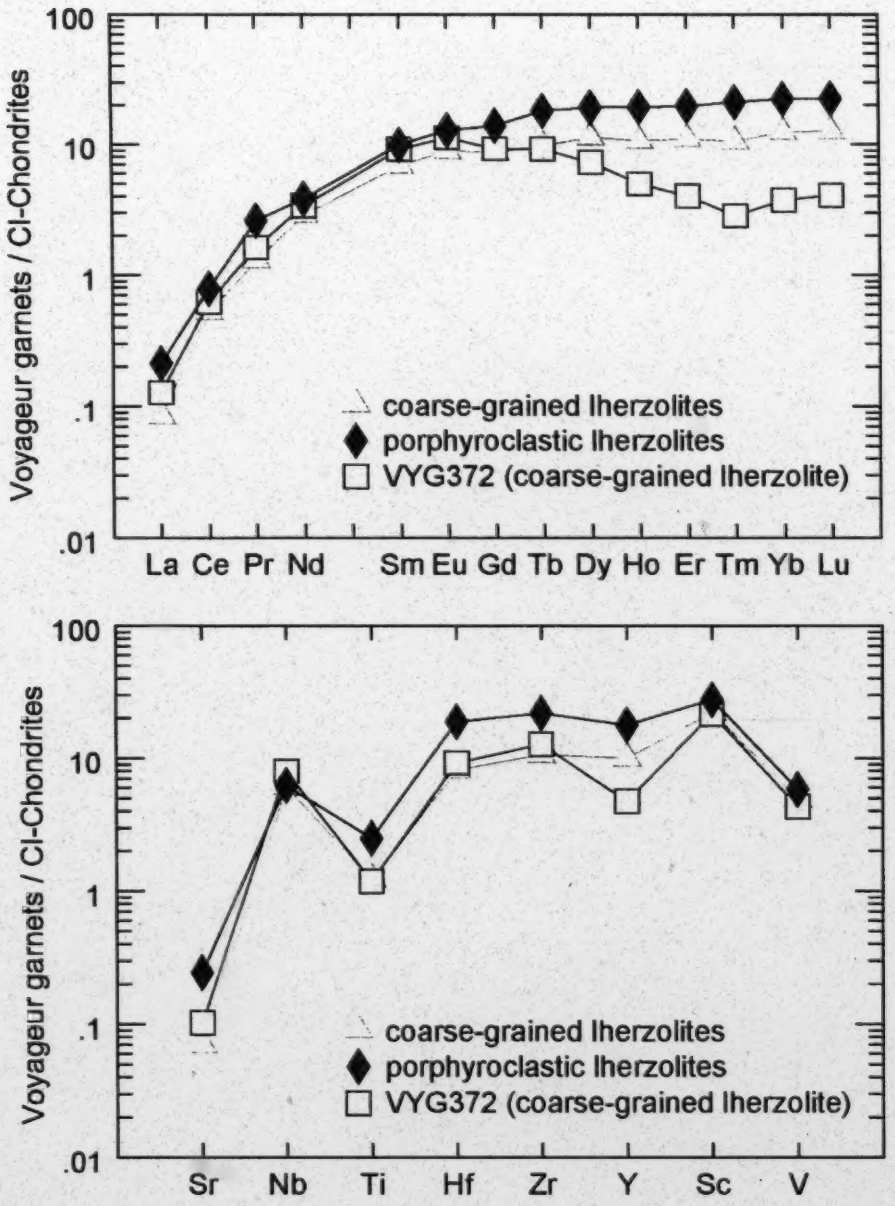

Fig. 3.4.1 Averaged trace elements abundances in lherzolitic garnets from Voyageur peridotite xenoliths normalized to the C1-chondrite composition of McDonough & Sun (1995) a) REE b) non-REE; element order of non-REE corresponds to increasing distribution coefficient between garnet and silicate liquid (Green, 1994).

VYG382 also has contrasting concentrations of Y (39-42ppm vs. 4-19ppm), Ti (>1300ppm vs. 382-820ppm), Zr (101-108ppm vs. 30-62ppm) and Hf (2.4-2.6ppm vs. 0.6-1.2ppm) relative to all other samples.

Clinopyroxenes from Voyageur lherzolites yielded similar convex-upward chondrite-normalized REE patterns disregarding the textural type of their host rocks (Fig. 3.4.2). They are consistently enriched in $LREE_N$ (with La and Ce concentrations over 10 times chondritic abundances) and depleted in $HREE_N$ (Er to Lu). $MREE_N$ (Sm to Ho) form a negative steep slope in the REE_N patterns. As opposed to garnets, clinopyroxenes from VYG372 have similar trace elements abundances to the ones from other coarse-grained lherzolites.

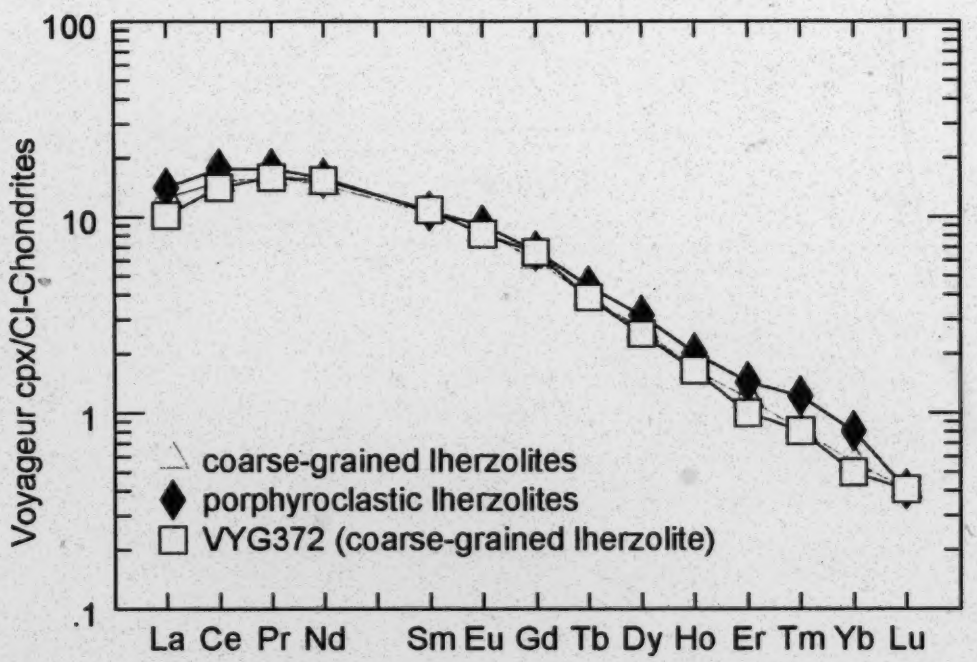

Fig. 3.4.2 Averaged REE abundances in lherzolitic clinopyroxenes from Voyageur peridotite xenoliths normalized to the C1 chondrite (McDonough & Sun, 1996)

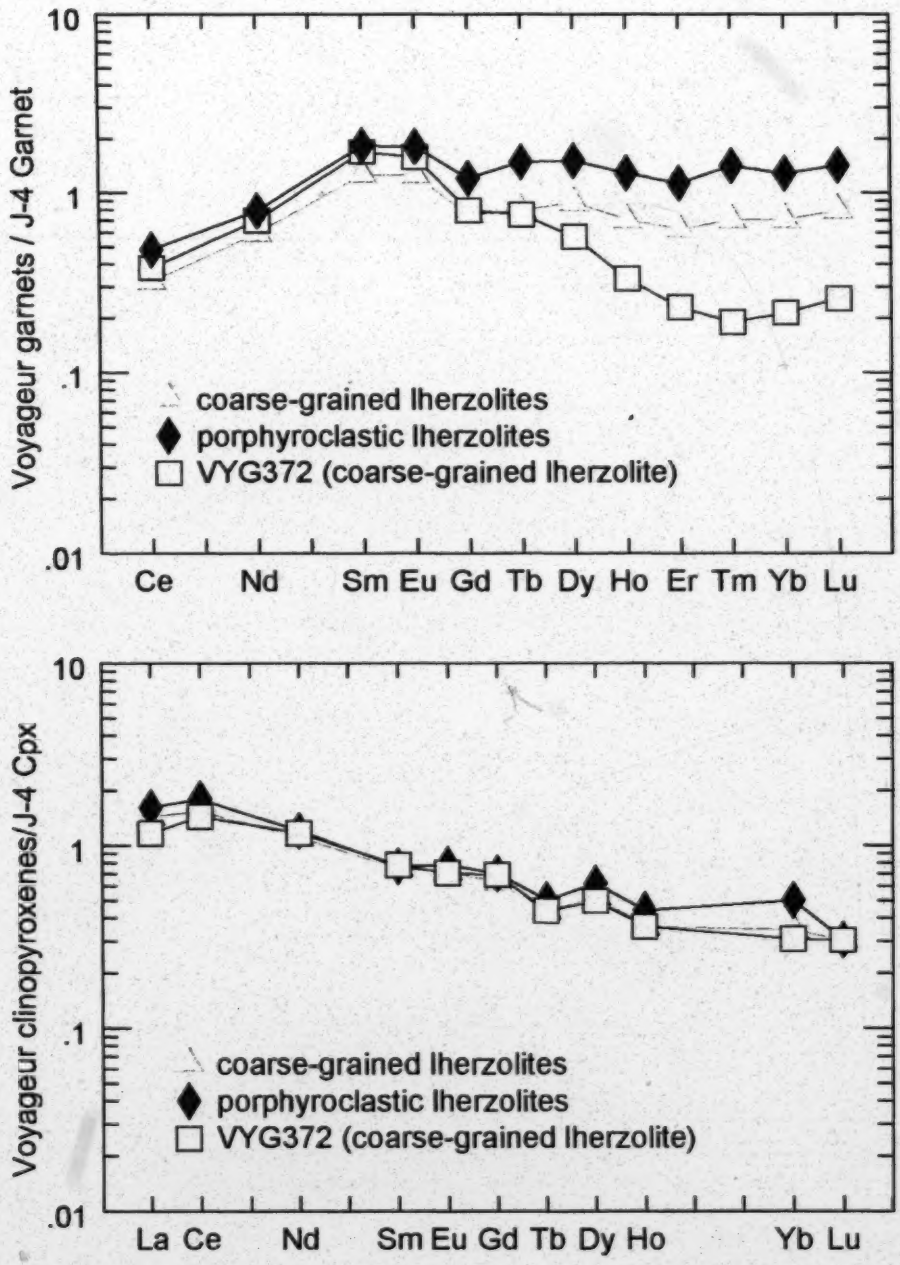

Fig. 3.4.3 Averaged REE abundances in lherzolitic garnets (a) and clinopyroxenes (b) from Voyageur peridotite xenoliths normalized to the composition of a primitive lherzolitic garnet/clinopyroxene (J4 of Jagoutz & Spettel).

The Sr, Ti and Zr concentrations (<200ppm, 250-290ppm and 9-13ppm, respectively) together with the features described above are characteristic of clinoproxenes from peridotite xenoliths in kimberlites.

When plotted against a primitive composition (J4 of Jagoutz & Spettel, unpublished; Fig. 3.4.3a) the REE patterns of lherzolitic garnets from Voyageur appear slightly depleted in $LREE_N$, with a slightly positive slope from Ce= 0.3-0.5 peaking at Sm-Eu and followed by a fairly horizontal pattern with $MREE_N$-$HREE_N$ approaching primitive abundances. VYG372 garnets deviate from this trend at Sm-Eu, showing depletion relative to J4, with a trough in $HREE_N$.

Normalization to primitive J4 clinopyroxene shows REE patterns approaching primitive abundances for all clinopyroxenes analyzed (Fig. 3.4.3b).

Constraints from the REE patterns

Voyageur lherzolitic garnets show both normal and moderately sinusoidal REE_N patterns, typical for garnets in mantle xenoliths worldwide (Shimizu, 1975; Stachel et al., 2004). When normalized to J4, both garnets and clinopyroxenes show virtually primitive or slightly enriched trace elements concentrations despite their overall depleted major element characteristics. This suggests an interaction of their mantle source rocks with metasomatic fluids and, as a consequence, a re-enrichment of the subcratonic lithosphere sampled by Voyageur kimberlite.

By analogy to the study of Hoal et al. (1994), the normal REE_N patterns showed by Voyageur lherzolitic garnets represent fully equilibrated metasomatic

compositions whereas the moderate sinusoidal REE_N patterns peaking at Sm-Eu should indicate an incomplete (but advanced) re-equilibration of more refractory garnets with a metasomatic fluid. It was pointed out that this disequilibrium model requires the larger LREE cations to diffuse faster than the smaller ones (HREE) and this has not been observed experimentally (Van Orman et al., 2002).

Stachel et al. (2004) explained the variability of REE_N patterns in lherzolitic garnets through a two-stage evolution model: starting from a highly depleted residual harzburgite composition, fluid metasomatism first causes the ubiquitously observed LREE enrichment of garnets in cratonic peridotites. In a second stage, beginning with such LREE enriched harzburgitic composition, the garnet is gradually enriched in MREE and HREE and turns into an average lherzolitic and then fully refertilized garnet with primitive composition (Fig. 3.4.4).

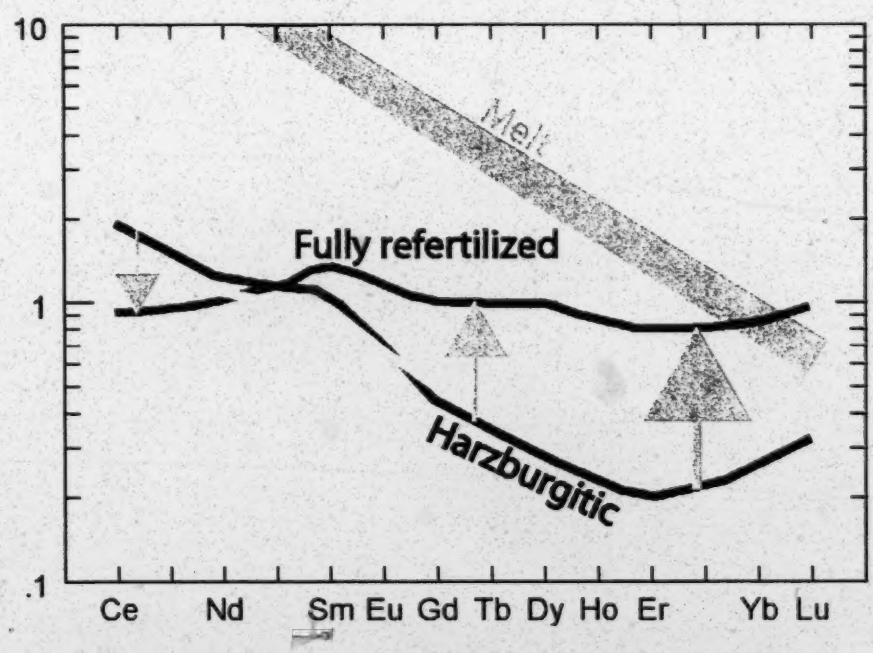

Fig. 3.4.4 Origin of lherzolitic garnets through metasomatic enrichment of former harzburgites. Modified after Stachel et al. (2004).

The equilibration of the lherzolitic garnet with clinopyroxene during the metasomatic enrichment process is responsible for the relative depletion in LREE and the composition of the percolating melt calculated is typical of low-volume mantle melts (kimberlites, lamroites etc.).

In the light of observations made by Stachel et al. (2004), the variability of patterns shown by Voyageur garnets when plotted individually represent different stages of adjustment of an initial harzburgitic composition with a percolating melt with LREE/HREE falling in the ranges observed for low volume partial melts (Fig. 3.4.5).

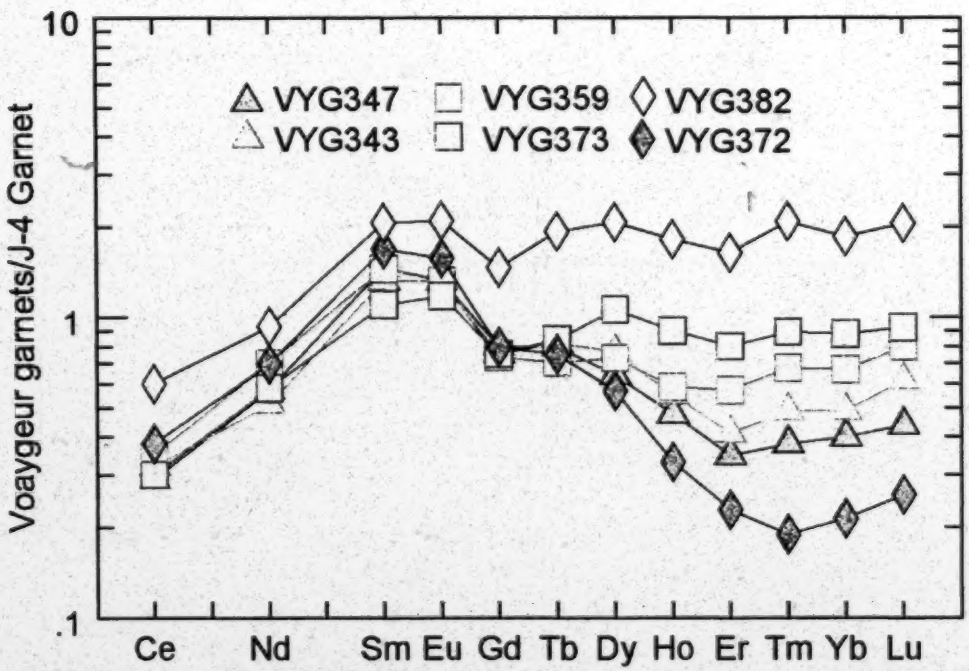

Fig. 3.4.5 Averaged REE abundances in lherzolitic garnets from Voyageur peridotite xenoliths normalized to the composition of the primitive J4 garnet (Jagoutz&Spettel)

"Depleted" garnets are completely absent from the peridotite xenoliths studied implying that the lithosphere sampled by Voyageur kimberlite is metasomatized throughout. The correlated enrichment of Zr and Y advocate for high-T, melt metasomatism affecting in different degrees the mantle source of Voyageur lherzolitic garnets (Fig. 3.4.4; Griffin & Ryan, 1995). A very intense melt-related metasomatism is highly evident in VYG382 garnets and is associated with enrichment in Zr, Y, Ti, Sr. The documented porphyroclastic texture and the high $T_{Ni\text{-}in\text{-}garnet}$ temperatures calculated for VYG382 (discussed in Chapter 4) support these findings.

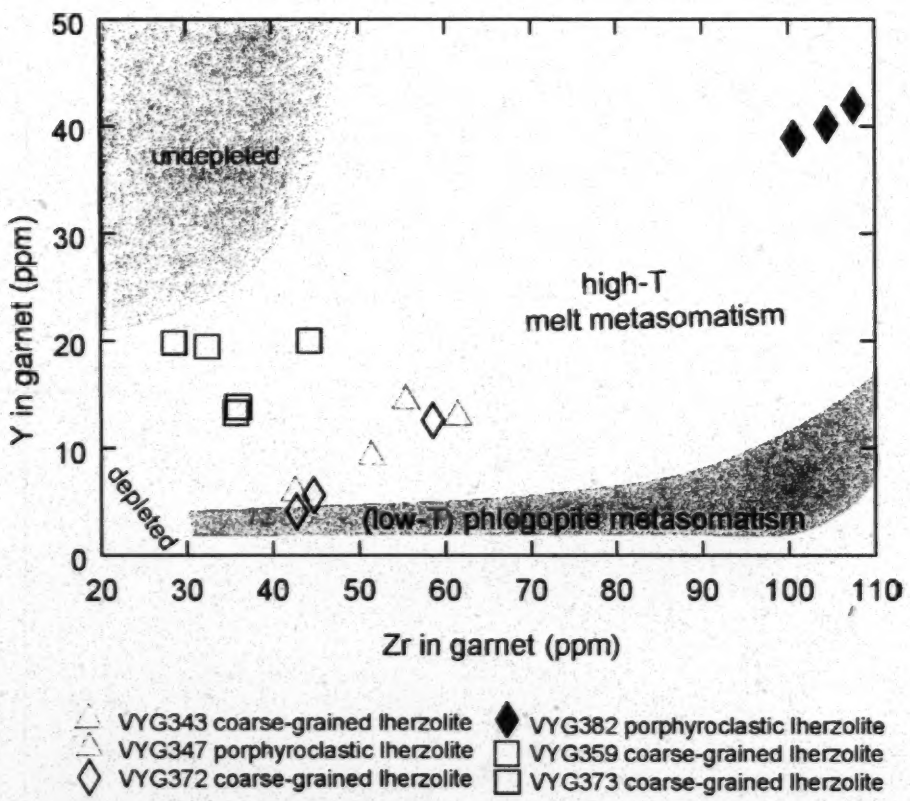

Fig. 3.4.6 Zr (ppm) Vs Y (ppm) concentrations in lherzolitic garnets from the Voyageur peridotite xenoliths. Metasomatic fields after Griffin & Ryan (1995).

LITERATURE CITED

- **Carbno, G.B. and Canil, D., 2002**– *Mantle Structure beneath SW Slave Craton, Canada: Constraints from Garnet Geochemistry in Drybones Bay Kimberlite*. Journal of Petrology 43: 129-142
- **Canil, D.; Schulze, D.J.; Hall, D.; Hearn, B.C. and Milliken, S.M., 2003** – *Lithospheric roots beneath western Laurentia: the geochemical signal in mantle garnets.* Canadian Journal of Earth Sciences 40: 1027-1051
- **Chen, Z., 1999** – *Inter-element fractionation and correction in laser ablation inductively coupled plasma mass spectrometry.* Journal of Analytical Atomic Spectrometry 14: 1823-1828
- **Gregoire, M.; Tinguely, C.; Bell, D.R. and le Roex, A.P., 2005 in press** – *Spinel lherzolite xenoliths from the Premier kimberlite (Kaapvaal craton, South Africa): Nature and evolution of the shallow upper mantle beneath Bushveld complex.* Lithos
- **Griffin, W.L. and Ryan, C.G., 1995** – *Trace elements in indicators minerals: area selection and targetevaluation in diamond exploration.* Journal of Geochemical Exploration 53: 311-337
- **Gurney, J. J., Harris, J. W. and Pickard, R. S., 1979** - *Silicate and oxide inclusions in diamonds from the Finsch kimberlite pipe*. In F. R. Boyd and H. O. A. Meyer, Eds., Kimberlites, Diatremes and Diamonds: Their Geology, Petrology and Geochemistry, p 1-15 American Geophysical Union, Washington, D.C.

- **Hoal, K.E.O.; Hoal, B.G.; Erlank, A.J.; Shimizu, N., 1994** – *Metasomatism of the mantle lithosphere recorded by rare earth elements in garnets*. Earth and Planetary Science Letters 126: 303-313
- **Kopylova, M.G.; Russell, J.K. and Cookenboo, H., 1999a** – *Petrology of peridotite and pyroxenite xenoliths from Jericho kimberlite: Implications for the thermal state of the mantle beneath the Slave craton, Northern Canada*. Journal of Petrology 40: 79-104
- **Kopylova, M.G.; Russell, J.K. and Cookenboo, H., 1999b** – *Mapping the lithosphere beneath the North Central Slave Craton*. In: Gurney, J.J.; Richardson, S.R. (Eds.) Proceedings to the 7th international Kimberlite Conference, Red Roof Designs, Cape Town pp: 468-479
- **Kopylova, M. G., Russell, J. K., Stanley, C. and Cookenboo, H., 2000** - *Garnet from Cr and Ca-saturated mantle: implications for diamond exploration*. Journal of Geochemical Exploration 68: 183–199.
- **Menzies, M.A.; Westerlund, K.; Grutter, H., Gurney, J., Carlson, J., Fung, A. and Nowicki, T., 2004** – *Peridotitic mantle xenoliths from kimberlites on the Ekati Diamond Mine property, N.W.T., Canada: major element compositions and implications for the lithosphere beneath the central Slave craton*
- **Norman, M.D.; Pearson, N.J.; Sharma, A. and Griffin, W.L., 1996** - *Quantitative analysis of trace elements in geological materials by laser ablation ICPMS: instrumental operating conditions and calibration values of NIST glasses*. Geostandards Newsletter 20, 247-261.

- **Norman, M. D., 1998** - *Melting and metasomatism in the continental lithosphere: laser ablation ICPMS analysis of minerals in spinel lherzolites from eastern Australia.* Contrib. Mineral. Petrol. 130: 240–255.
- **Shimizu, N., 1975** – *Rare earth elements in garnets and clinopyroxenes from garnet lherzolite nosules in kimberlites.* Earth and Planetary Science Letters 25: 26-32
- **Shimizu, N and Richardson, 1987** – *Trace elements abundance patterns of garnet inclusions in peridotite-suite diamonds.* Geochim. Cosmochim. Acta 51: 755-758
- **Smith, D., W.L. Griffin, C.G. Ryan, D.R. Cousens, S.H. Sie and G.F. Suter, 1991** - *Trace-element zoning of garnets from The Thumb: a guide to mantle processes.* Contrib. Mineral. Petrol. 107: 60-79
- **Smith,** *D. and Boyd, F. R., 1992 - Compositional zonation in garnets in peridotite xenoliths.* Contrib. Mineral. Petrol. 112: 134-147
- **Sobolev, N.V.; Laurent'ev, Yu, G.; Pokhilenko, N.P., and Usova, L.V., 1973** - *Chrome-rich garnets from the kimberlites of Yakutia and their parageneses.* Contrib. Mineral. Petrol. 40: 39-52.
- **Stachel, T.; Viljoen, K.S.; Brey, G. and Harris, J.W., 1998** – *Metasomatic processes in lherzolitic and harzburgitic domains of diamondiferous lithospheric mantle: REE in garnets from xenoliths and inclusions in diamonds.* Earth and Planetary Science Letters 159: 1-12

- **Stachel, T.; Aulbach, S.; Brey, G.P.; Harris, J.W.; Leost, I.; Tappert, R. and Viljoen, K.S., 2004** – *The trace element composition of silicate inclusions in diamonds: a review.* Lithos 77: 1-19
- **Van Achtenberg, E. Griffin, W.L.Stiefenhofer, J., 2001** – *Metasomatism in mantle xenoliths from the Letlhakane kimberlites: estimation of element fluxes.* Contrib. Mineral. Petrol. 141: 397-414
- **Van Orman, J.A.; Grove, T.L.; Shimizu, N. and Layne, G.D., 2002** – *Rare earth element diffusion in a natural pyropes single crystalat 2.8GPa.* Contrib. Mineral. Petrol. 142: 416-424

CHAPTER 4

GEOTHERMOBAROMETRY

Equilibrium pressure and temperature estimates were computed for the Voyageur peridotite xenoliths using published geothermometers and geobarometers recommended for cratonic peridotites:

- T_{BKN} [two-pyroxene thermometer of Brey and Köhler (1990)]
- $T_{O'Neill}$ [Fe-Mg exchange between olivine and garnet thermometer of O'Neill and Wood (1979) with correction of O'Neill (1980)]
- T_{Harley} [Fe-Mg exchange between orthopyroxene and garnet thermometer of Harley (1984)]

Each thermometer was combined with P_{BKN} [Al-in-opx barometer of Brey and Köhler (1990)]. The resulting solutions were used for different mineral assemblages: T_{BKN} - P_{BKN}, T_{Harley} - P_{BKN}, $T_{O'Neill}$ - P_{BKN} for garnet lherzolites and $T_{O'Neill}$ - P_{BKN}, T_{Harley} - P_{BKN} for the garnet harzburgite. T_{BKN} was demonstrated to be particularly suitable for high-temperature garnet peridotites and to give the best estimates of equilibrium conditions when combined with P_{BKN} (Brey&Köhler, 1990). $T_{O'Neill}$ is widely used and very convenient due to its applicability to both garnet lherzolites and harzburgites whereas T_{Harley} is used as a complementary thermobarometric solution, supposed to give the most realistic estimates (near concordance with T_{BKN}) in the interval 800-900°C (Smith, 1999).

In addition to the above thermobarometers, T_{NT} [single grain clinopyroxene thermometer of Nimis&Taylor (2000)] was applied in combination with P_{NT} [single

grain clinopyroxene barometer of Nimis&Taylor (2000)] on the Voyageur clinopyroxene-bearing peridotites. All clinopyroxenes from Voyageur garnet peridotite xenoliths plot in the garnet peridotite field of Ramsay & Tompkins (1994) so equilibrium with orthopyroxene and garnet can be inferred.

The $T_{Ni\text{-}in\text{-}garnet}$ geothermometer is based on the strongly temperature-dependent partitioning of Ni between garnet and olivine in mantle peridotites (assuming equilibration between the two coexisting phases and a uniform Ni content of olivine). It is insensitive to the major element composition of garnets and to pressure and can be used to approximate the depth of their origin if the results are reffered to a known geotherm (Griffin et al., 1989; Ryan et al.,1996; Canil, 1999 and references therein).

Averaged results of iteratively calculated P-T estimates for mineral cores are listed in Table 4.1.

For a better evaluation of the different solutions, thermometers were also applied at constant pressure and barometers at constant temperature. At a given pressure of 40kbar, T_{BKN} temperatures match well (maximum ~50°C hotter) with $T_{O'Neill}$ temperatures and are ~100°C hotter than T_{Harley} temperatures estimated for the garnet lherzolite xenoliths from the Voyageur kimberlite (Table 4.1). The exception is VYG382 (porphyroclastic peridotite) where the difference is slightly bigger in both cases. This may indicate that cpx-opx equilibria in this sample are disturbed. Overall, these results are in concordance with the observation made by Smith (1999) that at temperatures ~1100°C, T_{BKN} yields values at least 50-100°C hotter than the other widely used geothermometers.

Table 4.1 Averaged equilibration P–Ts for the mineral cores of peridotite xenoliths from the Voyageur kimberlite

Sample	Rock type	$T_{Ni\text{-}in\text{-}garnet}$ (Canil, 1999)	Preset pressure 40kb										
			T_{BKN}	$T_{O'Neill}$	T_{Harley}	T_{BKN} - P_{BKN}		$T_{O'Neill}$ - P_{BKN}		T_{Harley} - P_{BKN}		T_{NTcpx} - P_{NTcpx}	
VYG 343	grt lh	1057	1092	1085	1020	1112	51	1140	53	1066	47	1038	53
VYG 347	grt lh	1092	1108	1110	1115	1144	56	1193	60	1091	51	1063	57
VYG 359	grt lh	1021	1066	1047	987	1110	66	1194	73	1205	74	993	48
VYG 372	grt lh	997	1095	1047	987	1121	48	1081	48	1001	43	1008	50
VYG 373	grt lh	1048	1053	1103	958	1055	48	1098	51	1047	47	972	47
VYG 382	grt lh	1173	1153	1083	1027	1190	56	1140	52	1070	47	1130	61
VYG 403	grt hz	-	-	-	-	-	-	1053	44	963	39	-	-
VYG 368	sp-grt lh	-	-	-	-	622	25	604	23	790	39	529	32
VYG 402	sp-grt lh	-	-	-	-	-	-	541	18	834	37	434	27
VYG 345	wh	-	-	-	-	-	-	-	-	-	-	943	45
VYG 354	wh	-	-	-	-	-	-	-	-	-	-	851	40
VYG 358	wh	-	-	-	-	-	-	-	-	-	-	863	40
VYG 363	gt wh	-	-	-	-	-	-	-	-	-	-	996	50
VYG 398	gt wh	-	-	-	-	-	-	-	-	-	-	942	50

Voyageur peridotite xenoliths show a P-T range (on average from ~500 to 1200°C and up to 70kbar) suggesting that the kimberlite sampled a large section of the mantle. All garnet lherzolites plot within the diamond stability field when combining T_{BKN} and P_{BKN} (Fig. 4.1). With one exception, calculated P-T conditions define an array representing equilibration along a geothermal gradient equivalent to ca. 40mW/m^2 surface heat flow at the time of Voyageur kimberlite eruption. The porphyroclastic samples record pressures of ~55kbar and temperatures up to ~1200°C whereas the coarse-grained samples record slightly lower pressures (~50kbar) and temperatures (~1100°C or lower). Different chemistry, textural characteristics and P-T equilibration values are pointing to two groups of xenoliths present: a shallower, low-temperature coarse-grained group and a deeper, high-temperature porphyroclastic group.

One sample appears to be unrelated to the main trend and may indicate a different evolution in the mantle: the coarse-grained garnet lherzolite VYG359 plots on a cooler geotherm at high pressures (~65kbar) and temperatures of ~1100°C (Fig. 4.1). Calculated pressures and temperatures using the three different thermobarometers listed above are similar for VYG359. However, based on cpx thermobarometry the sample plots on a common geotherm as well and at depth similar to other coarse granular xenoliths hence disequilibrium between garnet-opx is suspected.

Two of the xenoliths (VYG368 and VYG402) contain coexisting spinel and garnet and define the spinel/garnet transition zone in the cratonic mantle sampled by Voyageur kimberlite. No suitable pair of minerals could be found for

VYG402, but VYG368 gave an average equilibration temperature of ~600°C at an average pressure of ~25kbar.

Because no suitable barometer is available for spinel peridotites, for the garnet-free sample T_{BKN} was computed at fixed pressure of 20kbar and 30kbar representing the maximum depth extent of the spinel-facies stability field. By projecting the results onto the 40mw/m^2 geotherm derived for garnet peridotites, an estimation of the depth of origin of the spinel lherzolite can be obtained (Fig. 4.1).

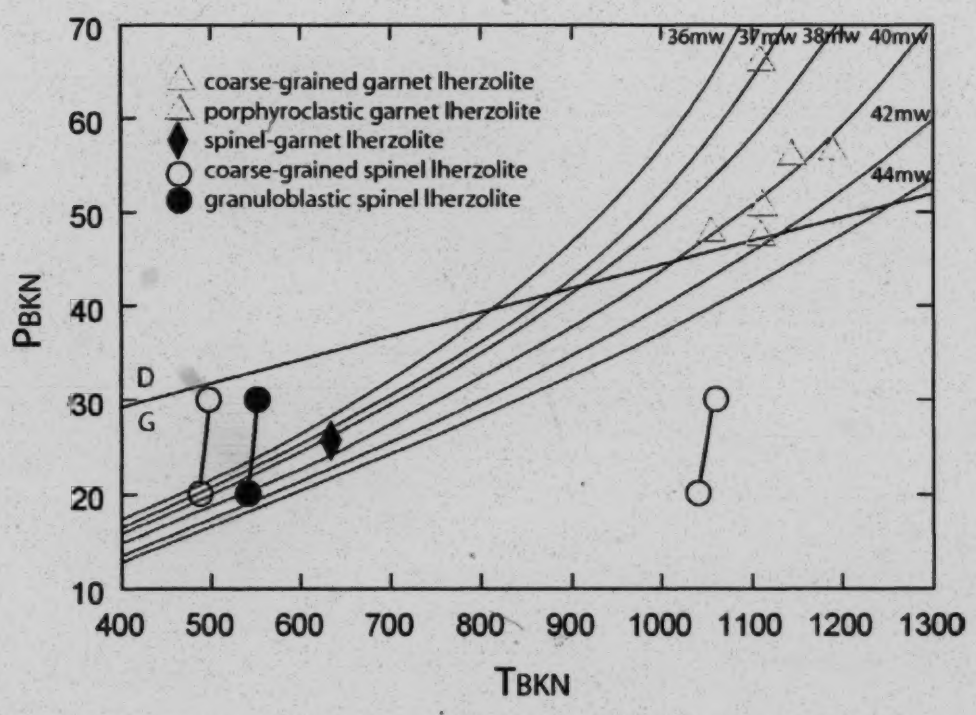

Fig. 4.1 Averaged P-T estimates of peridotite xenoliths from the Voyageur kimberlite calculated iteratively using T_{BKN} - P_{BKN}. Equilibrium temperatures for spinel lherzolites were calculated at 20kbar and 30kbar, respectively. Geotherms from Pollack & Chapman (1977).

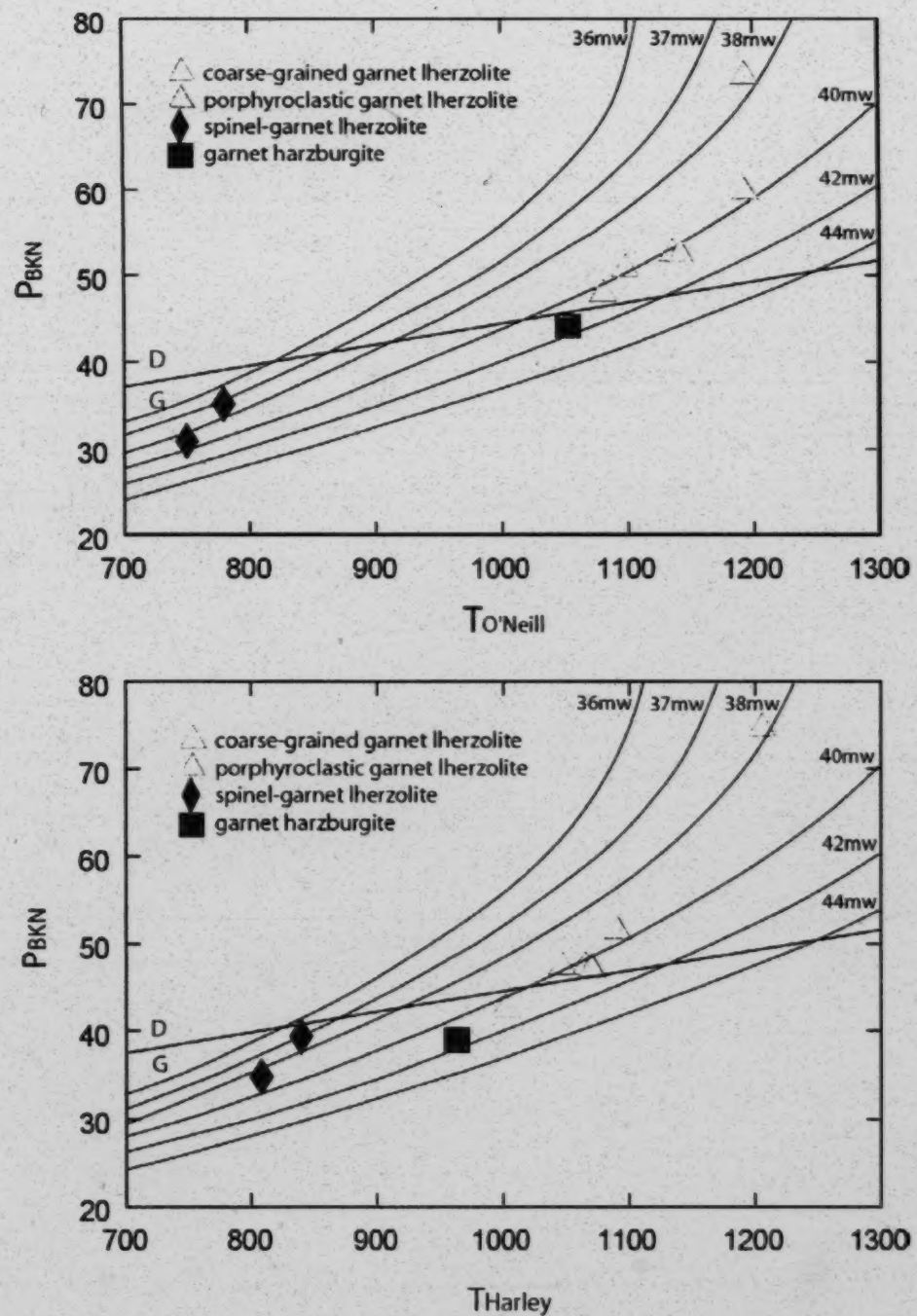

Fig. 4.2 Averaged P-T estimates of peridotite xenoliths from the Voyageur kimberlite calculated iteratively using a) $T_{O'Neill}$-P_{NTcpx} solution and b) T_{Harley}-P_{NTcpx} .
Geotherms from Pollack & Chapman (1977).

Excluding VYG359 lithospheric thickness of at least ~170km (for T_{BKN}-P_{BKN}) can be inferred from the maximum equilibration pressures and temperatures recorded by the garnet peridotite xenoliths from Voyageur kimberlite.

Irrespective of the geothermobarometric combination used, the resulting P-T array is similar (Fig. 4.1 and 4.2a-b). The depth range, however, varies somewhat.

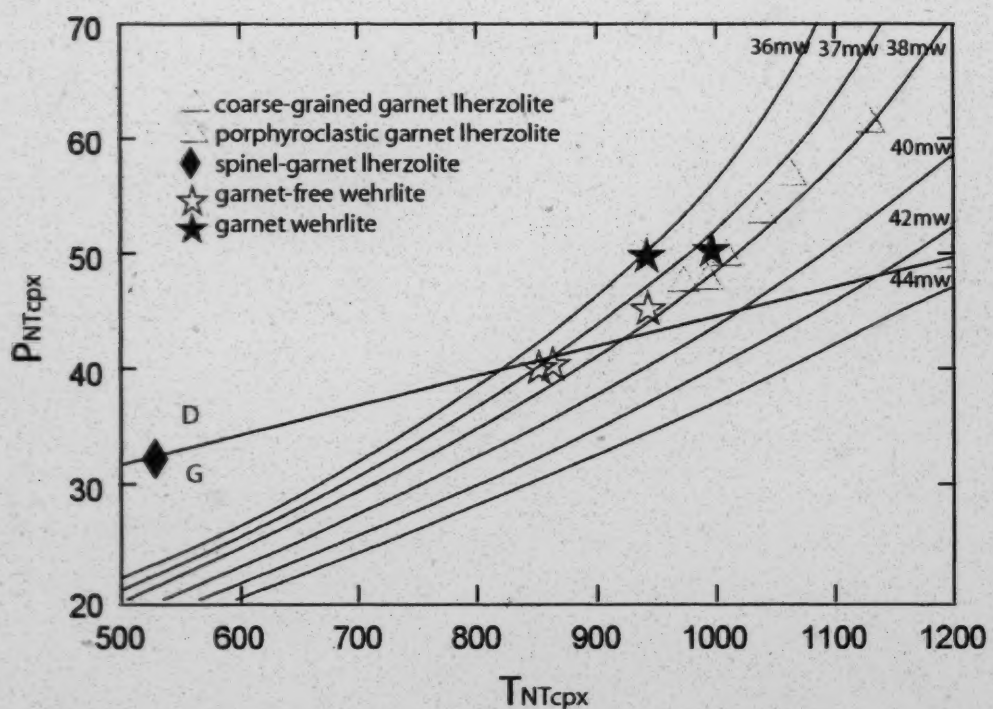

Fig. 4.3 Averaged P-T estimates of peridotite xenoliths from Voyageur kimberlite calculated iteratively using T_{NTcpx}-P_{NTcpx} . Geotherms from Pollack & Chapman (1977)

Temperature and pressure estimates obtained from the cores and rims of coexisting phases were compared in order to recognize any thermal perturbations resulting from magma generation or emplacement events.

Generally, when computed for the cores, pressures and temperatures are higher than the values obtained for the rims.

According to the Nimis and Taylor thermobarometer, the resulting pressure and temperature estimates define a slightly different geotherm (38mW/m^2) but compare favorably with T_{BKN}-P_{BKN} solution applied on the Voyageur garnet peridotites (Fig. 4.3). VYG359 also plots on the 38mW/m^2 geotherm, at less than 1000°C and ~48kbar.

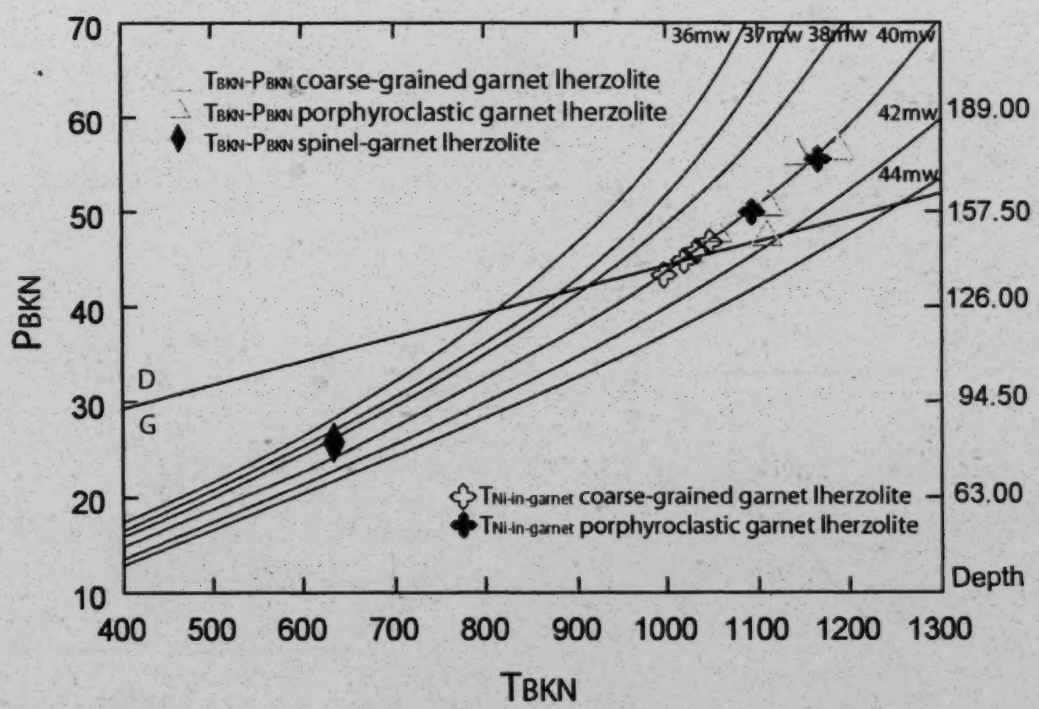

Fig. 4.4 Comparison of garnet equilibration temperatures calculated using $T_{Ni\text{-}in\text{-}garnet}$ (version of Canil, 1999) and T_{BKN}-P_{BKN} geothermometers

The range in T_{Ni} obtained using the experimental version of the thermometer (Canil, 1999) is between 997 and 1173°C (Table 4.1). A slightly different range (1024-1210°C) was found when using the empirical version of Ryan et al. (1996) but this does not affect the conclusion of this investigation.

The results are comparing favourably to the ones from conventional thermobarometry. When projected to the 40mw/m^2 geotherm, the pressure and depth of origin intervals are similar for $T_{Ni\text{-}in\text{-}garnet}$ and T_{BKN}-P_{BKN} solutions (Fig. 4.4). This supports the suggestion that garnet-opx are out of equilibrium in sample VYG359.

LITERATURE CITED

- **Brey, G.P. and Köhler, T. and Nickel, K.G., 1990** – *Geothermobarometry of four-phase lherzolites: I. Experimental results from 10 to 60kb*. Journal of Petrology 6: 1313-1352
- **Brey, G.P. and Köhler, T., 1990** – *Geothermobarometry in four-phase lherzolites: II. New thermometers and practical assessement of existing thermobarometers*. Journal of Petrology 31: 1353-1378
- **Canil D., 1999** - *The Ni-in-garnet geothermometer: calibration at natural abundances*. Contrib. Mineral. Petrol. 136: 240-246.
- **Griffin, W.L.; Cousens, D.R.; Ryan, C.G.; Sie, S.H.; Suter, G.F., 1989a** – *Ni in chrome pyropes garnets: A new geothermometers*. Contrib. Mineral. Petrol. 103: 199-202
- **Griffin, W.L.; Smith, D.; Boyd, F.R.; Cousens, D.R.; Ryan, C.G.; Sie, S.H. and Suter, G.F., 1989b** – *Trace element zoning in garnets from sheared mantle xenoliths*. Geochim. Cosmochim. Acta 53 (2): 561-567
- **Harley, S.L., 1984** – *An experimental study of the partitioning of Fe and Mg between garnet and orthopyroxene*. Contrib. Mineral. Petrol. 86: 359-373
- **Nickel, K.G. and Green, D.H., 1985** – *Empirical geothermobarometry for garnet peridotites and implications for the nature of the lithosphere, kimberlites and diamonds*. Earth and Planetary Science Letters 73: 158-168

- **Nimis, P and Taylor, W.R., 2000** – *Single clinopyroxene thermobarometry for garnet peridotites: Part 1. Calibration and testing of Cr-in-Cpx barometer and enstatite-in-Cpx thermometer.* Contrib. Mineral. Petrol. 139 (5): 541-554
- **O'Neill, H.St.C. and Wood, B.J., 1979** – *An experimental study of Fe-Mg partitioning between garnet and olivine, and its calibration as a geothermometer.* Contrib. Mineral. Petrol. 70: 59-70
- **ONeill H.St.C. and Wood, B.J., 1980** - *An experimental study of Fe-Mg partitioning between garnet and olivine, and its calibration as a geothermometers*: corrections. Contrib. Mineral. Petrol. 72: 337
- **O'Neill, H.St.C, 1981** - *The transition between spinel lherzolite and garnet lherzolite, and its use as a geobarometer.* Contrib. Mineral. Petrol. 77: 185-194
- **Pollack, H.N. and Chapman, D.S., 1977** – *On the regional variation of heat flow, geotherms, and lithospheric thickness.* Tectonophysics 38: 279-296
- **Ryan, C.G.; Griffin, W.L. and Pearson, N.J., 1996** – *Garnet geotherms: pressure-temperature data from Cr-pyrope garnet xenocrysts in volcanic rocks.* Journal of Geophysical Research 101 (B3): 5611-5625

- **Smith, D., 1999**. *Temperatures and pressures of mineral equilibration in peridotite xenoliths: review, discussion, and implications*. In: Fei, Y.; Bertka, C.M. and Mysen, B.O. (Eds.), Mantle Petrology: Field observations and High Pressure Experimentation: A tribute to Francis R. (Joe) Boyd. Geochemical Society Special Publication, vol. 6: 171-188

CHAPTER 6

DISCUSSION

The mantle underlying that part of the Slave craton sampled by Voyageur kimberlite is similar to cratonic mantle worldwide in many ways.

Only peridotitic samples were selected for this study (lherzolites, harzburgites and wehrlites). They are developed in spinel, garnet or spinel-garnet facies. Although generally coarse-grained, the peridotitic samples display the main textural varieties commonly described in cratonic xenoliths.

The olivines from Voyageur peridotite xenoliths are magnesium rich and range in mg-number of 0.879-0.933, similar to olivines in xenoliths recovered from other kimberlite pipes in the Slave craton: Jericho (mg# = 0.88-0.93; Kopylova et al, 1999), Torrie (mg# = 0.90-0.93; MacKenzie & Canil, 1999), Gahcho Kue (mg# = 0.87-0.93; Kopylova & Caro, 2004), Ekati (mg # = 0.85-0.94; Menzies et al., 2004). The averaged mg-number for this study (0.909) is comparable to that reported for the Jericho peridotites (0.913; Kopylova et al., 1999) but low when compared to Torrie (0.920 – MacKenzie & Canil, 1999), Kaapvaal (0.926 - Boyd & Nixon, 1987), Udachnaya (0.920 - Boyd et al., 1997) or Sommerset Island (0.921 - Kjarsgaard & Peterson, 1992; Schmidberger & Francis, 1999; Irvine, 2003) (Fig.5.1). The averaged concentration of NiO in olivines from Voyageur peridotite xenoliths is 0.35wt%, lower than Jericho (0.39wt% – Kopylova et al., 1999) and closer to Torrie and Panda averages (0.36wt% - MacKenzie & Canil, 1999; Menzies et al., 2004).

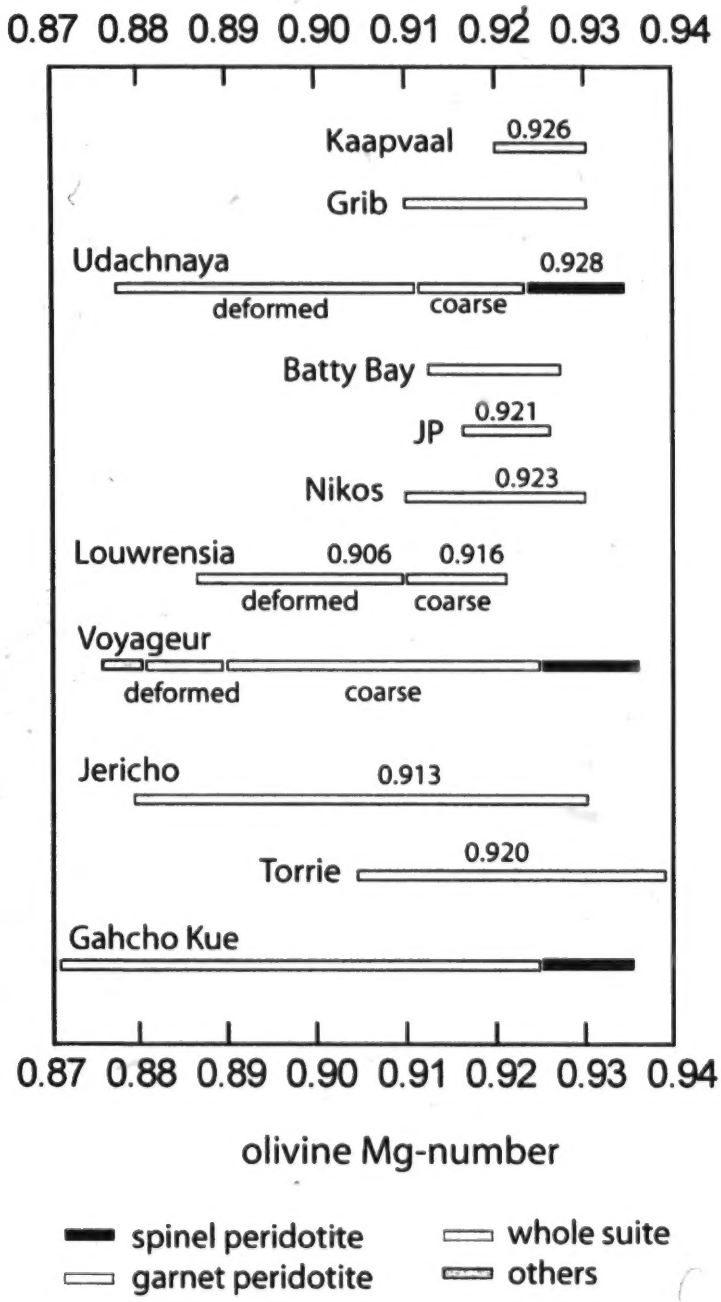

***Fig. 5.1** Mg-number of olivines from peridotite xenoliths worldwide*

In concordance with what can be generally observed in other cratonic xenoliths suites, olivines in spinel peridotites are more Mg-rich then olivines in garnet peridotites. As opposed to Gahcho Kue (Slave) and/or Nikos (Sommerset Island) where coarse and deformed peridotites are not chemically distinguishable, olivines and pyroxenes from Voyageur coarse-grained garnet peridotites are definitely more magnesium-rich in comparison with the ones from porphyroclastic varieties.

Voyageur spinel lherzolites have orthopyroxenes relatively low in Al_2O_3 (0.81-1.35wt%) with respect to the ones in worldwide cratonic spinel peridotites (1.5-4.0wt% Al_2O_3; Boyd, 1989). Low-Al compositions of orthopyroxenes have been reported in spinel lherzolites affected by kimberlite-related recrystallization from the SE Slave craton (Kopylova & Caro, 2004). The orthopyroxenes in spinel lherzolites from Premier kimberlite (0.4-1.4wt%Al_2O_3) are higher in CaO and TiO_2 in comparison with Voyageur orthopyroxenes.

The third type of clinopyroxene described in Voyageur spinel lherzolites resembles the late-stage Na-, Al- and Cr-depleted clinopyroxene reported in the peridotite xenoliths recovered from other pipes in the Slave craton: Jericho (Kopylova et al., 1999), Grizzly (Boyd & Canil, 1997), Gahcho Kue (Kopylova & Caro, 2004). A similar clinopyroxene described in a peridotite xenolith from Udachnaya was ascribed to secondary crystallization during eruption of the host kimberlite magma (Boyd et al., 1997).

Garnets from the clinopyroxene-free, harzburgitic sample plot within the lherzolitic field. The unique CCGE trend, which was first recognized in garnet

compositions from the Slave craton peridotite xenoliths by Kopylova et al. (1999), appears in garnets from the Voyageur xenoliths as well (Fig. 5.2). It derives mainly from garnet compositions in spinel-garnet lherzolites containing relatively high-Cr spinels (49.2-54.2wt% Cr_2O_3). In comparison with diamond inclusions, spinel from spinel-garnet lherzolites at Voyageur is definitely less Cr-enriched. As such, the presence of the CCGE trend implies sampling of relatively shallow mantle (Kopylova et al., 2000). Indeed, thermobarometric calculations for the spinel-garnet lherzolite VYG368 places it at 622°C and 25kbar, well within the graphite stability field.

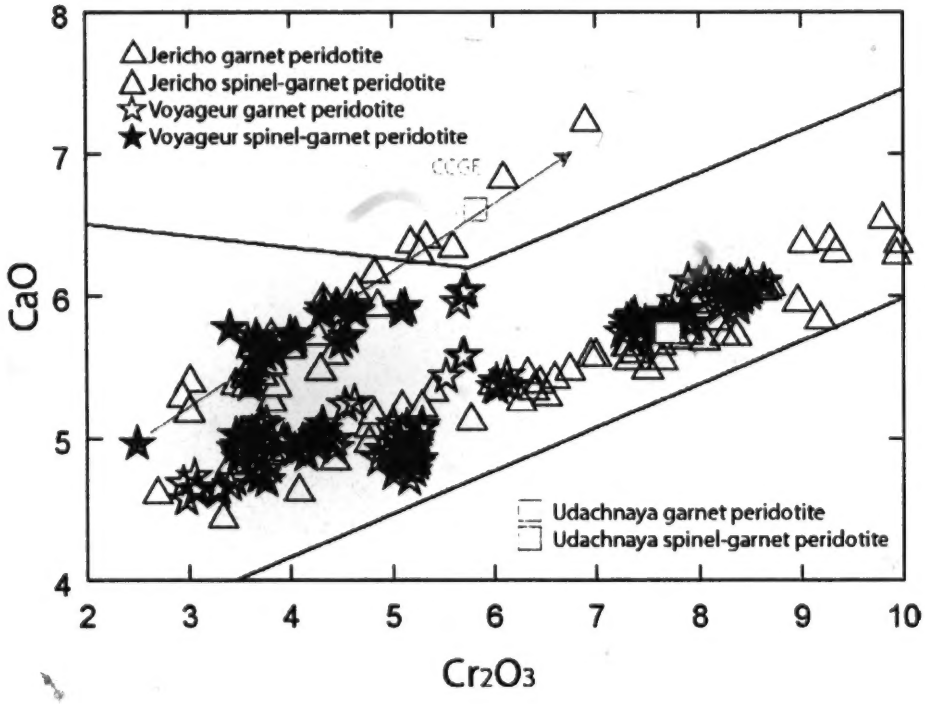

Fig. 5.2 Comparison of the CCGE trend in garnets from Voyageur and Jericho

Data for Jericho from Kopylova et al. (1999) and for Udachnaya from Boyd et al. (1997)

Kopylova et al. (2000) demonstrated that equilibrium between garnet and a lherzolitic mantle that includes Mg-chromite and cpx is necessary in order to develop this "exotic" trend. Hence, the VYG351 "harzburgitic" garnets plotting along CCGE must imply equilibration of the two compositionally different parts of the heterogeneous sample.

As opposed to Jericho, the CCGE trend developed in garnets from Voyageur xenoliths is not extending into the wehrlitic field (Fig. 5.2).

The CCGE trend was also apparent in peridotitic xenoliths from the Colorado Plateau (Ehrenberg, 1982; Smith et al., 1991), Lesotho (Smith & Boyd, 1992), and Drybones Bay (Carbno & Canil, 2002). In garnet xenocrysts from kimberlites in Kaavi-Kuopio (Finland) this compositional trend appears to be developed only in the wehrlitic field (Lehtonen, 2004).

As seen in many mantle sections worldwide, a pervasive metasomatic enrichment in the subcratonic lithospheric mantle sampled by Voyageur kimberlite is documented by the trace elements of lherzolitic garnets and clinopyroxenes. The garnets show an evolution that starts with a harzburgitic-like MREE-HREE composition and goes all the way to relatively primitive compositions. LREEs are depleted and slightly different from one garnet to another. Hence, interaction with a metasomatic fluid and enrichment in MREE-HREE was accompanied by equilibration of garnet with clinopyroxene. VYG382 (porphyroclastic sample) probably represents localized thermal perturbances related to the kimberlite activity short before eruption.

The bimodal distribution recognized in garnet peridotites from South Africa (Boyd, 1987) and in most of cratonic xenoliths worldwide can as well be observed in the Voyageur samples based on mineral chemistry and thermobarometry.

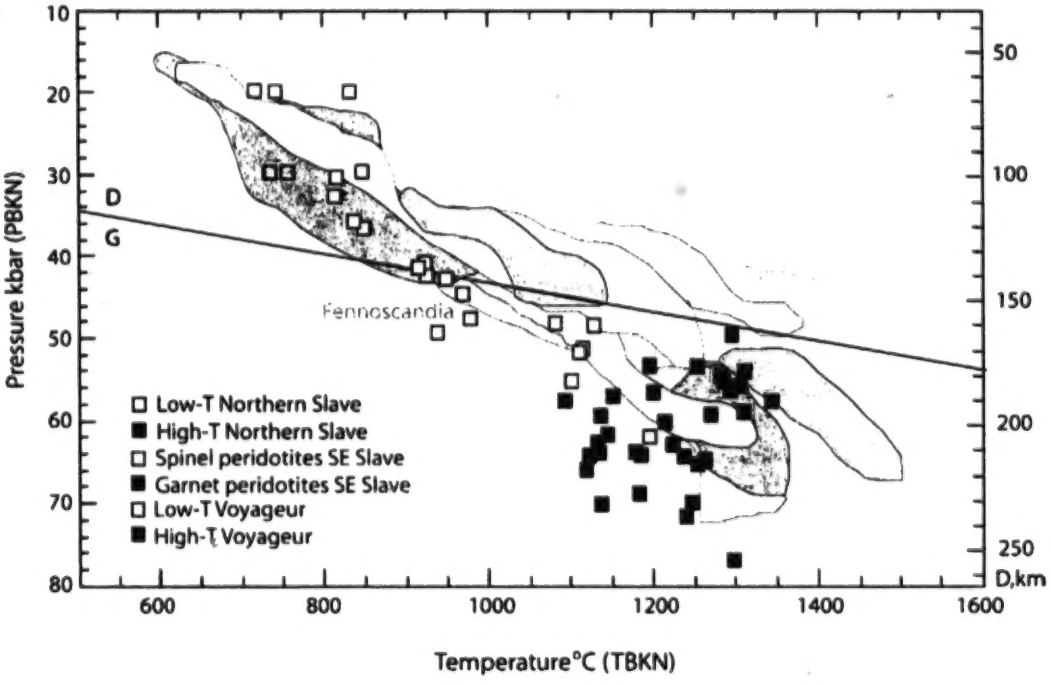

Fig. 5.3 Equilibrium pressure and temperature estimates calculated using the TBKN-PBKN geothermobarometer for Voyageur garnet peridotite xenoliths in comparison with data from cratonic mantle worldwide. Data points are from Kopylova et al., 1999 (Northern Slave) and Kopylova & Caro, 2004 (Southeastern Slave). P-T fields are based on data from Boyd, 1990 (unpublished, as cited in Kopylova and Caro, 2004) for the Kaapvaal craton; from Boyd et al., 1997 (Udachnaya) and Roden et al., 1999 (Mir) for the Siberian craton; from Kukkonen & Peltonen, 1999; Lehtonen et al., 2003 for the Fennoscandian craton; from Lee & Rudnick, 1999 for the Tanzanian craton; from Meyer et al., 1994 for the Superior craton; from Kjarsgaard & Peterson, 1992 and Schmidberger & Francis, 1999 for the Canadian Shield (Sommerset Island). Modified from Kopylova & Caro, 2004

Low-temperature (lithospheric) peridotites equilibrated at temperatures ~1100°C and pressures ~50kbar, have coarse-grained textures, Mg-rich compositions of olivines (mg# = 0.92-0.94) and orthopyroxenes (mg# = 0.92-0.93) and, compared to primitive mantle, overall depleted mineral chemistry.

The high-temperature peridotites (up to ~1200°C and ~56kbar), on the other hand, have porphyroclastic textures and fertile compositions (olivine mg# = 0.88; orthopyroxene mg# = 0.90). High-T suites of deformed peridotites are absent from Gahcho Kue and Ekati but have been reported in Torrie and Jericho xenoliths (MacKenzie & Canil, 1999; Kopylova et al., 1999). The majority of calculated P-T estimates for Voyageur garnet peridotites plot on a relatively cold geotherm of about 40mW/m², characteristic of Archean cratons, similar to Jericho but much higher than Gahcho Kùe (35mW/m²) and lower than Torrie (42mW/m²).

In concordance with the data reported from the Slave craton, the mantle sampled by Voyageur kimberlite is cooler than the mantle beneath other cratons (e.g. Kaapvaal, Canadian Shield, Tanzania) (Fig. 5.3).

LITERATURE CITED

- **Boyd, F.R. and Nixon, P.H., 1978** – *Ultramafic nodules from the Kimberley pipes, South Africa*. Geochim. Cosmochim. Acta 42: 1367-1382
- **Boyd, F.R., 1987** – *High- and low-temperature garnet peridotite xenoliths and their possible relation to the lithosphere-astenosphere boundary beneath South Africa*. In: P.H. Nixon (Ed.) Mantle xenoliths, John Wiley, New York, pp: 403-412
- **Boyd, F. R. and Canil, D., 1997** - *Peridotite xenoliths from the Slave craton, NWT. Lunar and Planetary Institute Contribution* 921: 34
- **Boyd, F.R.; Pokhilenko, N.P.; Pearson, D.G.; Mertzman, S.A. and Finger, L.W., 1997** – *Composition of the Siberian cratonic mantle: evidence from Udachnaya peridotite xenoliths*. Contrib. Mineral. Petrol. 128: 228-246
- **Boyd, F.R., 1989** – *Compositional distinction between oceanic and cratonic lithosphere*. Earth and Planetary Sciences 96: 15-26
- **Carbno, G.B. and Canil, D., 2002**– *Mantle Structure beneath SW Slave Craton, Canada: Constraints from Garnet Geochemistry in Drybones Bay Kimberlite*. Journal of Petrology 43: 129-142
- **Ehrenberg, S. N., 1982** - *Petrogenesis of garnet lherzolite and megacrystalline nodules from the Thumb, Navajo Volcanic Field*. Journal of Petrology 23: 507–547

- **Irvine, G.J.; Pearson, D.G.; Kjarsgaard, B.A.; Carlson. R.W.; Kopylova, M.G. and Dreibus, G., 2003** - *A Re-Os isotope and PGE studyof kimberlite-derivated peridotite xenoliths from Sommerset Island and a comparison to the Slave and Kaapvaal cratons*. Lithos 71: 461-488
- **Kjarsgaard, B.A. and Peterson, T.D., 1992** – *Kimberlite-derived ultramafic xenoliths from the diamond stability field: a new Cretaceous geotherm for Sommerset Island, Northwest Territories*. Geological Survey of Canada Paper 92-1B: 1-6
- **Kopylova, M.G.; Russell, J.K. and Cookenboo, H., 1999a** – *Petrology of peridotite and pyroxenite xenoliths from Jericho kimberlite: Implications for the thermal state of the mantle beneath the Slave craton, Northern Canada*. Journal of Petrology 40: 79-104
- **Kopylova, M.G.; Russell, J.K. and Cookenboo, H., 1999b** – *Mapping the lithosphere beneath the North Central Slave Craton*. In: Gurney, J.J.; Richardson, S.R. (Eds.) Proceedings to the 7th international Kimberlite Conference, Red Roof Designs, Cape Town p: 468-479
- **Kopylova, M. G., Russell, J. K., Stanley, C. and Cookenboo, H., 2000** - *Garnet from Cr and Ca-saturated mantle: implications for diamond exploration*. Journal of Geochemical Exploration 68: 183–199.
- **Kopylova, M.G. and Caro, G., 2004** – *Mantle Xenoliths from Southeastern Slave Craton: Evidence for a Chemical Zonation in a Thick, Cold Lithosphere*. Journal of Petrology 45: 1045-1067

- **Kukkonen, I. T. and Peltonen, P., 1999 -** *Xenolith-controlled geotherm for the central Fennoscandian Shield: implications for lithosphere–asthenosphere relations. Tectonophysics* 304: 301–315
- **Lee, C.-T. & Rudnick, R. L., 1999** - *Compositionally stratified cratonic lithosphere: petrology and geochemistry of peridotite xenoliths from the Labait tuff cone, Tanzania.* In: Gurney, J. J. & Richardson, S. R. (eds) Proceedings of the 7th International Kimberlite Conference. Cape Town: Red Roof Design, p.503-521
- **Lehtonen, M.; O'Brien, H., Peltonen, P., Johanson, B. & Pakkanen, L., 2004 -** *Layered mantle at the edge of the Karelian craton: P–T of mantle xenocrystals and xenoliths from Eastern Finland kimberlites.* Lithos 77: 593-608
- **MacKenzie J.M. and Canil D., 1999** - *Composition and thermal evolution of cratonic mantle beneath the central Archean Slave Province, NWT, Canada.* Contrib. Mineral. Petrol. 134: 313-324.
- **Menzies, M.A.; Westerlund, K.; Grutter, H., Gurney, J., Carlson, J., Fung, A. and Nowicki, T., 2004** – *Peridotitic mantle xenoliths from kimberlites on the Ekati Diamond Mine property, N.W.T., Canada: major element compositions and implications for the lithosphere beneath the central Slave craton Lithos 77: 395-412*
- **Meyer, H. O. A., Waldman, M. A. & Garwood, B. L., 1994** – *Mantle xenoliths from kimberlite near Kirkland Lake, Ontario.* Canadian Mineralogist 32: 295-306.

- **Roden, M.F.; Laz'ko, E.E.; Jagoutz, E., 1999** - *The role of garnet pyroxenites in the Siberian lithosphere: evidence from the Mir kimberlite.* In: Gurney, J.J., et al. (Ed.) Proceedings of the 7th International Kimberlite Conference, Cape Town, vol. 2: 714–720.
- **Schmidberger, S.S. and Francis, D., 1999** – *Nature of mantle roots beneath the North American craton: mantle xenoliths evidence from Sommerset Island kimberlites.* Lithos 48: 195-216
- **Smith, D., W.L. Griffin, C.G. Ryan, D.R. Cousens, S.H. Sie and G.F. Suter, 1991** - Trace element *zoning of garnets from The Thumb: a guide to mantle processes.* Contributions to Mineralogy and Petrology 107: 60-79
- **Smith, *D. and Boyd, F. R., 1992*** - *Compositional zonation in garnets in peridotite xenoliths.* Contributions to Mineralogy and Petrology 112: 134-147

CONCLUSIONS

- The peridotitic mantle sampled by the Voyageur kimberlite is developed in spinel, garnet or spinel-garnet facies and displays the main textural varieties commonly described in cratonic xenoliths worldwide
- There is a total absence of G10 (harzburgitic) garnets, even from modally clinopyroxene-free ("harzburgitic") samples
- The presence of the exotic CCGE trend in garnets implies the presence of Ca-saturated garnet in the shallow (spinel bearing) mantle sampled by Voyageur kimberlite
- Trace element characteristics of the lherzolitic garnets and clinopyroxenes suggest an interaction of the mantle sampled by Voyageur kimberlite with melts with LREE/HREE that is much lower than observed for typical fluid (low-T) metasomatism.
- Estimation of equilibrium temperatures and pressures for Voyageur peridotites define a cold, 40mW/m^2 geotherm, characteristic of Archean cratons
- Based on mineral compositions and P-T estimates a low-T coarse-grained, depleted group and a high-T porphyroclastic, fertile group are recognized in Voyageur xenoliths

- A lithospheric thickness of at least ~170km can be inferred from the maximum equilibration pressures and temperatures recorded by the garnet lherzolite xenoliths from Voyageur kimberlite
- The Slave mantle is colder than the mantle beneath other cratons worldwide (e.g. Kaapvaal, Canadian Shield, Tanzania)

APPENDICES

APPENDIX I

Electron microprobe core analyses of olivines from the Voyageur peridotite xenoliths

Sample	Rock type	SiO2	TiO2	Al2O3	Cr2O3	NiO	MgO	CaO	MnO	FeO	Total	X Mg	Fo
355-4.1	coarse spinel lherzolite	40.45	0.00	0.00	0.00	0.41	51.40	0.00	0.07	7.05	99.38	0.93	92.42
355-4.2	coarse spinel lherzolite	40.48	0.00	0.00	0.03	0.38	51.49	0.00	0.07	6.98	99.42	0.93	92.53
355-4.3	coarse spinel lherzolite	40.02	0.00	0.00	0.00	0.41	51.36	0.02	0.08	6.89	98.77	0.93	92.54
355-6.1	coarse spinel lherzolite	39.62	0.00	0.00	0.00	0.37	51.36	0.00	0.10	6.96	98.41	0.93	92.50
355-6.2	coarse spinel lherzolite	39.48	0.00	0.00	0.00	0.42	51.19	0.02	0.10	6.87	98.08	0.93	92.50
355-6.3	coarse spinel lherzolite	39.61	0.00	0.00	0.00	0.38	51.26	0.00	0.09	6.96	98.30	0.93	92.49
355-11.1	coarse spinel lherzolite	39.56	0.00	0.00	0.01	0.37	51.31	0.00	0.10	7.06	98.41	0.93	92.40
355-11.2	coarse spinel lherzolite	39.35	0.00	0.01	0.00	0.39	51.35	0.00	0.10	6.95	98.15	0.93	92.49
355-11.3	coarse spinel lherzolite	39.57	0.00	0.01	0.02	0.42	51.28	0.00	0.10	6.94	98.34	0.93	92.47
355-15.1	coarse spinel lherzolite	39.60	0.00	0.00	0.00	0.39	51.37	0.00	0.09	6.96	98.41	0.93	92.50
355-15.2	coarse spinel lherzolite	39.49	0.00	0.00	0.00	0.39	51.45	0.00	0.09	6.93	98.35	0.93	92.53
355-15.3	coarse spinel lherzolite	39.83	0.00	0.00	0.00	0.38	51.62	0.00	0.08	6.90	98.80	0.93	92.62
355-18.1	coarse spinel lherzolite	39.76	0.00	0.00	0.00	0.40	51.22	0.02	0.09	7.02	98.50	0.93	92.40
355-18.2	coarse spinel lherzolite	39.59	0.00	0.00	0.02	0.38	51.22	0.00	0.08	6.94	98.23	0.93	92.52
355-18.3	coarse spinel lherzolite	39.46	0.00	0.02	0.02	0.39	51.16	0.00	0.09	7.04	98.18	0.93	92.39
355-21.1	coarse spinel lherzolite	39.48	0.00	0.00	0.00	0.38	51.15	0.00	0.10	7.00	98.10	0.93	92.44
355-21.2	coarse spinel lherzolite	39.66	0.00	0.01	0.02	0.37	51.31	0.00	0.08	6.94	98.38	0.93	92.54
355-21.3	coarse spinel lherzolite	39.84	0.00	0.00	0.01	0.37	51.29	0.00	0.09	6.99	98.58	0.93	92.48
369-3.1	coarse spinel lherzolite	40.06	0.00	0.01	0.01	0.37	51.36	0.01	0.08	7.05	98.95	0.93	92.43
369-3.2	coarse spinel lherzolite	39.96	0.00	0.00	0.00	0.39	51.22	0.00	0.08	6.80	98.45	0.93	92.64
369-3.3	coarse spinel lherzolite	40.07	0.00	0.02	0.00	0.37	51.54	0.02	0.07	7.00	99.50	0.93	92.50
369-20.1	coarse spinel lherzolite	39.74	0.00	0.00	0.02	0.39	51.59	0.00	0.08	7.10	98.92	0.93	92.41
369-20.3	coarse spinel lherzolite	39.50	0.00	0.00	0.01	0.38	51.24	0.00	0.09	6.93	98.15	0.93	92.52
369-17.2	coarse spinel lherzolite	39.64	0.00	0.00	0.01	0.39	51.37	0.00	0.09	6.93	98.42	0.93	92.53

Continued APPENDIX I (olivine analyses)

Sample	Rock type	SiO2	TiO2	Al2O3	Cr2O3	NiO	MgO	CaO	MnO	FeO	Total	X Mg	Fo
369-17.3	coarse spinel lherzolite	39.65	0.00	0.00	0.01	0.39	51.26	0.00	0.09	7.04	98.45	0.93	92.41
369-12.1	coarse spinel lherzolite	39.73	0.00	0.01	0.00	0.38	51.22	0.00	0.09	7.01	98.44	0.93	92.45
369-12.3	coarse spinel lherzolite	39.65	0.00	0.00	0.00	0.39	51.42	0.02	0.09	6.84	98.40	0.93	92.60
371 - 2.1	coarse spinel lherzolite	39.47	0.00	0.00	0.00	0.36	51.32	0.01	0.09	6.78	98.02	0.93	92.68
371 - 2.2	coarse spinel lherzolite	39.38	0.00	0.00	0.01	0.42	51.55	0.00	0.09	6.75	98.20	0.93	92.69
371 - 2.3	coarse spinel lherzolite	39.58	0.00	0.00	0.00	0.39	51.24	0.00	0.10	6.83	98.14	0.93	92.60
371 - 6.1	coarse spinel lherzolite	40.00	0.00	0.01	0.01	0.35	51.38	0.00	0.08	6.94	98.78	0.93	92.56
371 - 6.2	coarse spinel lherzolite	39.84	0.00	0.01	0.03	0.36	51.18	0.00	0.07	6.76	98.25	0.93	92.71
371 - 6.3	coarse spinel lherzolite	39.82	0.00	0.00	0.01	0.36	51.50	0.00	0.09	7.00	98.74	0.93	92.54
371 - 8.1	coarse spinel lherzolite	40.17	0.00	0.00	0.00	0.39	51.23	0.00	0.10	7.00	98.60	0.93	92.52
371 - 8.2	coarse spinel lherzolite	39.54	0.00	0.03	0.00	0.41	51.26	0.01	0.09	6.81	98.20	0.93	92.73
371 - 8.3	coarse spinel lherzolite	39.94	0.00	0.00	0.00	0.37	51.12	0.00	0.11	6.91	98.30	0.93	92.62
371 - 11.1	coarse spinel lherzolite	39.77	0.00	0.00	0.01	0.36	51.85	0.03	0.10	6.84	99.05	0.93	92.64
371 - 11.2	coarse spinel lherzolite	40.00	0.00	0.00	0.02	0.40	51.34	0.00	0.07	7.01	98.76	0.93	92.55
371 - 11.3	coarse spinel lherzolite	40.09	0.00	0.02	0.00	0.38	51.53	0.00	0.08	7.01	98.97	0.93	92.59
411 - 2.1	coarse spinel lherzolite	40.72	0.00	0.00	0.00	0.41	51.69	0.00	0.10	6.88	99.98	0.93	92.61
411 - 2.2	coarse spinel lherzolite	40.76	0.00	0.00	0.00	0.41	52.21	0.00	0.10	6.91	100.59	0.93	92.64
411 - 2.3	coarse spinel lherzolite	40.70	0.00	0.00	0.00	0.40	51.90	0.03	0.09	6.83	100.36	0.93	92.71
411 - 5.1	coarse spinel lherzolite	40.89	0.00	0.00	0.00	0.39	52.12	0.00	0.09	7.00	100.42	0.93	92.55
411 - 5.2	coarse spinel lherzolite	40.47	0.00	0.00	0.00	0.39	51.90	0.00	0.08	6.68	99.77	0.93	92.79
356-2.2	granuloblastic spinel lherzolite	40.00	0.00	0.00	0.00	0.41	51.46	0.00	0.10	6.61	98.57	0.93	92.82
356-2.3	granuloblastic spinel lherzolite	39.82	0.00	0.02	0.00	0.40	51.77	0.01	0.08	6.66	98.76	0.93	92.82
356-6.1	granuloblastic spinel lherzolite	39.41	0.00	0.00	0.00	0.43	51.59	0.00	0.09	6.60	98.15	0.93	92.83
356-6.2	granuloblastic spinel lherzolite	40.32	0.00	0.00	0.01	0.41	52.19	0.00	0.10	6.56	99.60	0.93	92.95
356-6.3	granuloblastic spinel lherzolite	39.91	0.00	0.00	0.00	0.41	51.71	0.01	0.08	6.55	98.67	0.93	92.91
356-16.1	granuloblastic spinel lherzolite	40.37	0.00	0.00	0.00	0.39	51.49	0.00	0.10	6.65	99.00	0.93	92.80

Continued APPENDIX I (olivine analyses)

Sample	Rock type	SiO2	TiO2	Al2O3	Cr2O3	NiO	MgO	CaO	MnO	FeO	Total	X Mg	Fo
356-16.2	granuloblastic spinel lherzolite	40.16	0.00	0.00	0.00	0.38	51.65	0.00	0.08	6.67	98.94	0.93	92.82
356-16.3	granuloblastic spinel lherzolite	40.35	0.00	0.00	0.00	0.39	51.82	0.03	0.07	6.66	99.32	0.93	92.82
356-19.1	granuloblastic spinel lherzolite	39.72	0.00	0.00	0.00	0.40	51.31	0.00	0.08	6.71	98.22	0.93	92.73
356-19.2	granuloblastic spinel lherzolite	39.79	0.00	0.04	0.01	0.39	51.55	0.00	0.09	6.71	98.59	0.93	92.75
356-19.3	granuloblastic spinel lherzolite	39.81	0.00	0.01	0.00	0.40	51.51	0.02	0.09	6.67	98.51	0.93	92.75
343-22.1	coarse garnet lherzolite	40.09	0.05	0.02	0.03	0.39	50.41	0.01	0.11	8.98	100.09	0.91	90.46
343-22.2	coarse garnet lherzolite	40.28	0.04	0.00	0.02	0.38	50.32	0.02	0.12	8.74	99.93	0.91	90.64
343-22.3	coarse garnet lherzolite	40.27	0.05	0.00	0.04	0.39	50.28	0.02	0.10	8.66	99.81	0.91	90.73
343-2.1	coarse garnet lherzolite	40.31	0.00	0.02	0.04	0.39	50.36	0.00	0.10	8.67	99.89	0.91	90.75
343-2.2	coarse garnet lherzolite	40.28	0.02	0.00	0.03	0.40	50.66	0.03	0.10	8.75	100.26	0.91	90.69
343-2.3	coarse garnet lherzolite	40.40	0.00	0.00	0.04	0.38	50.42	0.02	0.10	8.59	99.97	0.91	90.81
343-13.1	coarse garnet lherzolite	40.11	0.04	0.00	0.03	0.41	50.38	0.02	0.12	8.71	99.81	0.91	90.67
343-13.2	coarse garnet lherzolite	40.36	0.00	0.01	0.04	0.41	50.37	0.02	0.12	8.67	100.01	0.91	90.70
343-13.3	coarse garnet lherzolite	40.40	0.04	0.01	0.03	0.39	50.44	0.02	0.11	8.74	100.19	0.91	90.67
343-23.1	coarse garnet lherzolite	40.19	0.00	0.01	0.04	0.37	50.32	0.02	0.13	8.71	99.80	0.91	90.68
343-23.2	coarse garnet lherzolite	40.20	0.03	0.00	0.03	0.40	50.73	0.03	0.11	8.79	100.32	0.91	90.65
343-23.3	coarse garnet lherzolite	40.27	0.04	0.02	0.05	0.40	50.54	0.03	0.11	8.76	100.20	0.91	90.66
343-6.1	coarse garnet lherzolite	40.38	0.04	0.00	0.03	0.38	50.10	0.02	0.10	8.69	99.73	0.91	90.68
343-6.2	coarse garnet lherzolite	40.29	0.00	0.00	0.03	0.36	50.39	0.02	0.10	8.70	99.91	0.91	90.73
343-6.3	coarse garnet lherzolite	40.32	0.04	0.00	0.02	0.38	50.66	0.01	0.10	8.81	100.34	0.91	90.67
343-4.1	coarse garnet lherzolite	40.07	0.05	0.00	0.03	0.38	50.17	0.03	0.13	8.72	99.58	0.91	90.62
343-4.2	coarse garnet lherzolite	40.16	0.04	0.01	0.03	0.39	50.27	0.02	0.12	8.74	99.77	0.91	90.64
343-4.3	coarse garnet lherzolite	40.39	0.03	0.02	0.03	0.35	50.40	0.03	0.13	8.59	99.96	0.91	90.81
343-24.1	coarse garnet lherzolite	40.30	0.04	0.01	0.03	0.43	50.34	0.03	0.11	8.71	99.99	0.91	90.64
343-24.2	coarse garnet lherzolite	40.37	0.03	0.00	0.02	0.36	50.53	0.04	0.10	8.74	100.19	0.91	90.71
343-24.3	coarse garnet lherzolite	40.35	0.00	0.01	0.04	0.37	50.70	0.02	0.10	8.73	100.31	0.91	90.76
359-5.1	coarse garnet lherzolite	40.08	0.02	0.02	0.03	0.35	50.71	0.03	0.08	8.01	99.34	0.92	91.43

Continued APPENDIX I (olivine analyses)

Sample	Rock type	SiO2	TiO2	Al2O3	Cr2O3	NiO	MgO	CaO	MnO	FeO	Total	X Mg	Fo
359-6.2	coarse garnet lherzolite	40.00	0.02	0.00	0.04	0.35	51.06	0.04	0.10	8.11	99.72	0.92	91.37
359-6.3	coarse garnet lherzolite	40.27	0.03	0.00	0.03	0.36	50.69	0.03	0.09	7.92	99.42	0.92	91.50
359-8.1	coarse garnet lherzolite	40.33	0.02	0.01	0.05	0.34	51.22	0.02	0.09	8.06	100.13	0.92	91.48
372 11.1	coarse garnet lherzolite	40.70	0.04	0.01	0.05	0.38	50.86	0.03	0.10	8.00	100.16	0.92	91.43
372 11.2	coarse garnet lherzolite	40.46	0.04	0.01	0.05	0.40	50.85	0.03	0.11	7.87	99.81	0.92	91.52
372 11.3	coarse garnet lherzolite	40.68	0.03	0.00	0.04	0.40	51.06	0.02	0.10	7.97	100.30	0.92	91.47
372 6.1	coarse garnet lherzolite	40.53	0.04	0.00	0.04	0.37	51.12	0.03	0.11	7.99	100.23	0.92	91.48
372 6.2	coarse garnet lherzolite	40.50	0.04	0.00	0.03	0.39	50.97	0.03	0.11	7.96	100.03	0.92	91.46
373 12.1	coarse garnet lherzolite	40.66	0.03	0.01	0.02	0.41	50.22	0.02	0.07	8.58	100.02	0.91	90.80
373 12.2	coarse garnet lherzolite	40.40	0.04	0.00	0.01	0.41	50.26	0.02	0.11	8.53	99.78	0.91	90.81
373 12.3	coarse garnet lherzolite	40.21	0.04	0.00	0.03	0.41	49.89	0.03	0.10	8.51	99.21	0.91	90.78
373 9.1	coarse garnet lherzolite	40.53	0.03	0.02	0.02	0.41	50.24	0.02	0.09	8.64	100.00	0.91	90.74
373 9.2	coarse garnet lherzolite	40.44	0.03	0.00	0.01	0.41	50.25	0.03	0.09	8.63	99.89	0.91	90.73
373 9.3	coarse garnet lherzolite	40.42	0.03	0.00	0.02	0.41	50.27	0.02	0.10	8.64	99.91	0.91	90.72
373 1.1	coarse garnet lherzolite	40.52	0.03	0.01	0.04	0.41	50.28	0.03	0.10	8.57	99.99	0.91	90.78
373 1.2	coarse garnet lherzolite	40.53	0.04	0.02	0.02	0.41	50.17	0.02	0.09	8.57	99.87	0.91	90.78
373 1.3	coarse garnet lherzolite	40.49	0.04	0.01	0.02	0.42	50.11	0.02	0.09	8.48	99.68	0.91	90.85
347-20.1	transitional garnet lherzolite	39.94	0.00	0.01	0.02	0.29	48.80	0.03	0.11	11.19	100.40	0.89	88.22
347-20.2	transitional garnet lherzolite	40.19	0.04	0.01	0.03	0.32	48.98	0.02	0.12	11.15	100.85	0.89	88.27
347-20.3	transitional garnet lherzolite	40.05	0.03	0.00	0.05	0.31	48.80	0.03	0.12	11.13	100.50	0.89	88.25
347-25.1	transitional garnet lherzolite	40.09	0.03	0.02	0.02	0.26	48.78	0.03	0.12	11.19	100.54	0.88	88.22
347-25.2	transitional garnet lherzolite	39.75	0.03	0.02	0.01	0.28	48.67	0.02	0.12	11.14	100.04	0.89	88.24
347-25.3	transitional garnet lherzolite	39.93	0.02	0.00	0.01	0.31	48.56	0.04	0.10	11.07	100.04	0.89	88.25
347-16.1	transitional garnet lherzolite	39.82	0.00	0.01	0.04	0.31	48.67	0.02	0.13	11.01	100.03	0.89	88.32
347-16.2	transitional garnet lherzolite	40.01	0.04	0.03	0.03	0.28	48.50	0.02	0.11	11.09	100.11	0.89	88.26
347-16.3	transitional garnet lherzolite	40.04	0.03	0.00	0.03	0.29	48.41	0.01	0.11	11.07	99.99	0.89	88.26

Continued APPENDIX I (olivine analyses)

Sample	Rock type	SiO2	TiO2	Al2O3	Cr2O3	NiO	MgO	CaO	MnO	FeO	Total	X Mg	Fo
347-28.1	transitional garnet lherzolite	40.07	0.02	0.01	0.03	0.30	48.71	0.00	0.13	11.10	100.37	0.89	88.28
347-28.2	transitional garnet lherzolite	40.04	0.03	0.01	0.00	0.28	48.65	0.02	0.12	11.32	100.47	0.88	88.08
347-28.3	transitional garnet lherzolite	40.01	0.00	0.02	0.04	0.32	48.55	0.02	0.12	11.16	100.25	0.88	88.16
347-30.1	transitional garnet lherzolite	39.87	0.04	0.03	0.01	0.30	48.53	0.02	0.13	11.15	100.07	0.88	88.18
347-30.2	transitional garnet lherzolite	39.79	0.00	0.02	0.03	0.29	48.51	0.01	0.12	11.29	100.05	0.88	88.08
347-30.3	transitional garnet lherzolite	39.68	0.03	0.01	0.02	0.28	48.72	0.03	0.11	11.26	100.14	0.88	88.14
347-12.1	transitional garnet lherzolite	39.75	0.03	0.01	0.02	0.27	48.51	0.03	0.12	11.09	99.83	0.89	88.26
347-12.2	transitional garnet lherzolite	39.69	0.04	0.01	0.02	0.28	48.64	0.03	0.11	11.13	99.94	0.89	88.25
347-12.3	transitional garnet lherzolite	39.97	0.03	0.01	0.03	0.27	48.92	0.04	0.11	11.18	100.56	0.89	88.26
382-21.3	porphyroclastic garnet lherzolite	39.98	0.03	0.01	0.05	0.30	48.94	0.03	0.11	11.01	100.45	0.89	88.40
382-25.1	porphyroclastic garnet lherzolite	39.91	0.00	0.01	0.03	0.31	49.01	0.02	0.10	11.21	100.61	0.89	88.25
382-25.2	porphyroclastic garnet lherzolite	40.20	0.04	0.00	0.03	0.32	48.82	0.04	0.14	11.21	100.78	0.88	88.15
382-25.3	porphyroclastic garnet lherzolite	40.00	0.06	0.03	0.05	0.32	48.87	0.03	0.10	11.17	100.64	0.89	88.23
382-16.1	porphyroclastic garnet lherzolite	39.91	0.00	0.01	0.04	0.30	49.05	0.05	0.12	11.27	100.74	0.88	88.16
382-16.2	porphyroclastic garnet lherzolite	40.03	0.00	0.02	0.03	0.32	49.12	0.02	0.10	11.32	100.97	0.88	88.16
382-16.3	porphyroclastic garnet lherzolite	40.00	0.00	0.01	0.02	0.33	49.08	0.02	0.13	11.29	100.88	0.88	88.15
382-1.3	porphyroclastic garnet lherzolite	40.16	0.02	0.02	0.02	0.31	49.06	0.03	0.12	11.17	100.91	0.89	88.27
382-5.1	porphyroclastic garnet lherzolite	39.71	0.00	0.02	0.02	0.33	48.72	0.01	0.11	11.26	100.17	0.88	88.13
382-5.2	porphyroclastic garnet lherzolite	39.89	0.00	0.01	0.02	0.29	48.83	0.02	0.12	11.29	100.48	0.88	88.14
382-5.3	porphyroclastic garnet lherzolite	39.84	0.00	0.00	0.02	0.31	49.05	0.03	0.12	11.23	100.61	0.89	88.21
382-12.1	porphyroclastic garnet lherzolite	39.99	0.00	0.01	0.04	0.31	48.74	0.01	0.12	11.17	100.39	0.89	88.22
382-12.2	porphyroclastic garnet lherzolite	39.94	0.03	0.02	0.04	0.31	48.58	0.03	0.12	11.17	100.24	0.88	88.16
382-12.3	porphyroclastic garnet lherzolite	39.85	0.03	0.01	0.04	0.32	48.87	0.05	0.13	11.27	100.56	0.88	88.10
375 - 2.1	spinel harzburgite	39.06	0.00	0.00	0.00	0.36	51.17	0.02	0.09	7.34	98.03	0.92	92.13
375 - 2.2	spinel harzburgite	39.51	0.00	0.00	0.01	0.37	51.01	0.01	0.08	7.06	98.05	0.93	92.37
375 - 2.3	spinel harzburgite	39.49	0.00	0.00	0.00	0.34	51.18	0.00	0.08	7.26	98.35	0.93	92.25
375 - 6.1	spinel harzburgite	38.55	0.00	0.00	0.00	0.35	51.06	0.00	0.09	7.24	97.29	0.93	92.23

Continued APPENDIX I (olivine analyses)

Sample	Rock type	SiO2	TiO2	Al2O3	Cr2O3	NiO	MgO	CaO	MnO	FeO	Total	X Mg	Fo
375 - 6.2	spinel harzburgite	38.89	0.00	0.00	0.00	0.37	51.10	0.01	0.08	7.26	97.72	0.93	92.19
375 - 6.3	spinel harzburgite	38.55	0.00	0.00	0.00	0.33	50.86	0.02	0.11	7.13	97.01	0.93	92.28
375 - 9.1	spinel harzburgite	38.86	0.00	0.00	0.00	0.34	51.18	0.00	0.11	7.28	97.77	0.93	92.20
375 - 9.2	spinel harzburgite	38.81	0.00	0.00	0.00	0.37	51.27	0.00	0.09	7.33	97.87	0.92	92.16
375 - 9.3	spinel harzburgite	38.78	0.00	0.00	0.01	0.35	51.28	0.00	0.10	7.28	97.80	0.93	92.21
375 - 12.1	spinel harzburgite	39.27	0.00	0.00	0.00	0.35	51.09	0.00	0.10	7.30	98.11	0.92	92.17
375 - 12.2	spinel harzburgite	39.21	0.00	0.01	0.01	0.35	50.96	0.00	0.09	7.27	97.90	0.93	92.19
375 - 12.3	spinel harzburgite	39.23	0.00	0.00	0.00	0.34	51.05	0.01	0.09	7.34	98.06	0.92	92.14
375 - 14.1	spinel harzburgite	39.47	0.00	0.00	0.00	0.37	51.62	0.00	0.09	7.27	98.82	0.93	92.26
375 - 14.2	spinel harzburgite	39.46	0.00	0.00	0.01	0.31	51.30	0.03	0.07	7.28	98.45	0.93	92.26
375 - 14.3	spinel harzburgite	39.61	0.00	0.00	0.01	0.40	51.25	0.00	0.09	7.25	98.60	0.93	92.21
403-6.1	garnet harzburgite	40.28	0.02	0.01	0.04	0.38	50.97	0.03	0.12	8.11	99.96	0.92	91.33
403-6.2	garnet harzburgite	40.31	0.03	0.01	0.05	0.37	51.00	0.03	0.08	8.05	99.92	0.92	91.43
403-6.3	garnet harzburgite	40.25	0.00	0.01	0.04	0.39	50.89	0.02	0.09	7.96	99.64	0.92	91.49
403-2.1	garnet harzburgite	40.44	0.04	0.00	0.04	0.40	50.89	0.02	0.09	8.03	99.93	0.92	91.41
403-2.2	garnet harzburgite	40.50	0.00	0.02	0.06	0.38	51.20	0.03	0.10	8.11	100.40	0.92	91.38
403-2.3	garnet harzburgite	40.43	0.00	0.00	0.04	0.42	51.15	0.00	0.08	8.04	100.17	0.92	91.45
403-16.1	garnet harzburgite	40.39	0.00	0.02	0.05	0.36	51.12	0.02	0.08	8.11	100.14	0.92	91.41
403-16.2	garnet harzburgite	40.40	0.00	0.01	0.05	0.39	50.97	0.02	0.09	8.10	100.03	0.92	91.36
403-16.3	garnet harzburgite	40.36	0.03	0.01	0.03	0.38	50.67	0.02	0.10	7.96	99.56	0.92	91.44
403-13.1	garnet harzburgite	40.21	0.00	0.02	0.03	0.41	50.98	0.01	0.08	8.22	99.96	0.92	91.26
403-13.2	garnet harzburgite	40.01	0.02	0.00	0.02	0.41	50.91	0.03	0.08	8.11	99.58	0.92	91.33
403-13.3	garnet harzburgite	40.29	0.03	0.01	0.02	0.37	50.93	0.03	0.09	8.12	99.89	0.92	91.34
403-10.1	garnet harzburgite	40.27	0.00	0.00	0.04	0.36	51.14	0.05	0.11	8.15	100.12	0.92	91.32
403-10.2	garnet harzburgite	40.43	0.00	0.01	0.03	0.37	51.05	0.01	0.11	8.08	100.10	0.92	91.41
403-10.3	garnet harzburgite	40.39	0.02	0.00	0.04	0.41	51.00	0.01	0.09	8.00	99.96	0.92	91.45

Continued APPENDIX I (olivine analyses)

Sample	Rock type	SiO2	TiO2	Al2O3	Cr2O3	NiO	MgO	CaO	MnO	FeO	Total	X Mg	Fo
351 8.1	heterogeneous sample	40.48	0.00	0.00	0.00	0.39	51.31	0.01	0.09	7.51	99.80	0.92	91.97
351 8.2	heterogeneous sample	40.20	0.00	0.00	0.00	0.39	50.90	0.00	0.09	7.41	99.00	0.92	92.01
351 8.3	heterogeneous sample	40.27	0.00	0.02	0.00	0.38	50.72	0.01	0.10	7.45	98.94	0.92	91.94
351 6.1	heterogeneous sample	40.75	0.00	0.18	0.01	0.38	51.83	0.08	0.08	7.39	100.70	0.93	92.09
351 6.2	heterogeneous sample	40.27	0.00	0.00	0.00	0.38	51.05	0.01	0.08	7.47	99.27	0.92	91.98
351 6.3	heterogeneous sample	40.19	0.00	0.01	0.01	0.37	50.72	0.01	0.08	7.38	98.77	0.92	92.03
351 12.1	heterogeneous sample	40.47	0.00	0.00	0.00	0.38	50.70	0.01	0.09	7.48	99.13	0.92	91.91
351 12.2	heterogeneous sample	40.77	0.00	0.01	0.00	0.39	51.00	0.01	0.08	7.42	99.68	0.92	92.01
351 12.3	heterogeneous sample	40.63	0.00	0.00	0.00	0.38	51.04	0.01	0.08	7.37	99.51	0.92	92.08
351 11.1	heterogeneous sample	40.85	0.00	0.00	0.01	0.38	51.39	0.01	0.08	7.38	100.10	0.92	92.12
351 11.2	heterogeneous sample	40.84	0.00	0.00	0.00	0.38	51.21	0.00	0.09	7.45	99.97	0.92	92.03
351 11.3	heterogeneous sample	40.51	0.00	0.01	0.00	0.40	50.94	0.01	0.10	7.40	99.38	0.92	92.00
351 9.1	heterogeneous sample	40.53	0.00	0.01	0.01	0.36	51.18	0.01	0.09	7.42	99.60	0.92	92.06
351 9.2	heterogeneous sample	40.75	0.00	0.00	0.00	0.39	51.33	0.01	0.10	7.35	99.93	0.92	92.11
351 9.3	heterogeneous sample	40.53	0.00	0.00	0.01	0.38	51.34	0.00	0.10	7.40	99.76	0.92	92.09
351 21.1	heterogeneous sample	40.54	0.00	0.00	0.00	0.37	51.06	0.02	0.10	7.34	99.42	0.92	92.09
351 21.2	heterogeneous sample	40.24	0.00	0.02	0.00	0.36	50.76	0.02	0.09	7.37	98.87	0.92	92.03
351 21.3	heterogeneous sample	40.53	0.00	0.00	0.02	0.38	51.07	0.01	0.09	7.40	99.51	0.92	92.05
351 18.1	heterogeneous sample	40.45	0.00	0.00	0.01	0.38	50.98	0.01	0.08	7.42	99.34	0.92	92.02
351 18.2	heterogeneous sample	40.51	0.00	0.00	0.02	0.38	50.55	0.01	0.10	7.43	99.00	0.92	91.93
351 18.3	heterogeneous sample	40.37	0.00	0.01	0.00	0.38	50.86	0.01	0.08	7.42	99.14	0.92	92.01
394 - 23.1	heterogeneous sample	40.22	0.00	0.00	0.01	0.38	51.22	0.00	0.07	7.44	99.34	0.92	92.06
394 - 23.2	heterogeneous sample	40.38	0.00	0.00	0.01	0.36	51.76	0.00	0.09	7.39	99.99	0.92	92.18
394 - 23.3	heterogeneous sample	40.33	0.00	0.00	0.01	0.33	51.53	0.00	0.08	7.56	99.84	0.92	92.03
394 - 21.1	heterogeneous sample	39.69	0.00	0.00	0.03	0.36	51.14	0.00	0.08	7.43	98.74	0.92	92.06
394 - 21.2	heterogeneous sample	39.81	0.04	0.00	0.01	0.36	51.37	0.00	0.07	7.56	99.21	0.92	91.99
394 - 21.3	heterogeneous sample	40.00	0.00	0.00	0.00	0.36	51.25	0.00	0.07	7.39	99.07	0.92	92.13

Continued APPENDIX I (olivine)

Sample	Rock type	SiO2	TiO2	Al2O3	Cr2O3	NiO	MgO	CaO	MnO	FeO	Total	X Mg	Fo
394 - 18.1	heterogeneous sample	39.82	0.00	0.00	0.03	0.39	51.18	0.01	0.09	7.41	98.93	0.92	92.04
394 - 18.2	heterogeneous sample	39.91	0.00	0.00	0.01	0.37	51.34	0.00	0.08	7.44	99.16	0.92	92.08
394 - 18.3	heterogeneous sample	40.14	0.00	0.00	0.03	0.32	51.29	0.02	0.08	7.65	99.53	0.92	91.89
394 - 4.1	heterogeneous sample	39.78	0.00	0.01	0.00	0.34	51.00	0.00	0.08	7.31	98.52	0.92	92.17
394 - 4.2	heterogeneous sample	39.72	0.03	0.00	0.00	0.36	51.18	0.00	0.08	7.58	98.96	0.92	91.93
394 - 4.3	heterogeneous sample	39.77	0.00	0.01	0.00	0.33	51.25	0.00	0.09	7.38	98.83	0.92	92.14
394 - 3.1	heterogeneous sample	39.90	0.00	0.01	0.01	0.38	50.71	0.00	0.08	7.40	98.49	0.92	92.02
394 - 3.2	heterogeneous sample	39.92	0.00	0.00	0.01	0.37	51.01	0.01	0.08	7.48	98.88	0.92	91.98
394 - 3.3	heterogeneous sample	40.05	0.00	0.00	0.01	0.39	51.02	0.04	0.08	7.50	99.09	0.92	91.91
394 - 19.1	heterogeneous sample	39.93	0.00	0.00	0.02	0.39	51.21	0.00	0.09	7.53	99.17	0.92	91.95
394 - 19.2	heterogeneous sample	39.61	0.00	0.00	0.04	0.37	51.48	0.00	0.09	7.58	99.16	0.92	91.96
394 - 19.3	heterogeneous sample	39.66	0.00	0.00	0.00	0.36	51.65	0.01	0.09	7.54	99.31	0.92	92.02
368 8.1	spinel-garnet lherzolite	40.54	0.02	0.01	0.02	0.37	50.98	0.00	0.09	7.82	99.85	0.92	91.66
368 8.2	spinel-garnet lherzolite	40.60	0.00	0.00	0.00	0.37	50.91	0.01	0.07	7.81	99.79	0.92	91.66
368 8.3	spinel-garnet lherzolite	40.51	0.00	0.01	0.01	0.36	50.97	0.01	0.08	7.84	99.80	0.92	91.65
368 31.1	spinel-garnet lherzolite	40.47	0.02	0.00	0.00	0.35	51.18	0.01	0.09	7.79	99.91	0.92	91.73
368 31.2	spinel-garnet lherzolite	40.58	0.00	0.01	0.00	0.36	50.95	0.01	0.09	7.90	99.92	0.92	91.58
368 31.3	spinel-garnet lherzolite	40.52	0.02	0.00	0.00	0.36	50.90	0.01	0.07	7.85	99.71	0.92	91.65
368 29.1	spinel-garnet lherzolite	40.42	0.00	0.00	0.00	0.35	50.89	0.00	0.09	7.79	99.55	0.92	91.70
368 29.2	spinel-garnet lherzolite	40.56	0.00	0.00	0.00	0.37	50.81	0.01	0.09	7.82	99.67	0.92	91.63
368 29.3	spinel-garnet lherzolite	40.55	0.00	0.00	0.01	0.36	50.72	0.01	0.09	7.81	99.55	0.92	91.64
368 27.1	spinel-garnet lherzolite	40.51	0.02	0.00	0.00	0.37	50.71	0.01	0.09	7.76	99.46	0.92	91.67
368 27.2	spinel-garnet lherzolite	40.44	0.00	0.00	0.00	0.36	50.91	0.01	0.10	7.85	99.67	0.92	91.61
368 27.3	spinel-garnet lherzolite	40.61	0.00	0.00	0.02	0.36	50.97	0.01	0.09	7.82	99.90	0.92	91.65
368 26.1	spinel-garnet lherzolite	40.62	0.00	0.00	0.01	0.36	50.94	0.01	0.08	7.84	99.87	0.92	91.65
368 26.2	spinel-garnet lherzolite	40.68	0.02	0.00	0.00	0.37	50.86	0.01	0.09	7.80	99.82	0.92	91.66
368 26.3	spinel-garnet lherzolite	40.65	0.00	0.01	0.00	0.36	50.89	0.01	0.08	7.87	99.87	0.92	91.61

Continued APPENDIX I (olivine analyses)

Sample	Rock type	SiO2	TiO2	Al2O3	Cr2O3	NiO	MgO	CaO	MnO	FeO	Total	X Mg	Fo
402-19.1	spinel-garnet lherzolite	40.17	0.00	0.00	0.01	0.40	51.48	0.00	0.09	7.75	99.90	0.92	91.77
402-19.2	spinel-garnet lherzolite	40.40	0.00	0.01	0.00	0.40	51.43	0.00	0.10	7.70	100.03	0.92	91.81
402-19.3	spinel-garnet lherzolite	40.44	0.00	0.01	0.01	0.39	51.13	0.00	0.08	7.74	99.81	0.92	91.75
402-20.1	spinel-garnet lherzolite	40.17	0.00	0.00	0.00	0.40	51.19	0.01	0.07	7.75	99.61	0.92	91.73
402-20.2	spinel-garnet lherzolite	40.24	0.00	0.00	0.00	0.39	51.07	0.00	0.07	7.72	99.50	0.92	91.77
402-20.3	spinel-garnet lherzolite	40.40	0.00	0.01	0.02	0.38	51.22	0.00	0.12	7.68	99.83	0.92	91.80
402-16.2	spinel-garnet lherzolite	40.34	0.00	0.00	0.01	0.39	51.00	0.00	0.09	7.65	99.47	0.92	91.81
402-16.3	spinel-garnet lherzolite	40.28	0.00	0.00	0.00	0.38	51.16	0.01	0.08	7.68	99.59	0.92	91.80
402-15.1	spinel-garnet lherzolite	39.87	0.00	0.01	0.02	0.38	51.21	0.00	0.10	7.83	99.42	0.92	91.67
402-15.2	spinel-garnet lherzolite	40.28	0.00	0.00	0.00	0.36	51.32	0.00	0.08	7.82	99.85	0.92	91.74
402-15.3	spinel-garnet lherzolite	40.23	0.02	0.03	0.00	0.36	51.39	0.00	0.08	7.73	99.84	0.92	91.82
402-10.1	spinel-garnet lherzolite	40.29	0.00	0.00	0.01	0.38	50.99	0.00	0.08	7.49	99.24	0.92	91.97
402-10.2	spinel-garnet lherzolite	40.26	0.00	0.00	0.03	0.38	50.95	0.00	0.09	7.48	99.18	0.92	91.97
402-10.3	spinel-garnet lherzolite	40.01	0.00	0.00	0.01	0.39	51.22	0.00	0.11	7.65	99.39	0.92	91.82
402-8.1	spinel-garnet lherzolite	40.04	0.03	0.00	0.01	0.33	51.03	0.00	0.10	7.72	99.26	0.92	91.79
402-8.2	spinel-garnet lherzolite	40.26	0.03	0.02	0.02	0.36	51.20	0.01	0.10	7.63	99.63	0.92	91.85
402-8.3	spinel-garnet lherzolite	40.28	0.00	0.00	0.00	0.37	51.11	0.01	0.08	7.80	99.65	0.92	91.70
402-7.1	spinel-garnet lherzolite	40.63	0.00	0.02	0.00	0.34	51.09	0.02	0.10	7.61	99.82	0.92	91.86
402-7.2	spinel-garnet lherzolite	40.31	0.02	0.01	0.00	0.40	51.30	0.00	0.08	7.74	99.85	0.92	91.77
402-7.3	spinel-garnet lherzolite	40.56	0.00	0.02	0.00	0.35	50.98	0.00	0.08	7.65	99.64	0.92	91.84
402-4.2	spinel-garnet lherzolite	40.51	0.00	0.01	0.01	0.37	51.16	0.00	0.08	7.59	99.74	0.92	91.92
402-4.3	spinel-garnet lherzolite	40.44	0.00	0.01	0.01	0.37	51.17	0.00	0.08	7.63	99.72	0.92	91.88
402-23.1	spinel-garnet lherzolite	40.08	0.00	0.00	0.01	0.35	50.84	0.00	0.09	7.79	99.17	0.92	91.69
402-23.2	spinel-garnet lherzolite	40.35	0.00	0.00	0.02	0.36	50.68	0.00	0.09	7.62	99.13	0.92	91.81
402-23.3	spinel-garnet lherzolite	40.22	0.00	0.00	0.00	0.40	50.86	0.01	0.08	7.47	99.05	0.92	91.94
345-1.1	wehrlite	39.28	0.08	0.00	0.02	0.26	48.41	0.01	0.13	11.35	99.54	0.88	88.02
345-1.2	wehrlite	39.61	0.04	0.00	0.03	0.27	48.41	0.01	0.10	11.30	99.76	0.88	88.08
345-1.3	wehrlite	39.49	0.00	0.03	0.02	0.27	48.04	0.01	0.13	11.18	99.16	0.88	88.09

Continued APPENDIX I (olivine analyses)

Sample	Rock type	SiO2	TiO2	Al2O3	Cr2O3	NiO	MgO	CaO	MnO	FeO	Total	X Mg	Fo
345-5.1	wehrlite	39.25	0.02	0.01	0.02	0.25	48.36	0.01	0.13	11.41	99.46	0.88	87.97
345-5.2	wehrlite	39.50	0.00	0.00	0.00	0.27	48.22	0.02	0.13	11.27	99.42	0.88	88.03
345-6.2	wehrlite	40.31	0.00	0.01	0.01	0.26	48.71	0.02	0.12	11.28	100.72	0.88	88.15
345-6.3	wehrlite	40.19	0.00	0.01	0.01	0.25	48.81	0.00	0.12	11.30	100.70	0.88	88.18
345-7.1	wehrlite	39.73	0.00	0.00	0.01	0.27	48.30	0.01	0.12	11.39	99.83	0.88	87.96
345-7.2	wehrlite	39.94	0.00	0.00	0.01	0.25	48.69	0.00	0.12	11.39	100.41	0.88	88.08
345-8.1	wehrlite	39.68	0.00	0.03	0.01	0.24	48.47	0.02	0.14	11.22	99.80	0.88	88.15
345-8.2	wehrlite	39.69	0.00	0.02	0.01	0.26	48.61	0.00	0.14	11.41	100.14	0.88	88.01
345-8.3	wehrlite	39.79	0.00	0.00	0.02	0.23	48.77	0.02	0.13	11.37	100.34	0.88	88.10
345-9.1	wehrlite	39.46	0.00	0.01	0.02	0.25	48.33	0.00	0.10	11.38	99.55	0.88	88.02
345-9.2	wehrlite	39.68	0.00	0.01	0.01	0.24	48.60	0.00	0.11	11.25	99.91	0.88	88.19
345-9.3	wehrlite	39.27	0.02	0.00	0.01	0.25	48.75	0.01	0.13	11.33	99.77	0.88	88.12
345-12.1	wehrlite	39.68	0.06	0.00	0.01	0.23	48.05	0.00	0.11	11.38	99.52	0.88	87.97
345-12.2	wehrlite	39.54	0.00	0.04	0.03	0.27	48.10	0.00	0.14	11.38	99.49	0.88	87.92
345-12.3	wehrlite	39.51	0.08	0.00	0.01	0.24	48.32	0.03	0.12	11.37	99.69	0.88	87.98
354-1.1	wehrlite	38.74	0.00	0.03	0.02	0.23	48.01	0.00	0.13	11.27	98.44	0.88	88.04
354-1.2	wehrlite	38.86	0.00	0.01	0.01	0.21	47.76	0.02	0.12	11.59	98.58	0.88	87.70
354-1.3	wehrlite	38.99	0.02	0.00	0.02	0.21	47.89	0.02	0.13	11.42	98.69	0.88	87.88
354-5.1	wehrlite	39.39	0.06	0.00	0.00	0.22	48.26	0.03	0.15	11.40	99.50	0.88	87.95
354-5.2	wehrlite	39.37	0.00	0.00	0.02	0.22	48.19	0.01	0.13	11.57	99.52	0.88	87.80
354-5.3	wehrlite	39.27	0.00	0.00	0.02	0.21	48.22	0.00	0.13	11.34	99.19	0.88	88.05
354-7.1	wehrlite	39.89	0.00	0.00	0.02	0.18	48.34	0.02	0.13	11.47	100.05	0.88	87.95
354-7.2	wehrlites	39.46	0.02	0.01	0.02	0.21	48.25	0.00	0.13	11.41	99.51	0.88	87.98
354-7.3	wehrlite	39.45	0.00	0.00	0.01	0.20	48.17	0.00	0.13	11.42	99.39	0.88	87.97
354-8.1	wehrlite	39.77	0.02	0.01	0.01	0.23	48.39	0.00	0.13	11.43	100.00	0.88	87.98
354-8.2	wehrlite	39.79	0.04	0.00	0.01	0.21	48.59	0.01	0.11	11.37	100.12	0.88	88.11
354-8.3	wehrlite	39.90	0.00	0.00	0.01	0.23	48.13	0.01	0.12	11.27	99.67	0.88	88.07

Continued APPENDIX I (olivine analyses)

Sample	Rock type	SiO2	TiO2	Al2O3	Cr2O3	NiO	MgO	CaO	MnO	FeO	Total	X Mg	Fo
358-1.1	Wehrlite	39.06	0.00	0.00	0.01	0.22	48.79	0.10	0.11	11.58	99.88	0.88	87.85
358-1.2	wehrlite	39.09	0.00	0.00	0.01	0.23	48.87	0.00	0.12	11.59	99.91	0.88	87.96
358-1.3	wehrlite	39.06	0.00	0.01	0.01	0.23	48.68	0.00	0.14	11.54	99.66	0.88	87.94
358-4.1	wehrlite	39.91	0.03	0.03	0.02	0.21	48.77	0.01	0.12	11.64	100.75	0.88	87.88
358-4.2	wehrlite	39.65	0.00	0.00	0.00	0.20	48.63	0.01	0.14	11.62	100.25	0.88	87.87
358-6.1	wehrlite	39.76	0.00	0.01	0.02	0.19	48.68	0.05	0.13	11.56	100.40	0.88	87.90
358-6.2	wehrlite	39.96	0.00	0.02	0.00	0.24	48.94	0.00	0.12	11.67	100.95	0.88	87.89
363 6.2	garnet wehrlite	39.73	0.05	0.01	0.04	0.39	49.20	0.02	0.12	9.77	99.33	0.90	89.49
363 6.3	garnet wehrlite	39.27	0.03	0.00	0.03	0.38	49.50	0.02	0.12	9.89	99.25	0.90	89.45
363 5.1	garnet wehrlite	40.18	0.04	0.01	0.03	0.38	49.48	0.03	0.12	9.88	100.15	0.90	89.45
363 5.2	garnet wehrlite	40.09	0.04	0.00	0.02	0.38	49.38	0.03	0.13	9.93	99.99	0.90	89.38
363 5.3	garnet wehrlite	40.24	0.02	0.03	0.02	0.37	49.63	0.03	0.11	9.87	100.32	0.90	89.51
363 11.1	garnet wehrlite	40.10	0.04	0.01	0.03	0.38	49.12	0.03	0.11	9.98	99.80	0.90	89.29
363 11.2	garnet wehrlite	40.26	0.04	0.02	0.03	0.37	49.37	0.07	0.12	9.90	100.17	0.90	89.38
363 9.1	garnet wehrlite	40.42	0.04	0.00	0.03	0.39	49.67	0.03	0.12	9.93	100.63	0.90	89.44
363 9.2	garnet wehrlite	40.21	0.03	0.01	0.02	0.38	49.32	0.02	0.12	9.86	99.97	0.90	89.44
363 9.3	garnet wehrlite	40.03	0.03	0.00	0.02	0.39	49.44	0.02	0.12	9.96	100.01	0.90	89.37
363 8.1	garnet wehrlite	40.04	0.04	0.00	0.03	0.37	49.22	0.03	0.12	9.85	99.70	0.90	89.44
363 8.2	garnet wehrlite	40.27	0.05	0.01	0.01	0.38	49.39	0.03	0.13	9.97	100.23	0.90	89.35
363 8.3	garnet wehrlite	40.07	0.04	0.00	0.02	0.36	49.30	0.03	0.12	10.01	99.96	0.90	89.31
363 13.1	garnet wehrlite	40.18	0.03	0.01	0.03	0.38	49.25	0.03	0.12	9.82	99.84	0.90	89.47
363 13.2	garnet wehrlite	39.96	0.03	0.05	0.03	0.40	48.75	0.03	0.11	9.76	99.12	0.90	89.40
363 13.3	garnet wehrlite	40.04	0.04	0.00	0.03	0.39	49.39	0.02	0.13	9.97	100.01	0.90	89.34
398-4.1	garnet wehrlite	39.96	0.00	0.01	0.05	0.29	49.22	0.01	0.12	10.54	100.21	0.89	88.90
398-4.2	garnet wehrlite	40.00	0.05	0.00	0.01	0.31	49.34	0.03	0.12	10.65	100.49	0.89	88.80
398-4.3	garnet wehrlite	40.05	0.02	0.00	0.02	0.29	49.55	0.01	0.10	10.71	100.76	0.89	88.83
398-2.1	garnet wehrlite	39.87	0.04	0.00	0.03	0.30	48.82	0.01	0.11	11.22	100.41	0.88	88.21

Continued APPENDIX I (olivine analyses)

Sample	Rock type	SiO2	TiO2	Al2O3	Cr2O3	NiO	MgO	CaO	MnO	FeO	Total	X Mg	Fo
398-2.2	garnet wehrlite	39.93	0.03	0.01	0.01	0.26	48.83	0.04	0.13	11.26	100.49	0.88	88.16
398-2.3	garnet wehrlite	39.94	0.04	0.00	0.04	0.28	48.78	0.02	0.11	11.23	100.43	0.88	88.21
398-5.1	garnet wehrlite	40.08	0.00	0.00	0.02	0.28	48.88	0.03	0.11	11.32	100.72	0.88	88.14
398-5.2	garnet wehrlites	39.94	0.00	0.02	0.02	0.26	48.84	0.01	0.10	11.30	100.50	0.88	88.19
398-5.3	garnet wehrlite	40.00	0.03	0.00	0.03	0.28	48.99	0.01	0.14	11.34	100.83	0.88	88.12
398-15.1	garnet wehrlite	40.04	0.07	0.01	0.02	0.26	48.94	0.01	0.13	11.39	100.86	0.88	88.10
398-15.2	garnet wehrlite	39.97	0.03	0.00	0.01	0.29	48.93	0.01	0.12	11.28	100.64	0.88	88.18
398-15.3	garnet wehrlite	40.12	0.02	0.00	0.01	0.28	48.81	0.02	0.11	11.34	100.72	0.88	88.10
399-17.3	garnet wehrlite	40.11	0.05	0.01	0.02	0.30	48.70	0.00	0.12	11.21	100.52	0.88	88.19
398-18.1	garnet wehrlite	40.04	0.05	0.02	0.03	0.27	48.76	0.03	0.11	11.24	100.54	0.88	88.19
398-18.2	garnet wehrlite	40.07	0.04	0.00	0.00	0.25	48.54	0.02	0.11	11.33	100.36	0.88	88.08
398-18.3	garnet wehrlite	40.13	0.03	0.01	0.00	0.29	48.61	0.03	0.13	11.29	100.53	0.88	88.06
398-18.1	garnet wehrlite	40.04	0.03	0.00	0.02	0.26	48.68	0.02	0.14	11.30	100.48	0.88	88.11
398-18.2	garnet wehrlite	40.08	0.02	0.01	0.01	0.25	48.65	0.04	0.12	11.34	100.52	0.88	88.06
398-18.3	garnet wehrlite	40.10	0.04	0.00	0.01	0.29	48.98	0.02	0.12	11.28	100.84	0.88	88.18
398-13.1	garnet wehrlite	40.05	0.05	0.03	0.02	0.28	48.66	0.03	0.13	11.33	100.57	0.88	88.05
398-13.2	garnet wehrlite	40.06	0.02	0.00	0.02	0.28	48.72	0.02	0.12	11.36	100.61	0.88	88.05
398-13.3	garnet wehrlite	39.97	0.03	0.01	0.02	0.27	48.94	0.00	0.12	11.35	100.71	0.88	88.15

APPENDIX II

Electron microprobe core analyses of orthopyroxenes from the Voyageur peridotite xenoliths

Sample	Rock type	SiO2	TiO2	Al2O3	Cr2O3	MgO	CaO	MnO	FeO	Na2O	K2O	Total	X Mg
343-1.1	coarse garnet lherzolite	56.89	0.10	0.56	0.24	34.81	0.56	0.09	5.04	0.16	0.00	98.45	0.92
343-1.2	coarse garnet lherzolite	56.81	0.14	0.57	0.23	34.68	0.58	0.10	5.09	0.17	0.00	98.38	0.92
343-1.3	coarse garnet lherzolite	56.94	0.13	0.56	0.23	34.56	0.59	0.10	5.04	0.16	0.00	98.32	0.92
343-9.1	coarse garnet lherzolite	56.88	0.12	0.60	0.24	34.89	0.60	0.10	5.08	0.15	0.01	98.68	0.92
343-9.2	coarse garnet lherzolite	57.11	0.13	0.57	0.24	34.84	0.58	0.10	5.03	0.17	0.01	98.78	0.93
343-9.3	coarse garnet lherzolite	57.11	0.12	0.58	0.24	35.01	0.60	0.13	5.01	0.16	0.00	98.94	0.93
343 - 30.1	coarse garnet lherzolite	56.13	0.10	0.56	0.24	35.15	0.61	0.13	5.23	0.12	0.02	98.28	0.92
343 - 30.2	coarse garnet lherzolite	56.27	0.09	0.59	0.26	34.88	0.63	0.13	5.18	0.14	0.01	98.16	0.92
343 - 31.1	coarse garnet lherzolite	56.48	0.12	0.60	0.21	34.89	0.59	0.11	5.22	0.10	0.00	98.33	0.92
343 - 31.2	coarse garnet lherzolite	56.27	0.09	0.58	0.25	34.85	0.60	0.11	5.23	0.17	0.00	98.16	0.92
343 - 31.3	coarse garnet lherzolite	56.56	0.08	0.59	0.24	34.89	0.62	0.11	5.15	0.15	0.01	98.39	0.92
343 - 32.2	coarse garnet lherzolite	56.38	0.06	0.61	0.26	34.83	0.61	0.11	5.10	0.13	0.00	98.08	0.92
343 - 32.3	coarse garnet lherzolite	56.50	0.11	0.59	0.25	34.85	0.58	0.13	5.12	0.11	0.00	98.24	0.92
347-1.1	transitional garnet lherzolite	56.67	0.14	0.60	0.19	34.14	0.64	0.11	6.49	0.16	0.00	99.14	0.90
347-1.2	transitional garnet lherzolite	56.63	0.13	0.54	0.19	34.17	0.63	0.14	6.49	0.14	0.01	99.05	0.90
347-1.3	transitional garnet lherzolite	56.70	0.15	0.58	0.19	34.05	0.67	0.12	6.55	0.16	0.00	99.17	0.90
347-19.1	transitional garnet lherzolite	56.74	0.13	0.58	0.20	34.29	0.64	0.13	6.47	0.15	0.00	99.33	0.90
347-19.2	transitional garnet lherzolite	56.62	0.13	0.58	0.20	34.19	0.64	0.14	6.45	0.17	0.00	99.12	0.90
347-19.3	transitional garnet lherzolite	56.34	0.16	0.60	0.20	33.81	0.65	0.14	6.50	0.16	0.01	98.56	0.90
347-3.1	transitional garnet lherzolite	56.53	0.15	0.58	0.23	34.31	0.60	0.12	6.51	0.15	0.01	99.18	0.90
347-3.2	transitional garnet lherzolite	56.67	0.12	0.57	0.22	34.19	0.60	0.11	6.37	0.15	0.00	98.99	0.91
347-3.3	transitional garnet lherzolite	56.38	0.13	0.57	0.22	34.07	0.61	0.13	6.39	0.16	0.01	98.66	0.90
347-4.1	transitional garnet lherzolite	56.64	0.13	0.53	0.20	34.35	0.66	0.13	6.51	0.19	0.00	99.34	0.90
347-4.2	transitional garnet lherzolite	56.96	0.14	0.56	0.20	34.28	0.65	0.12	6.46	0.15	0.01	99.54	0.90
347-4.3	transitional garnet lherzolite	56.79	0.14	0.56	0.19	34.30	0.64	0.13	6.38	0.14	0.00	99.27	0.91
347-7.1	transitional garnet lherzolite	56.86	0.13	0.55	0.21	34.19	0.60	0.13	6.40	0.12	0.01	99.20	0.90
347-7.2	transitional garnet lherzolite	56.50	0.14	0.55	0.19	34.27	0.63	0.12	6.47	0.16	0.00	99.03	0.90

Continued APPENDIX II (opx analyses)

Sample	Rock type	SiO2	TiO2	Al2O3	Cr2O3	MgO	CaO	MnO	FeO	Na2O	K2O	Total	X Mg
347-7.3	transitional garnet lherzolite	56.41	0.13	0.56	0.20	34.27	0.62	0.12	6.49	0.17	0.00	98.96	0.90
347-27.1	transitional garnet lherzolite	56.49	0.14	0.56	0.20	34.06	0.62	0.12	6.40	0.14	0.00	98.73	0.90
347-27.2	transitional garnet lherzolite	56.51	0.13	0.59	0.20	34.02	0.63	0.13	6.44	0.13	0.00	98.77	0.90
347-27.3	transitional garnet lherzolite	56.60	0.13	0.58	0.21	34.15	0.64	0.12	6.41	0.10	0.01	98.94	0.90
347-27.1	transitional garnet lherzolite	56.63	0.14	0.61	0.20	34.27	0.64	0.13	6.40	0.18	0.00	99.21	0.91
347-27.2	transitional garnet lherzolite	56.69	0.14	0.60	0.19	34.28	0.67	0.14	6.48	0.16	0.00	99.35	0.90
347-27-3	transitional garnet lherzolite	56.74	0.13	0.58	0.18	34.26	0.68	0.11	6.54	0.15	0.02	99.39	0.90
347-29.1	transitional garnet lherzolite	56.61	0.13	0.57	0.21	34.25	0.60	0.12	6.44	0.17	0.00	99.10	0.90
347-29.2	transitional garnet lherzolite	56.67	0.11	0.60	0.22	34.22	0.64	0.12	6.48	0.14	0.01	99.20	0.90
347-29.3	transitional garnet lherzolite	56.87	0.11	0.64	0.22	34.08	0.63	0.11	6.47	0.14	0.00	99.27	0.90
347-13.1	transitional garnet lherzolite	56.36	0.11	0.58	0.19	34.22	0.61	0.11	6.52	0.16	0.00	98.86	0.90
347-13.2	transitional garnet lherzolite	56.37	0.13	0.59	0.21	34.24	0.63	0.13	6.40	0.16	0.00	98.85	0.91
347-13.3	transitional garnet lherzolite	56.49	0.12	0.53	0.20	34.16	0.60	0.13	6.44	0.14	0.00	98.81	0.90
347-11.1	transitional garnet lherzolite	56.37	0.17	0.58	0.22	34.26	0.63	0.12	6.43	0.17	0.00	98.94	0.90
347-11.2	transitional garnet lherzolite	56.41	0.16	0.61	0.23	34.45	0.62	0.13	6.46	0.13	0.00	99.20	0.90
347-11.3	transitional garnet lherzolite	56.55	0.11	0.61	0.23	34.24	0.63	0.12	6.34	0.15	0.02	98.99	0.91
359-12.1	coarse garnet lherzolite	57.15	0.14	0.58	0.28	35.62	0.57	0.10	4.72	0.16	0.00	99.32	0.93
359-12.2	coarse garnet lherzolite	57.40	0.15	0.55	0.28	35.84	0.59	0.09	4.67	0.16	0.00	99.74	0.93
359-12.3	coarse garnet lherzolite	57.26	0.14	0.54	0.28	35.51	0.58	0.09	4.70	0.15	0.01	99.26	0.93
359-14.1	coarse garnet lherzolite	57.12	0.15	0.55	0.24	35.65	0.56	0.10	4.72	0.17	0.00	99.26	0.93
359-14.2	coarse garnet lherzolite	57.25	0.12	0.55	0.26	35.70	0.62	0.11	4.65	0.18	0.01	99.45	0.93
359-14.3	coarse garnet lherzolite	57.04	0.11	0.55	0.30	35.51	0.56	0.09	4.72	0.16	0.00	99.05	0.93
359 - 17.1	coarse garnet lherzolite	57.14	0.11	0.56	0.30	35.57	0.58	0.12	4.69	0.16	0.00	99.23	0.93
359 - 17.2	coarse garnet lherzolite	57.48	0.19	0.59	0.30	35.60	0.52	0.11	4.82	0.14	0.00	99.76	0.93
359 - 17.3	coarse garnet lherzolite	57.34	0.11	0.60	0.26	35.47	0.57	0.11	4.77	0.23	0.00	99.44	0.93
372-22.1	coarse garnet lherzolite	56.60	0.14	0.54	0.35	35.46	0.59	0.10	4.68	0.16	0.00	98.62	0.93
372-22.2	coarse garnet lherzolite	56.70	0.16	0.54	0.32	35.29	0.53	0.10	4.71	0.16	0.01	98.50	0.93
372-13.1	coarse garnet lherzolite	56.82	0.13	0.55	0.36	34.86	0.59	0.11	4.68	0.20	0.00	98.29	0.93
372-13.2	coarse garnet lherzolite	56.78	0.14	0.53	0.36	35.12	0.53	0.08	4.66	0.16	0.01	98.37	0.93
372-13.3	coarse garnet lherzolite	56.64	0.12	0.54	0.34	35.13	0.55	0.11	4.70	0.16	0.00	98.29	0.93

Continued APPENDIX II (opx analyses)

Sample	Rock type	SiO2	TiO2	Al2O3	Cr2O3	MgO	CaO	MnO	FeO	Na2O	K2O	Total	X Mg
372-10.1	coarse garnet lherzolite	56.91	0.12	0.55	0.36	35.18	0.55	0.10	4.65	0.19	0.00	98.60	0.93
372-10.2	coarse garnet lherzolite	56.80	0.15	0.60	0.36	35.22	0.57	0.12	4.65	0.16	0.00	98.62	0.93
372-10.3	coarse garnet lherzolite	56.80	0.14	0.56	0.36	35.33	0.54	0.09	4.68	0.16	0.01	98.66	0.93
372-9.1	coarse garnet lherzolite	56.88	0.13	0.57	0.35	35.00	0.56	0.12	4.66	0.17	0.01	98.45	0.93
372-9.2	coarse garnet lherzolite	56.60	0.15	0.54	0.36	35.11	0.57	0.10	4.64	0.15	0.00	98.23	0.93
372-9.3	coarse garnet lherzolite	56.49	0.12	0.54	0.33	35.28	0.56	0.11	4.67	0.14	0.00	98.23	0.93
372-1.2	coarse garnet lherzolite	56.58	0.10	0.55	0.33	35.23	0.54	0.10	4.71	0.18	0.01	98.32	0.93
372-1.3	coarse garnet lherzolite	56.46	0.09	0.58	0.34	35.27	0.55	0.10	4.67	0.18	0.00	98.23	0.93
373-3.1	coarse garnet lherzolite	56.84	0.13	0.57	0.17	35.19	0.52	0.07	5.10	0.17	0.00	98.77	0.92
373-4.1	coarse garnet lherzolite	56.70	0.09	0.58	0.17	35.30	0.55	0.11	5.10	0.11	0.00	98.71	0.93
373-4.2	coarse garnet lherzolite	56.67	0.08	0.57	0.16	35.44	0.52	0.09	5.13	0.12	0.00	98.79	0.92
373-4.3	coarse garnet lherzolite	56.86	0.07	0.56	0.17	35.32	0.56	0.09	5.13	0.14	0.00	98.90	0.92
382-4.1	porphyroclastic garnet lherzolite	56.82	0.13	0.64	0.23	34.21	0.72	0.12	6.67	0.23	0.00	99.77	0.90
382-4.2	porphyroclastic garnet lherzolite	56.77	0.11	0.65	0.22	34.18	0.75	0.11	6.59	0.19	0.00	99.57	0.90
382-4.3	porphyroclastic garnet lherzolite	56.44	0.12	0.65	0.22	34.23	0.73	0.15	6.66	0.20	0.00	99.40	0.90
382-27.1	porphyroclastic garnet lherzolite	56.66	0.12	0.65	0.21	34.31	0.74	0.13	6.61	0.21	0.00	99.64	0.90
382-27.2	porphyroclastic garnet lherzolite	56.93	0.14	0.65	0.24	34.25	0.78	0.12	6.62	0.19	0.01	99.93	0.90
382-27.3	porphyroclastic garnet lherzolite	57.12	0.14	0.64	0.24	34.05	0.75	0.14	6.61	0.17	0.01	99.86	0.90
382-10.1	porphyroclastic garnet lherzolite	56.64	0.11	0.62	0.23	34.15	0.78	0.12	6.54	0.21	0.01	99.42	0.90
382-10.2	porphyroclastic garnet lherzolite	56.62	0.11	0.68	0.23	34.39	0.79	0.14	6.64	0.21	0.00	99.81	0.90
382-10.3	porphyroclastic garnet lherzolite	56.56	0.14	0.68	0.23	34.11	0.76	0.11	6.73	0.23	0.02	99.57	0.90
382-13.1	porphyroclastic garnet lherzolite	56.59	0.10	0.66	0.24	34.28	0.74	0.13	6.57	0.21	0.00	99.51	0.90
382-13.2	porphyroclastic garnet lherzolite	56.78	0.13	0.65	0.24	34.22	0.72	0.14	6.66	0.21	0.00	99.75	0.90
382-13.3	porphyroclastic garnet lherzolite	56.79	0.13	0.64	0.24	34.02	0.75	0.12	6.66	0.21	0.00	99.56	0.90
382-14.1	porphyroclastic garnet lherzolite	56.90	0.12	0.67	0.23	34.24	0.78	0.13	6.58	0.18	0.00	99.84	0.90
382-14.2	porphyroclastic garnet lherzolite	56.68	0.12	0.63	0.21	34.15	0.76	0.12	6.63	0.22	0.01	99.53	0.90
382-14.3	porphyroclastic garnet lherzolite	57.02	0.13	0.65	0.23	34.16	0.77	0.14	6.60	0.20	0.00	99.91	0.90
382-15.1	porphyroclastic garnet lherzolite	56.79	0.11	0.64	0.20	34.15	0.75	0.14	6.65	0.18	0.00	99.60	0.90
382-15.2	porphyroclastic garnet lherzolite	56.83	0.13	0.66	0.25	34.07	0.78	0.13	6.72	0.20	0.00	99.76	0.90
382-15.3	porphyroclastic garnet lherzolite	56.59	0.16	0.63	0.24	34.06	0.75	0.11	6.61	0.19	0.00	99.34	0.90
375 - 8.1	spinel harzburgite	55.90	0.02	0.99	0.22	35.71	0.17	0.11	4.54	0.05	0.00	97.71	0.93

Continued APPENDIX II (opx analyses)

Sample	Rock type	SiO2	TiO2	Al2O3	Cr2O3	MgO	CaO	MnO	FeO	Na2O	K2O	Total	X Mg
375 - 8.3	spinel harzburgite	55.78	0.00	0.92	0.25	35.70	0.09	0.13	4.69	0.06	0.00	97.61	0.93
375 - 7.1	spinel harzburgite	55.25	0.00	1.06	0.24	35.61	0.16	0.10	4.58	0.06	0.00	97.07	0.93
375 - 7.2	spinel harzburgite	55.55	0.02	0.98	0.27	35.36	0.16	0.10	4.57	0.00	0.00	97.01	0.93
375 - 7.3	spinel harzburgite	55.62	0.00	1.00	0.25	35.76	0.16	0.12	4.57	0.02	0.00	97.50	0.93
375 - 10.1	spinel harzburgite	56.04	0.00	0.95	0.22	35.78	0.13	0.13	4.60	0.06	0.00	97.91	0.93
375 - 10.2	spinel harzburgite	55.19	0.00	1.06	0.23	35.22	0.16	0.11	4.70	0.03	0.00	96.69	0.93
375 - 10.3	spinel harzburgite	56.07	0.00	0.96	0.23	35.66	0.16	0.12	4.73	0.01	0.00	97.94	0.93
375 - 11.1	spinel harzburgite	55.28	0.00	1.13	0.30	35.48	0.14	0.12	4.65	0.00	0.01	97.10	0.93
375 - 11.3	spinel harzburgite	55.37	0.00	1.14	0.34	35.47	0.16	0.11	4.64	0.02	0.00	97.24	0.93
375 - 15.2	spinel harzburgite	56.29	0.00	0.97	0.22	35.65	0.13	0.11	4.69	0.02	0.02	98.10	0.93
375 - 15.3	spinel harzburgite	56.29	0.00	1.03	0.27	35.86	0.14	0.12	4.59	0.02	0.01	98.33	0.93
403-3.1	garnet harzburgite	57.39	0.05	0.54	0.39	35.20	0.52	0.09	4.71	0.12	0.00	99.00	0.93
403-3.2	garnet harzburgite	57.17	0.05	0.57	0.36	35.31	0.55	0.10	4.78	0.23	0.00	99.12	0.93
403-3.3	garnet harzburgite	57.11	0.04	0.56	0.38	35.55	0.53	0.10	4.74	0.18	0.00	99.19	0.93
403-2.1	garnet harzburgite	57.17	0.05	0.55	0.38	35.40	0.53	0.09	4.75	0.15	0.00	99.08	0.93
403-2.2	garnet harzburgite	57.31	0.06	0.54	0.37	35.42	0.55	0.10	4.66	0.20	0.00	99.20	0.93
403-2.3	garnet harzburgite	57.13	0.04	0.55	0.38	35.42	0.56	0.09	4.74	0.18	0.00	99.09	0.93
403-1.1	garnet harzburgite	57.32	0.08	0.53	0.39	35.48	0.56	0.08	4.68	0.19	0.01	99.31	0.93
403-1.2	garnet harzburgite	57.52	0.04	0.54	0.37	35.76	0.55	0.09	4.68	0.20	0.01	99.76	0.93
403-1.3	garnet harzburgite	57.03	0.08	0.54	0.36	35.44	0.53	0.11	4.74	0.12	0.01	98.95	0.93
403-12.1	garnet harzburgite	57.02	0.07	0.55	0.35	35.53	0.55	0.09	4.70	0.17	0.01	99.04	0.93
403-12.2	garnet harzburgite	57.13	0.07	0.56	0.40	35.46	0.56	0.10	4.74	0.19	0.02	99.22	0.93
403-12.3	garnet harzburgite	57.22	0.04	0.58	0.35	35.48	0.54	0.10	4.75	0.18	0.00	99.22	0.93
403-9.1	garnet harzburgite	56.91	0.07	0.56	0.38	35.52	0.54	0.10	4.67	0.17	0.00	98.92	0.93
403-9.2	garnet harzburgite	57.39	0.06	0.53	0.38	35.70	0.56	0.11	4.76	0.15	0.00	99.64	0.93
403-9.3	garnet harzburgite	57.44	0.08	0.58	0.38	35.66	0.52	0.08	4.58	0.18	0.00	99.50	0.93
403-21.1	garnet harzburgite	57.10	0.07	0.56	0.38	35.41	0.54	0.11	4.71	0.14	0.00	99.02	0.93
403-21.2	garnet harzburgite	57.23	0.05	0.52	0.39	35.49	0.52	0.11	4.70	0.23	0.00	99.24	0.93
403-21.3	garnet harzburgite	56.86	0.05	0.54	0.39	35.54	0.57	0.09	4.67	0.22	0.00	98.94	0.93
403-17.1	garnet harzburgite	57.36	0.04	0.56	0.33	35.60	0.53	0.09	4.78	0.20	0.02	99.51	0.93

Continued APPENDIX II (opx analyses)

Sample	Rock type	SiO2	TiO2	Al2O3	Cr2O3	MgO	CaO	MnO	FeO	Na2O	K2O	Total	X Mg
403-17.2	garnet harzburgite	57.22	0.07	0.55	0.37	35.74	0.53	0.12	4.74	0.13	0.00	99.47	0.93
403-17.3	garnet harzburgite	57.35	0.04	0.56	0.39	35.52	0.56	0.10	4.70	0.17	0.01	99.40	0.93
403-19.1	garnet harzburgite	56.91	0.06	0.55	0.40	35.28	0.52	0.08	4.71	0.17	0.00	98.69	0.93
403-19.2	garnet harzburgite	57.16	0.05	0.57	0.36	35.59	0.54	0.11	4.70	0.20	0.01	99.29	0.93
403-19.3	garnet harzburgite	57.41	0.05	0.55	0.37	35.55	0.55	0.10	4.68	0.16	0.01	99.42	0.93
351-3.1	heterogeneous	57.42	0.03	0.46	0.18	36.04	0.16	0.09	4.56	0.05	0.00	98.98	0.93
351-3.2	heterogeneous	57.65	0.01	0.44	0.20	36.79	0.16	0.10	4.70	0.07	0.00	100.12	0.93
351-3.3	heterogeneous	57.69	0.01	0.49	0.17	36.73	0.18	0.11	4.71	0.03	0.01	100.11	0.93
351-5.1	heterogeneous	57.55	0.02	0.53	0.19	36.16	0.18	0.10	4.63	0.04	0.00	99.39	0.93
351-5.2	heterogeneous	57.42	0.02	0.53	0.19	36.37	0.19	0.11	4.59	0.03	0.01	99.45	0.93
351-5.3	heterogeneous	57.79	0.02	0.51	0.23	36.42	0.19	0.07	4.64	0.05	0.01	99.94	0.93
351-12.1	heterogeneous	57.73	0.03	0.49	0.18	36.17	0.20	0.11	4.59	0.04	0.00	99.53	0.93
351-12.3	heterogeneous	57.44	0.02	0.46	0.19	36.31	0.21	0.14	4.66	0.08	0.00	99.51	0.93
394 - 6.1	heterogeneous	56.59	0.00	0.47	0.22	36.03	0.17	0.08	4.66	0.07	0.00	98.30	0.93
394 - 6.2	heterogeneous	57.03	0.00	0.51	0.20	35.99	0.20	0.09	4.66	0.07	0.00	98.75	0.93
394 - 6.3	heterogeneous	56.68	0.00	0.49	0.22	35.94	0.21	0.08	4.68	0.07	0.01	98.38	0.93
394 - 1.2	heterogeneous	56.53	0.00	0.52	0.19	36.01	0.18	0.08	4.62	0.08	0.00	98.21	0.93
394 - 25.1	heterogeneous	57.07	0.00	0.48	0.22	36.19	0.20	0.11	4.67	0.04	0.00	98.98	0.93
394 - 25.2	heterogeneous	57.07	0.00	0.46	0.20	36.25	0.17	0.10	4.62	0.06	0.00	98.92	0.93
394 - 25.3	heterogeneous	57.04	0.00	0.49	0.20	36.31	0.22	0.10	4.63	0.05	0.00	99.03	0.93
368-20.1	spinel-garnet lherzolite	58.03	0.01	0.50	0.18	36.61	0.16	0.09	4.86	0.04	0.00	100.48	0.93
368-20.2	spinel-garnet lherzolite	58.20	0.05	0.48	0.16	36.58	0.18	0.09	4.84	0.03	0.00	100.61	0.93
368-20.3	spinel-garnet lherzolite	56.68	0.06	0.54	0.17	36.23	0.24	0.10	4.96	0.02	0.00	99.00	0.93
368-30.1	spinel-garnet lherzolite	57.64	0.05	0.56	0.20	36.30	0.20	0.10	4.93	0.03	0.00	100.02	0.93
368-30.2	spinel-garnet lherzolite	57.90	0.05	0.50	0.19	36.47	0.19	0.10	5.00	0.01	0.00	100.42	0.93
368-30.3	spinel-garnet lherzolite	57.83	0.03	0.52	0.20	36.57	0.21	0.10	4.91	0.01	0.00	100.38	0.93
368-16.1	spinel-garnet lherzolite	58.05	0.04	0.47	0.20	36.40	0.18	0.10	4.82	0.05	0.00	100.31	0.93
368-16.2	spinel-garnet lherzolite	58.00	0.06	0.47	0.19	36.55	0.18	0.10	4.90	0.05	0.00	100.49	0.93
368-16.3	spinel-garnet lherzolite	57.92	0.04	0.47	0.17	36.80	0.18	0.08	4.85	0.02	0.02	100.54	0.93
368-11.1	spinel-garnet lherzolite	58.03	0.06	0.45	0.13	36.69	0.16	0.10	4.93	0.04	0.00	100.60	0.93

Continued APPENDIX II (opx analyses)

Sample	Rock type	SiO2	TiO2	Al2O3	Cr2O3	MgO	CaO	MnO	FeO	Na2O	K2O	Total	X Mg
368-11.2	spinel-garnet lherzolite	57.96	0.05	0.50	0.16	36.52	0.17	0.11	4.90	0.01	0.00	100.38	0.93
368-11.3	spinel-garnet lherzolite	58.10	0.02	0.49	0.17	36.54	0.19	0.10	4.80	0.06	0.00	100.45	0.93
368-32.1	spinel-garnet lherzolite	57.88	0.07	0.50	0.19	36.65	0.20	0.10	4.87	0.04	0.00	100.51	0.93
368-32.2	spinel-garnet lherzolite	58.01	0.05	0.46	0.19	36.79	0.22	0.11	4.86	0.03	0.00	100.72	0.93
368-32.3	spinel-garnet lherzolite	57.72	0.06	0.48	0.17	36.42	0.21	0.10	4.85	0.06	0.00	100.07	0.93
368-3.1	spinel-garnet lherzolite	57.42	0.03	0.46	0.18	36.04	0.16	0.09	4.56	0.05	0.00	98.98	0.93
368-3.2	spinel-garnet lherzolite	57.65	0.01	0.44	0.20	36.79	0.16	0.10	4.70	0.07	0.00	100.12	0.93
368-3.3	spinel-garnet lherzolite	57.69	0.01	0.49	0.17	36.73	0.18	0.11	4.71	0.03	0.01	100.11	0.93
368-5.1	spinel-garnet lherzolite	57.55	0.02	0.53	0.19	36.16	0.18	0.10	4.63	0.04	0.00	99.39	0.93
368-5.2	spinel-garnet lherzolite	57.42	0.02	0.53	0.19	36.37	0.19	0.11	4.59	0.03	0.01	99.45	0.93
368-5.3	spinel-garnet lherzolite	57.79	0.02	0.51	0.23	36.42	0.19	0.07	4.64	0.05	0.01	99.94	0.93
402-14.1	spinel-garnet lherzolite	57.03	0.01	0.51	0.17	35.87	0.18	0.10	4.73	0.04	0.00	98.64	0.93
402-14.2	spinel-garnet lherzolite	57.42	0.03	0.53	0.16	36.03	0.18	0.09	4.67	0.03	0.00	99.15	0.93
402-14.3	spinel-garnet lherzolite	57.52	0.00	0.47	0.17	36.04	0.19	0.09	4.79	0.03	0.00	99.30	0.93
402-12.1	spinel-garnet lherzolite	57.30	0.04	0.48	0.17	36.04	0.18	0.10	4.70	0.03	0.00	99.03	0.93
402-12.2	spinel-garnet lherzolite	56.98	0.02	0.50	0.17	36.09	0.18	0.10	4.72	0.03	0.01	98.80	0.93
402-12.3	spinel-garnet lherzolite	57.45	0.03	0.49	0.17	35.93	0.20	0.09	4.66	0.03	0.00	99.05	0.93
402-9.1	spinel-garnet lherzolite	57.13	0.02	0.50	0.17	36.02	0.19	0.11	4.69	0.02	0.00	98.85	0.93
402-9.2	spinel-garnet lherzolite	57.25	0.00	0.51	0.15	36.17	0.16	0.10	4.70	0.04	0.00	99.07	0.93
402-9.3	spinel-garnet lherzolite	57.40	0.01	0.51	0.19	35.90	0.17	0.09	4.65	0.06	0.00	98.99	0.93
402-5.1	spinel-garnet lherzolite	56.85	0.01	0.51	0.18	35.66	0.17	0.11	4.63	0.06	0.00	98.20	0.93
402-5.2	spinel-garnet lherzolite	56.79	0.03	0.49	0.16	35.90	0.17	0.09	4.76	0.03	0.00	98.43	0.93
402-5.3	spinel-garnet lherzolite	57.09	0.04	0.52	0.16	36.02	0.18	0.11	4.75	0.02	0.00	98.90	0.93
402-21.2	spinel-garnet lherzolite	57.14	0.02	0.53	0.18	35.96	0.18	0.10	4.71	0.03	0.00	98.84	0.93
402-21.3	spinel-garnet lherzolite	57.16	0.02	0.53	0.17	35.96	0.16	0.10	4.77	0.03	0.00	98.90	0.93
355-12.1	coarse spinel lherzolite	56.55	0.00	1.07	0.22	35.65	0.15	0.12	4.50	0.01	0.01	98.28	0.93
355-12.2	coarse spinel lherzolite	56.44	0.00	1.11	0.22	35.93	0.12	0.11	4.51	0.02	0.01	98.46	0.93
355-12.3	coarse spinel lherzolite	56.30	0.00	1.11	0.21	35.90	0.15	0.13	4.48	0.02	0.00	98.30	0.93
356-4.1	granuloblastic spinel lherzolite	56.59	0.00	1.35	0.36	35.12	0.42	0.09	4.52	0.02	0.00	98.47	0.93
356-4.2	granuloblastic spinel lherzolite	56.68	0.00	1.32	0.35	35.11	0.39	0.11	4.49	0.01	0.00	98.45	0.93

Continued APPENDIX II (opx analyses)

Sample	Rock type	SiO2	TiO2	Al2O3	Cr2O3	MgO	CaO	MnO	FeO	Na2O	K2O	Total	X Mg
356-4.3	granuloblastic spinel lherzolite	56.51	0.00	1.33	0.35	35.41	0.39	0.10	4.59	0.00	0.01	98.70	0.93
356-7.1	granuloblastic spinel lherzolite	56.98	0.00	1.29	0.34	35.25	0.38	0.10	4.59	0.00	0.02	98.95	0.93
356-7.2	granuloblastic spinel lherzolite	57.48	0.00	1.24	0.30	35.36	0.32	0.11	4.57	0.00	0.00	99.38	0.93
356-7.3	granuloblastic spinel lherzolite	57.24	0.00	1.26	0.34	35.29	0.34	0.09	4.50	0.00	0.00	99.05	0.93
356-11.1	granuloblastic spinel lherzolite	56.78	0.00	1.31	0.44	34.83	0.51	0.11	4.35	0.02	0.01	98.36	0.93
356-11.2	granuloblastic spinel lherzolite	57.20	0.00	1.32	0.41	34.93	0.63	0.09	4.38	0.00	0.00	98.95	0.93
356-11.3	granuloblastic spinel lherzolite	57.00	0.00	1.32	0.39	35.07	0.53	0.09	4.37	0.00	0.00	98.77	0.93
356-18.1	granuloblastic spinel lherzolite	56.90	0.00	1.21	0.29	35.10	0.32	0.10	4.62	0.01	0.00	98.54	0.93
356-18.2	granuloblastic spinel lherzolite	56.74	0.00	1.25	0.34	35.13	0.31	0.10	4.58	0.03	0.00	98.48	0.93
356-18.3	granuloblastic spinel lherzolite	56.57	0.00	1.21	0.28	35.57	0.30	0.11	4.60	0.00	0.02	98.66	0.93
369-2.1	coarse spinel lherzolite	56.00	0.00	1.02	0.25	35.72	0.14	0.10	4.50	0.00	0.01	97.74	0.93
369-2.2	coarse spinel lherzolite	56.61	0.00	1.02	0.24	36.22	0.19	0.10	4.42	0.00	0.01	98.81	0.94
369-2.3	coarse spinel lherzolite	56.71	0.00	0.95	0.24	36.06	0.13	0.09	4.57	0.00	0.03	98.78	0.93
369-5.1	coarse spinel lherzolite	56.81	0.00	1.28	0.32	35.99	0.16	0.09	4.42	0.00	0.00	99.08	0.94
369-5.2	coarse spinel lherzolite	56.34	0.00	1.31	0.33	35.79	0.13	0.09	4.52	0.00	0.00	98.52	0.93
369-5.3	coarse spinel lherzolite	56.73	0.00	1.22	0.29	35.98	0.13	0.11	4.55	0.00	0.06	99.07	0.93
369-9.2	coarse spinel lherzolite	56.00	0.00	0.83	0.20	36.06	0.16	0.09	4.58	0.00	0.04	97.96	0.93
369-9.3	coarse spinel lherzolite	55.76	0.00	0.88	0.22	35.78	0.10	0.12	4.49	0.00	0.04	97.38	0.93
369-9.5	coarse spinel lherzolite	55.68	0.00	0.81	0.20	35.75	0.15	0.11	4.54	0.00	0.02	97.28	0.93
369 - 21.1	coarse spinel lherzolite	55.82	0.00	1.47	0.36	35.77	0.12	0.10	4.58	0.00	0.05	98.26	0.93
369 - 21.2	coarse spinel lherzolite	55.68	0.00	1.39	0.36	35.63	0.14	0.10	4.53	0.00	0.02	97.84	0.93
369 - 21.3	coarse spinel lherzolite	56.17	0.00	1.36	0.35	35.48	0.13	0.08	4.43	0.00	0.02	98.02	0.93
369 - 18.1	coarse spinel lherzolite	55.74	0.00	1.22	0.29	35.94	0.17	0.12	4.56	0.00	0.01	98.05	0.93
369 - 18.2	coarse spinel lherzolite	56.00	0.00	1.24	0.28	35.90	0.14	0.09	4.47	0.00	0.00	98.13	0.93
369 - 18.3	coarse spinel lherzolite	55.68	0.00	1.15	0.24	35.93	0.14	0.10	4.44	0.00	0.02	97.70	0.94
369 - 11.1	coarse spinel lherzolite	55.91	0.01	1.32	0.31	35.84	0.18	0.14	4.55	0.00	0.01	98.27	0.93
369 - 11.2	coarse spinel lherzolite	55.41	0.00	1.31	0.31	35.80	0.14	0.10	4.55	0.00	0.04	97.65	0.93
369 - 11.3	coarse spinel lherzolite	55.30	0.00	1.31	0.31	35.60	0.16	0.10	4.46	0.00	0.00	97.23	0.93
371 - 3.2	coarse spinel lherzolite	56.32	0.00	1.28	0.35	35.71	0.14	0.10	4.47	0.02	0.01	98.39	0.93
371 - 6.1	coarse spinel lherzolite	56.59	0.04	0.99	0.28	35.94	0.15	0.11	4.30	0.02	0.00	98.43	0.94

Continued APPENDIX II (opx analyses)

Sample	Rock type	SiO2	TiO2	Al2O3	Cr2O3	MgO	CaO	MnO	FeO	Na2O	K2O	Total	X Mg
371 - 6.2	coarse spinel lherzolite	57.15	0.00	1.10	0.30	36.04	0.13	0.11	4.42	0.00	0.00	99.25	0.94
371 - 6.3	coarse spinel lherzolite	56.74	0.01	0.92	0.24	35.96	0.18	0.12	4.40	0.04	0.00	98.60	0.94
371 - 9.1	coarse spinel lherzolite	56.51	0.00	0.84	0.19	36.03	0.14	0.11	4.30	0.05	0.00	98.17	0.94
371 - 9.2	coarse spinel lherzolite	56.84	0.04	0.82	0.22	36.17	0.14	0.10	4.43	0.03	0.00	98.80	0.94
371 - 9.3	coarse spinel lherzolite	56.88	0.00	0.87	0.22	36.11	0.15	0.10	4.46	0.04	0.04	98.85	0.94
371 - 12.1	coarse spinel lherzolite	56.61	0.00	0.95	0.21	36.10	0.11	0.10	4.49	0.01	0.00	98.58	0.93
371 - 12.2	coarse spinel lherzolite	56.70	0.04	0.96	0.24	36.00	0.13	0.13	4.48	0.03	0.00	98.70	0.93
371 - 12.3	coarse spinel lherzolite	56.57	0.00	0.92	0.22	35.93	0.15	0.10	4.48	0.06	0.00	98.43	0.93
411 - 3.1	coarse spinel lherzolite	57.35	0.00	1.15	0.25	36.27	0.11	0.11	4.47	0.02	0.01	99.74	0.94
411 - 3.2	coarse spinel lherzolite	57.20	0.00	1.22	0.24	36.08	0.15	0.12	4.52	0.03	0.00	99.56	0.93
411 - 3.3	coarse spinel lherzolite	57.42	0.00	1.21	0.28	36.34	0.13	0.10	4.48	0.01	0.00	99.97	0.94
411 - 7.1	coarse spinel lherzolite	57.09	0.00	1.22	0.30	36.12	0.18	0.09	4.47	0.01	0.01	99.48	0.94
411 - 7.2	coarse spinel lherzolite	57.28	0.00	1.24	0.33	36.29	0.17	0.11	4.36	0.08	0.00	99.86	0.94
411 - 7.3	coarse spinel lherzolite	57.45	0.00	1.36	0.30	36.30	0.15	0.10	4.47	0.04	0.00	100.17	0.94
411 - 15.1	coarse spinel lherzolite	56.72	0.00	1.12	0.24	36.28	0.15	0.10	4.47	0.03	0.01	99.11	0.94
411 – 15.2	coarse spinel lherzolite	57.03	0.00	1.09	0.27	36.22	0.15	0.09	4.41	0.04	0.01	99.31	0.94
411 - 10.1	coarse spinel lherzolite	56.94	0.00	1.17	0.23	36.13	0.13	0.13	4.43	0.00	0.00	99.16	0.94
411 - 10.2	coarse spinel lherzolite	57.09	0.01	1.10	0.23	36.37	0.13	0.11	4.48	0.03	0.02	99.57	0.94
411 - 10.3	coarse spinel lherzolite	57.41	0.00	1.16	0.29	36.46	0.13	0.10	4.41	0.04	0.00	99.98	0.94
411 - 13.1	coarse spinel lherzolite	57.29	0.00	1.19	0.29	36.21	0.17	0.09	4.47	0.04	0.00	99.75	0.94
411 - 13.2	coarse spinel lherzolite	57.48	0.00	1.20	0.27	36.33	0.16	0.11	4.48	0.02	0.00	100.05	0.94
411 - 13.3	coarse spinel lherzolite	57.81	0.00	1.20	0.24	36.25	0.13	0.12	4.43	0.01	0.02	100.21	0.94

APPENDIX III

Electron microprobe core analyses of clinopyroxenes from the Voyageur peridotite xenoliths

Sample	Rock type	SiO2	TiO2	Al2O3	Cr2O3	MgO	CaO	MnO	FeO	Na2O	K2O	Total	X Mg
343 12.1	coarse garnet lherzolite	54.23	0.25	1.90	1.42	17.51	19.26	0.04	2.65	1.94	0.04	99.25	0.92
343 12.2	coarse garnet lherzolite	53.99	0.22	1.93	1.44	17.34	19.48	0.05	2.71	1.95	0.04	99.15	0.92
343 12.3	coarse garnet lherzolite	54.41	0.26	1.93	1.46	17.47	19.36	0.04	2.77	1.88	0.03	99.59	0.92
343 11.1	coarse garnet lherzolite	54.47	0.26	2.00	1.45	17.53	19.32	0.05	2.74	1.91	0.02	99.76	0.92
343 11.2	coarse garnet lherzolite	54.48	0.29	1.97	1.45	17.54	19.30	0.05	2.78	1.86	0.02	99.75	0.92
343 11.3	coarse garnet lherzolite	54.18	0.27	1.92	1.51	17.47	19.34	0.06	2.72	1.83	0.04	99.34	0.92
343 5.1	coarse garnet lherzolite	54.32	0.28	1.95	1.55	17.46	19.27	0.04	2.65	2.05	0.02	99.60	0.92
343 5.2	coarse garnet lherzolite	54.31	0.27	1.98	1.48	17.53	19.39	0.05	2.71	1.96	0.01	99.69	0.92
343 5.3	coarse garnet lherzolite	54.16	0.27	2.02	1.53	17.27	19.24	0.04	2.75	1.98	0.02	99.28	0.92
343 5.2.1	coarse garnet lherzolite	54.13	0.25	1.95	1.56	17.29	19.29	0.04	2.66	2.01	0.01	99.18	0.92
343 5.2.2	coarse garnet lherzolite	54.14	0.25	1.93	1.62	17.45	19.29	0.04	2.68	1.86	0.03	99.28	0.92
343 5.2.3	coarse garnet lherzolite	54.26	0.28	1.93	1.63	17.54	19.18	0.05	2.70	2.03	0.02	99.61	0.92
343 20.1	coarse garnet lherzolite	54.23	0.24	1.96	1.70	17.40	19.28	0.03	2.65	1.95	0.04	99.48	0.92
343 20.2	coarse garnet lherzolite	53.90	0.28	1.89	1.65	18.18	18.98	0.05	2.82	1.87	0.03	99.65	0.92
343 20.3	coarse garnet lherzolite	54.33	0.25	1.92	1.65	17.39	19.28	0.03	2.68	2.01	0.03	99.57	0.92
343 21.1	coarse garnet lherzolite	54.16	0.31	1.93	1.53	17.41	19.32	0.04	2.73	1.90	0.03	99.35	0.92
343 21.2	coarse garnet lherzolite	54.22	0.26	1.97	1.49	17.28	19.43	0.05	2.71	2.01	0.03	99.46	0.92
343 21.3	coarse garnet lherzolite	54.38	0.28	1.91	1.54	17.43	19.32	0.06	2.76	1.99	0.02	99.70	0.92
343 14.1	coarse garnet lherzolite	54.45	0.27	1.91	1.48	17.59	19.27	0.04	2.79	2.01	0.02	99.84	0.92
343 14.2	coarse garnet lherzolite	54.07	0.26	1.93	1.50	17.44	19.39	0.05	2.72	1.97	0.04	99.36	0.92
343 14.3	coarse garnet lherzolite	54.39	0.26	2.01	1.45	17.41	19.28	0.06	2.76	1.83	0.02	99.47	0.92
347-2.1	transitional garnet lherzolite	54.00	0.28	1.98	1.25	17.07	19.03	0.06	3.85	1.92	0.01	99.45	0.89
347-2.2	transitional garnet lherzolite	54.20	0.26	2.02	1.25	17.07	19.11	0.07	3.85	1.85	0.04	99.72	0.89
347-2.3	transitional garnet lherzolite	54.19	0.25	2.02	1.20	17.01	19.02	0.07	3.86	1.93	0.03	99.58	0.89
347-21.1	transitional garnet lherzolite	54.21	0.28	2.02	1.29	17.33	19.21	0.07	3.89	1.82	0.02	100.14	0.89
347-21.2	transitional garnet lherzolite	54.32	0.26	2.04	1.30	17.23	19.18	0.08	3.88	1.86	0.03	100.19	0.89
347-21.3	transitional garnet lherzolite	54.14	0.29	1.99	1.25	17.17	19.20	0.06	3.89	1.84	0.09	99.92	0.89

Continued APPENDIX III (cpx analyses)

Sample	Rock type	SiO2	TiO2	Al2O3	Cr2O3	MgO	CaO	MnO	FeO	Na2O	K2O	Total	X Mg
347-24.1	transitional garnet lherzolite	54.11	0.23	1.94	1.25	17.23	19.12	0.08	4.00	1.75	0.03	99.73	0.88
347-24.2	transitional garnet lherzolite	54.29	0.26	2.02	1.16	17.17	19.46	0.07	3.95	1.86	0.03	100.27	0.89
347-24.3	transitional garnet lherzolite	54.24	0.25	1.95	1.26	17.21	19.22	0.08	3.95	1.86	0.02	100.03	0.89
347-6.1	transitional garnet lherzolite	54.24	0.26	1.98	1.17	17.06	19.10	0.07	3.87	1.93	0.04	99.71	0.89
347-6.2	transitional garnet lherzolite	53.89	0.27	1.99	1.13	17.17	19.16	0.06	3.82	1.74	0.01	99.25	0.89
347-6.3	transitional garnet lherzolite	54.03	0.24	1.99	1.15	17.11	19.02	0.09	3.92	1.92	0.02	99.49	0.89
347-9.1	transitional garnet lherzolite	54.07	0.27	1.94	1.30	16.85	19.03	0.05	3.77	1.88	0.02	99.18	0.89
347-9.2	transitional garnet lherzolite	53.90	0.25	1.93	1.28	16.95	19.09	0.06	3.95	1.94	0.02	99.36	0.88
347-9.3	transitional garnet lherzolite	53.85	0.28	1.96	1.25	16.83	19.01	0.08	3.90	1.99	0.04	99.19	0.89
347-26.3	transitional garnet lherzolite	53.92	0.27	1.98	1.30	17.04	19.24	0.07	3.89	1.90	0.04	99.65	0.89
347-31.1	transitional garnet lherzolite	54.27	0.25	2.08	1.17	17.05	19.23	0.06	3.98	1.81	0.03	99.92	0.88
347-31.3	transitional garnet lherzolite	54.30	0.26	1.98	1.17	17.17	19.18	0.07	3.83	1.87	0.01	99.84	0.89
359-1.1	coarse garnet lherzolite	53.89	0.27	1.96	1.95	17.12	19.44	0.04	2.82	2.03	0.04	99.56	0.92
359-1.2	coarse garnet lherzolite	54.23	0.28	2.03	1.90	17.05	19.31	0.02	2.78	2.10	0.03	99.72	0.92
359-1.3	coarse garnet lherzolite	54.52	0.23	2.00	1.89	17.08	19.29	0.04	2.69	2.04	0.01	99.79	0.92
359-3.1	coarse garnet lherzolite	54.55	0.30	2.01	1.89	17.16	19.23	0.06	2.64	2.08	0.05	99.96	0.92
359-3.2	coarse garnet lherzolite	54.53	0.29	1.85	1.91	17.29	19.63	0.04	2.81	2.00	0.02	100.37	0.92
359-3.3	coarse garnet lherzolite	54.60	0.27	2.01	1.90	17.02	19.28	0.05	2.77	2.12	0.04	100.06	0.92
359-4.1	coarse garnet lherzolite	52.74	0.26	2.30	1.82	16.51	19.13	0.03	2.67	1.98	1.30	98.73	0.92
359-4.2	coarse garnet lherzolite	54.19	0.26	1.98	1.89	16.97	19.49	0.04	2.64	1.98	0.03	99.48	0.92
359-4.3	coarse garnet lherzolite	54.35	0.29	2.01	1.90	17.15	19.40	0.04	2.82	2.22	0.03	100.22	0.92
359 - 15.1	coarse garnet lherzolite	54.37	0.28	2.03	1.94	17.01	19.34	0.03	2.53	1.90	0.02	99.45	0.92
359 - 15.2	coarse garnet lherzolite	54.10	0.20	1.98	1.92	16.76	19.32	0.06	2.50	1.81	0.05	98.69	0.92
359 - 15.3	coarse garnet lherzolite	54.22	0.19	1.98	1.90	16.96	19.47	0.05	2.50	1.89	0.04	99.20	0.92
359 - 16.1	coarse garnet lherzolite	54.26	0.25	2.00	1.94	17.13	19.39	0.06	2.50	1.96	0.04	99.53	0.92
359 - 16.2	coarse garnet lherzolite	54.58	0.17	2.07	1.84	17.09	19.52	0.02	2.49	2.07	0.04	99.89	0.92
359 - 16.3	coarse garnet lherzolite	54.23	0.19	2.04	1.89	17.08	19.35	0.04	2.52	1.97	0.05	99.36	0.92
372-17.1	coarse garnet lherzolite	54.15	0.18	2.24	1.21	16.83	19.71	0.06	2.98	1.85	0.02	99.22	0.91
372-17.2	coarse garnet lherzolite	54.20	0.16	2.27	1.15	16.99	19.61	0.04	3.06	1.98	0.03	99.48	0.91
372-17.3	coarse garnet lherzolite	54.19	0.18	2.30	1.19	17.12	19.63	0.04	3.04	2.00	0.03	99.70	0.91

Continued APPENDIX III (cpx analyses)

Sample	Rock type	SiO2	TiO2	Al2O3	Cr2O3	MgO	CaO	MnO	FeO	Na2O	K2O	Total	X Mg
373-18.2	coarse garnet lherzolite	53.12	0.45	2.23	1.06	17.40	20.97	0.09	3.31	1.07	0.01	99.72	0.90
373-18.3	coarse garnet lherzolite	53.67	0.31	2.28	1.22	16.88	19.45	0.06	3.11	2.22	0.05	99.25	0.91
373-19.2	coarse garnet lherzolite	53.75	0.25	2.23	1.15	16.69	19.31	0.06	3.04	1.99	0.04	98.50	0.91
373-19.3	coarse garnet lherzolite	53.92	0.28	2.30	1.15	17.04	19.28	0.04	3.08	2.15	0.05	99.28	0.91
373-14.1	coarse garnet lherzolite	53.84	0.24	2.25	1.18	16.94	19.36	0.06	3.11	2.02	0.03	99.02	0.91
373-14.2	coarse garnet lherzolite	53.89	0.27	2.29	1.18	16.95	19.62	0.04	3.05	2.06	0.05	99.38	0.91
373-14.3	coarse garnet lherzolite	53.70	0.24	2.26	1.18	16.84	19.35	0.06	3.07	1.97	0.01	98.68	0.91
373-22.1	coarse garnet lherzolite	54.25	0.27	2.20	1.19	17.01	19.61	0.06	3.07	2.14	0.03	99.84	0.91
373-22.2	coarse garnet lherzolite	54.21	0.24	2.25	1.15	16.97	19.53	0.05	3.04	2.00	0.02	99.46	0.91
373-22.3	coarse garnet lherzolite	53.84	0.25	2.34	1.23	16.95	19.49	0.05	3.12	2.02	0.03	99.31	0.91
382-23.1	porphyroclastic garnet lherzolite	54.34	0.25	2.01	1.18	17.42	18.59	0.06	4.17	1.93	0.04	99.99	0.88
382-23.2	porphyroclastic garnet lherzolite	54.10	0.23	2.02	1.17	17.45	18.62	0.06	4.27	1.82	0.03	99.76	0.88
382-23.3	porphyroclastic garnet lherzolite	54.29	0.23	2.03	1.14	17.48	18.49	0.05	4.20	1.96	0.03	99.91	0.88
382-24.1	porphyroclastic garnet lherzolite	54.11	0.21	2.05	1.25	17.44	18.34	0.07	4.10	1.83	0.03	99.43	0.88
382-24.2	porphyroclastic garnet lherzolite	54.48	0.25	2.02	1.27	17.58	18.42	0.07	4.10	1.95	0.02	100.16	0.88
382-24.3	porphyroclastic garnet lherzolite	54.60	0.24	1.97	1.29	17.40	18.30	0.08	4.04	2.01	0.03	99.96	0.88
382-18.1	porphyroclastic garnet lherzolite	54.45	0.24	1.97	1.19	17.74	18.64	0.05	4.04	1.83	0.02	100.18	0.89
382-18.2	porphyroclastic garnet lherzolite	54.48	0.23	1.97	1.17	17.59	18.71	0.07	4.00	1.80	0.03	100.05	0.89
382-18.3	porphyroclastic garnet lherzolite	54.40	0.23	1.96	1.14	17.60	18.52	0.06	3.87	1.77	0.02	99.58	0.89
382-2.1	porphyroclastic garnet lherzolite	54.46	0.25	1.93	1.16	17.57	18.68	0.06	4.06	1.95	0.02	100.14	0.89
382-2.2	porphyroclastic garnet lherzolite	54.68	0.24	1.97	1.19	17.61	18.55	0.08	3.93	1.79	0.03	100.08	0.89
382-2.3	porphyroclastic garnet lherzolite	54.50	0.25	1.98	1.17	17.62	18.69	0.07	4.05	1.83	0.03	100.20	0.89
382-8.1	porphyroclastic garnet lherzolite	54.37	0.26	2.00	1.21	17.73	18.32	0.07	4.16	2.03	0.03	100.19	0.88
382-8.2	porphyroclastic garnet lherzolite	54.46	0.24	2.06	1.17	17.57	18.55	0.09	4.19	1.89	0.03	100.25	0.88
382-8.3	porphyroclastic garnet lherzolite	54.11	0.16	0.95	1.07	17.75	20.85	0.09	3.68	0.98	0.00	99.64	0.90
382-11.1	porphyroclastic garnet lherzolite	54.46	0.24	1.96	1.19	17.56	18.69	0.09	4.02	1.96	0.04	100.21	0.89
382-11.2	porphyroclastic garnet lherzolite	54.40	0.26	1.91	1.16	17.65	18.77	0.10	4.11	1.86	0.04	100.25	0.88
382-11.3	porphyroclastic garnet lherzolite	54.39	0.24	1.99	1.17	17.52	18.67	0.07	3.96	1.74	0.03	99.77	0.89
394 - 24.1	heterogeneous	54.33	0.14	3.19	2.75	14.05	19.02	0.00	2.49	3.25	0.00	99.22	0.91
394 - 24.1	heterogeneous	54.33	0.14	3.19	2.75	14.05	19.02	0.00	2.49	3.25	0.00	99.22	0.91

Continued APPENDIX III (cpx analyses)

Sample	Rock type	SiO2	TiO2	Al2O3	Cr2O3	MgO	CaO	MnO	FeO	Na2O	K2O	Total	X Mg
394 - 24.2	Heterogeneous	54.94	0.16	4.04	2.87	13.57	17.65	0.01	2.41	3.79	0.01	99.45	0.91
394 - 24.3	heterogeneous	54.78	0.17	4.22	3.14	13.43	17.67	0.00	2.31	3.97	0.00	99.69	0.91
394 - 22.1	heterogeneous	54.51	0.13	4.17	3.04	13.41	17.56	0.00	2.36	3.78	0.00	98.96	0.91
394 - 22.2	heterogeneous	54.78	0.16	4.19	3.24	13.25	17.56	0.00	2.32	3.83	0.00	99.33	0.91
394 - 22.3	heterogeneous	55.05	0.07	4.17	2.84	13.48	17.66	0.00	2.36	3.89	0.01	99.53	0.91
394 - 20.1	heterogeneous	54.86	0.14	3.66	2.63	14.02	18.15	0.00	2.57	3.59	0.01	99.63	0.91
394 - 20.2	heterogeneous	55.16	0.18	3.72	2.63	14.01	18.12	0.00	2.53	3.79	0.00	100.14	0.91
394 - 20.3	heterogeneous	55.02	0.11	3.68	2.69	14.05	18.17	0.00	2.52	3.59	0.00	99.83	0.91
394 - 17.1	heterogeneous	54.60	0.14	3.70	2.97	13.64	18.03	0.00	2.48	3.70	0.01	99.27	0.91
394 - 17.2	heterogeneous	54.80	0.12	3.66	3.03	13.74	18.21	0.00	2.35	3.75	0.00	99.66	0.91
394 - 17.3	heterogeneous	54.71	0.18	3.78	2.80	13.85	18.11	0.00	2.48	3.43	0.00	99.34	0.91
394 - 11.1	heterogeneous	54.50	0.13	2.42	2.60	14.94	20.18	0.02	2.32	2.66	0.00	99.77	0.92
394 - 11.2	heterogeneous	54.60	0.09	2.38	2.63	14.79	20.21	0.01	2.28	2.59	0.03	99.61	0.92
394 - 11.3	heterogeneous	54.36	0.07	2.41	2.63	14.63	20.12	0.00	2.30	2.58	0.03	99.13	0.92
368-29.1	spinel–garnet lherzolite	54.76	0.10	1.76	1.55	16.23	21.94	0.01	2.47	1.76	0.01	100.59	0.92
368-29.2	spinel–garnet lherzolite	54.82	0.10	1.74	1.61	16.25	21.95	0.01	2.52	1.78	0.01	100.78	0.92
368-29.3	spinel–garnet lherzolite	54.74	0.13	1.67	1.57	16.16	21.98	0.02	2.46	1.77	0.01	100.51	0.92
368-1.1	spinel–garnet lherzolite	54.79	0.11	1.79	1.61	16.13	21.99	0.02	2.47	1.90	0.01	100.81	0.92
368-1.2	spinel–garnet lherzolite	54.77	0.10	1.82	1.65	16.28	21.95	0.02	2.47	1.84	0.01	100.90	0.92
368-1.3	spinel–garnet lherzolite	54.28	0.08	1.84	1.60	15.98	22.11	0.01	2.46	1.76	0.00	100.12	0.92
402-3.1	spinel–garnet lherzolite	53.88	0.06	1.69	1.60	16.14	22.29	0.00	2.10	1.56	0.00	99.32	0.93
402-3.2	spinel–garnet lherzolite	53.99	0.05	1.70	1.63	16.23	22.35	0.02	2.01	1.54	0.01	99.52	0.94
402-22.1	spinel–garnet lherzolite	53.99	0.03	1.65	1.52	16.06	22.53	0.02	2.08	1.66	0.00	99.53	0.93
402-22.2	spinel–garnet lherzolite	54.04	0.03	1.61	1.62	16.15	22.51	0.02	2.11	1.58	0.01	99.68	0.93
402-22.3	spinel–garnet lherzolite	53.95	0.02	1.75	1.50	16.14	22.46	0.02	2.01	1.56	0.01	99.42	0.93
402-1.1	spinel–garnet lherzolite	53.96	0.05	1.65	1.56	16.23	22.67	0.02	2.07	1.61	0.00	99.81	0.93
402-1.2	spinel–garnet lherzolite	54.19	0.03	1.66	1.55	16.35	22.47	0.02	2.07	1.61	0.01	99.94	0.93
402-1.3	spinel–garnet lherzolite	54.12	0.05	1.69	1.51	16.13	22.43	0.03	2.04	1.50	0.00	99.49	0.93
355-1.1	coarse spinel lherzolite	53.87	0.00	2.82	1.41	15.54	22.82	0.03	1.19	1.60	0.00	99.28	0.96
355-1.2	coarse spinel lherzolite	54.04	0.03	2.72	1.46	15.44	22.85	0.01	1.17	1.64	0.00	99.37	0.96

Continued APPENDIX III (cpx analyses)

Sample	Rock type	SiO2	TiO2	Al2O3	Cr2O3	MgO	CaO	MnO	FeO	Na2O	K2O	Total	X Mg
355-1.3	coarse spinel lherzolite	53.66	0.00	2.69	1.46	15.69	22.90	0.04	1.20	1.73	0.00	99.37	0.96
355-2.1	coarse spinel lherzolite	53.04	0.00	2.68	1.41	15.48	22.72	0.04	1.19	1.55	0.00	98.11	0.96
355-2.2	coarse spinel lherzolite	52.89	0.00	2.80	1.38	15.58	22.60	0.04	1.22	1.56	0.00	98.07	0.96
356-3.1	coarse spinel lherzolite	53.84	0.00	1.22	0.69	17.28	24.78	0.05	1.26	0.43	0.00	99.55	0.96
356-3.2	coarse spinel lherzolite	53.74	0.00	1.20	0.69	17.57	24.58	0.05	1.24	0.42	0.00	99.49	0.96
356-3.3	coarse spinel lherzolite	54.03	0.00	1.25	0.75	17.62	24.60	0.04	1.22	0.41	0.01	99.94	0.96
356-9.1	coarse spinel lherzolite	54.01	0.00	1.24	0.72	17.56	24.46	0.03	1.47	0.33	0.01	99.83	0.96
356-9.2	coarse spinel lherzolite	53.74	0.00	1.25	0.71	17.62	24.24	0.02	1.50	0.35	0.00	99.43	0.95
356-9.3	coarse spinel lherzolite	53.83	0.01	1.21	0.75	17.65	24.34	0.04	1.48	0.33	0.03	99.66	0.96
371 - 5.1	coarse spinel lherzolite	54.42	0.00	2.34	1.67	15.76	22.53	0.01	1.19	1.64	0.02	99.59	0.96
371 - 5.2	coarse spinel lherzolite	54.31	0.00	2.37	1.55	15.89	22.68	0.01	1.22	1.64	0.00	99.67	0.96
371 - 5.3	coarse spinel lherzolite	54.15	0.01	2.33	1.58	15.62	22.70	0.01	1.24	1.66	0.00	99.31	0.96
411 - 1.1	coarse spinel lherzolite	54.92	0.00	2.73	1.46	15.94	22.61	0.02	1.21	1.63	0.00	100.52	0.96
411 - 1.2	coarse spinel lherzolite	55.13	0.00	2.61	1.43	16.05	22.51	0.03	1.21	1.55	0.01	100.53	0.96
411 - 4.2	coarse spinel lherzolite	54.60	0.00	2.56	1.43	15.90	22.67	0.02	1.25	1.67	0.00	100.10	0.96
411 - 4.3	coarse spinel lherzolite	54.70	0.00	2.53	1.47	15.73	22.81	0.02	1.16	1.55	0.02	99.99	0.96
411 - 14.1	coarse spinel lherzolite	54.66	0.00	2.79	1.44	15.85	22.51	0.02	1.24	1.56	0.01	100.07	0.96
411 - 14.2	coarse spinel lherzolite	55.05	0.00	2.72	1.41	15.83	22.74	0.04	1.18	1.68	0.02	100.67	0.96
411 - 11.1	coarse spinel lherzolite	54.77	0.93	0.72	0.36	18.32	21.51	0.14	3.26	0.89	0.02	100.92	0.91
411 - 11.3	coarse spinel lherzolite	54.92	0.90	0.69	0.45	18.16	21.33	0.13	3.29	0.82	0.00	100.69	0.91
345-3.1	wehrlite	54.01	0.24	2.10	1.17	16.18	20.06	0.07	3.34	1.71	0.05	98.94	0.90
345-3.2	wehrlite	54.19	0.22	2.07	1.13	16.09	20.20	0.06	3.48	1.82	0.03	99.29	0.89
345-3.3	wehrlite	54.24	0.22	2.04	1.14	16.20	20.06	0.07	3.39	1.83	0.02	99.20	0.89
345-4.2	wehrlite	54.47	0.27	2.04	1.20	16.35	20.04	0.05	3.31	1.83	0.02	99.58	0.90
345-4.3	wehrlite	54.72	0.23	2.12	1.21	16.19	20.18	0.06	3.24	1.85	0.02	99.82	0.90
345-10.1	wehrlite	55.25	0.15	2.03	1.21	16.51	20.20	0.07	3.43	1.82	0.02	100.68	0.90
345-10.2	wehrlite	54.96	0.33	2.06	1.23	16.35	20.34	0.07	3.43	1.91	0.03	100.70	0.89
345-10.3	wehrlite	55.22	0.25	2.00	1.22	16.46	20.26	0.07	3.31	1.85	0.03	100.66	0.90
345-11.1	wehrlite	54.09	0.23	2.12	1.52	16.26	19.99	0.07	3.38	1.87	0.02	99.54	0.90
345-11.2	wehrlite	54.44	0.25	2.14	1.54	16.17	20.00	0.05	3.40	1.92	0.02	99.93	0.89

Continued APPENDIX III (cpx analyses)

Sample	Rock type	SiO2	TiO2	Al2O3	Cr2O3	MgO	CaO	MnO	FeO	Na2O	K2O	Total	X Mg
345-11.3	wehrlite	54.37	0.18	2.11	1.58	16.28	19.95	0.05	3.38	1.97	0.03	99.89	0.90
345-13.1	wehrlite	53.50	0.21	2.08	1.02	16.12	20.24	0.06	3.45	1.87	0.02	98.56	0.89
354-2.1	wehrlite	53.90	0.24	2.16	0.72	16.07	20.81	0.08	3.26	1.67	0.03	98.95	0.90
354-2.2	wehrlite	54.17	0.15	2.06	0.73	16.24	20.71	0.06	3.36	1.69	0.02	99.19	0.90
354-2.3	wehrlite	54.13	0.23	2.15	0.76	16.26	20.80	0.08	3.29	1.55	0.00	99.25	0.90
354-4.1	wehrlite	54.88	0.24	2.23	0.79	16.21	21.04	0.06	3.19	1.72	0.02	100.37	0.90
354-4.2	wehrlite	54.78	0.26	2.23	0.81	16.16	21.16	0.08	3.18	1.65	0.01	100.32	0.90
354-4.3	wehrlite	54.07	0.19	2.22	0.68	16.12	20.95	0.05	3.05	1.61	0.03	98.97	0.90
354-6.1	wehrlite	54.57	0.18	2.15	0.84	16.13	20.86	0.09	3.34	1.78	0.03	99.97	0.90
354-6.2	wehrlite	54.72	0.22	2.13	0.80	16.06	20.85	0.07	3.38	1.75	0.04	100.01	0.89
354-6.3	wehrlite	54.80	0.18	2.10	0.78	16.34	20.98	0.08	3.35	1.73	0.01	100.35	0.90
354-9.1	wehrlite	54.79	0.24	2.19	0.85	16.08	21.03	0.08	3.06	1.71	0.05	100.08	0.90
354-9.2	wehrlite	54.81	0.23	2.11	0.82	16.29	21.08	0.08	3.16	1.74	0.04	100.36	0.90
354-9.3	wehrlite	54.89	0.18	2.16	0.89	16.17	21.08	0.06	3.13	1.69	0.03	100.28	0.90
358-2.1	wehrlite	54.43	0.22	2.20	0.87	16.29	20.78	0.06	3.34	1.60	0.03	99.82	0.90
358-2.2	wehrlite	54.46	0.26	2.16	0.85	16.38	20.96	0.07	3.35	1.71	0.01	100.21	0.90
358-2.3	wehrlite	54.33	0.27	2.17	0.84	16.30	20.89	0.07	3.33	1.67	0.03	99.90	0.90
358-3.1	wehrlite	54.86	0.23	2.18	0.75	16.24	20.94	0.08	3.33	1.77	0.02	100.40	0.90
358-3.2	wehrlite	54.65	0.11	2.19	0.77	16.26	21.08	0.08	3.25	1.83	0.02	100.24	0.90
358-3.3	wehrlite	54.76	0.24	2.18	0.81	16.31	20.88	0.05	3.21	1.68	0.03	100.14	0.90
358-5.1	wehrlite	54.87	0.23	2.17	0.88	16.31	20.94	0.05	3.15	1.82	0.01	100.43	0.90
358-5.2	wehrlite	54.88	0.18	2.18	0.89	16.38	20.93	0.07	3.25	1.75	0.02	100.53	0.90
358-5.3	wehrlite	55.14	0.19	2.16	0.88	16.27	21.06	0.08	3.31	1.69	0.01	100.79	0.90
363-1.1	garnet wehrlite	53.52	0.30	2.09	1.47	16.75	19.68	0.04	3.25	1.90	0.03	99.03	0.90
363-1.2	garnet wehrlite	53.36	0.28	2.05	1.43	16.75	19.65	0.05	3.32	2.07	0.03	99.00	0.90
363-1.3	garnet wehrlite	53.23	0.31	2.09	1.54	16.83	19.57	0.08	3.40	1.86	0.03	98.94	0.90
363-3.1	garnet wehrlite	53.93	0.28	2.00	1.48	16.87	19.86	0.05	3.39	1.98	0.03	99.86	0.90
363-3.2	garnet wehrlite	54.18	0.25	1.99	1.46	16.88	19.81	0.05	3.39	1.97	0.03	100.01	0.90
363-3.3	garnet wehrlite	54.30	0.28	2.02	1.46	17.02	19.74	0.04	3.26	2.05	0.02	100.19	0.90
363-7.1	garnet wehrlite	54.71	0.30	2.02	1.31	17.02	19.95	0.07	3.28	1.92	0.03	100.61	0.90
363-7.2	garnet wehrlite	54.89	0.26	2.06	1.26	17.02	19.71	0.07	3.37	1.97	0.03	100.64	0.90
363-7.3	garnet wehrlite	54.52	0.25	2.08	1.34	17.00	19.82	0.06	3.19	1.87	0.02	100.14	0.90

Continued APPENDIX III (cpx analyses)

Sample	Rock type	SiO2	TiO2	Al2O3	Cr2O3	MgO	CaO	MnO	FeO	Na2O	K2O	Total	X Mg
363-12.1	garnet wehrlite	54.73	0.28	2.04	1.43	17.00	19.73	0.06	3.27	1.88	0.02	100.44	0.90
363-12.2	garnet wehrlite	54.90	0.28	2.00	1.45	17.06	19.90	0.07	3.30	1.93	0.04	100.94	0.90
363-12.3	garnet wehrlite	54.60	0.27	2.00	1.37	16.85	19.71	0.08	3.27	1.90	0.04	100.08	0.90
398-16.1	garnet wehrlite	54.06	0.28	2.02	1.13	16.59	20.15	0.07	3.63	1.88	0.04	99.85	0.89
398-16.2	garnet wehrlite	54.08	0.29	2.00	1.12	16.45	20.10	0.05	3.68	1.84	0.03	99.64	0.89
398-16.3	garnet wehrlite	54.24	0.29	2.02	1.12	16.58	20.10	0.07	3.59	1.83	0.02	99.87	0.89
398-6.1	garnet wehrlite	54.15	0.29	2.10	2.05	15.94	19.79	0.02	3.54	2.19	0.04	100.10	0.89
398-6.2	garnet wehrlite	54.24	0.27	2.12	2.08	16.04	19.50	0.04	3.60	2.34	0.04	100.28	0.89
398-6.3	garnet wehrlite	53.92	0.28	2.10	2.06	16.06	19.66	0.02	3.63	2.32	0.03	100.08	0.89
398-7.1	garnet wehrlite	54.25	0.24	2.23	1.06	16.57	19.97	0.06	3.65	2.01	0.03	100.06	0.89
398-7.2	garnet wehrlite	54.32	0.31	2.22	1.12	16.69	19.81	0.07	3.68	1.93	0.03	100.18	0.89
398-7.3	garnet wehrlite	54.21	0.30	2.18	1.08	16.65	19.89	0.06	3.66	1.96	0.03	100.02	0.89
398-10.1	garnet wehrlite	54.24	0.28	1.92	1.07	16.73	19.97	0.09	3.69	1.80	0.03	99.82	0.89
398-10.2	garnet wehrlite	54.02	0.25	2.00	1.01	16.62	20.05	0.06	3.70	1.85	0.03	99.58	0.89
398-10.3	garnet wehrlite	54.05	0.27	1.99	1.05	16.57	20.13	0.06	3.72	1.80	0.03	99.66	0.89
398-12.1	garnet wehrlite	54.20	0.26	1.99	0.88	16.76	20.19	0.08	3.73	1.87	0.03	99.99	0.89
398-12.2	garnet wehrlite	54.30	0.28	2.09	0.91	16.88	20.22	0.07	3.75	1.76	0.02	100.27	0.89
398-12.3	garnet wehrlite	54.06	0.29	2.03	0.96	16.81	20.15	0.06	3.68	1.73	0.03	99.78	0.89

APPENDIX IV

Electron microprobe core analyses of garnets from the Voyageur peridotite xenoliths

Sample	Rock type	SiO2	TiO2	Al2O3	Cr2O3	MgO	CaO	MnO	FeO	Total	X Mg
343-10.1	coarse garnet lherzolite	41.30	0.34	19.75	5.16	20.83	4.71	0.20	7.37	99.65	0.83
343-10.2	coarse garnet lherzolite	41.27	0.37	19.53	5.21	20.59	4.77	0.23	7.42	99.39	0.83
343-10.3	coarse garnet lherzolite	41.25	0.40	19.54	5.13	20.77	4.91	0.20	7.41	99.61	0.83
343-8.1	coarse garnet lherzolite	41.38	0.49	19.24	5.09	20.93	4.80	0.21	7.49	99.64	0.83
343-8.2	coarse garnet lherzolite	41.37	0.43	19.40	5.01	20.88	4.75	0.20	7.44	99.48	0.83
343-8.3	coarse garnet lherzolite	41.33	0.41	19.42	5.05	20.78	4.81	0.20	7.43	99.43	0.83
343-7.1	coarse garnet lherzolite	41.47	0.57	19.22	5.02	20.80	4.90	0.19	7.63	99.80	0.83
343-7.2	coarse garnet lherzolite	41.38	0.60	19.16	4.89	20.56	4.92	0.20	7.49	99.20	0.83
343-7.3	coarse garnet lherzolite	41.58	0.54	19.29	4.94	20.66	4.89	0.20	7.51	99.60	0.83
343-3.1	coarse garnet lherzolite	41.34	0.41	19.27	4.86	20.74	4.85	0.23	7.45	99.14	0.83
343-3.2	coarse garnet lherzolite	41.56	0.41	19.53	5.07	20.78	4.87	0.21	7.41	99.84	0.83
343-3.3	coarse garnet lherzolite	41.38	0.44	19.52	5.04	20.77	4.84	0.23	7.40	99.62	0.83
343-18.1	coarse garnet lherzolite	41.42	0.41	19.43	5.26	20.89	4.85	0.19	7.47	99.92	0.83
343-18.2	coarse garnet lherzolite	41.50	0.42	19.35	5.10	20.84	4.85	0.21	7.44	99.71	0.83
343-18.3	coarse garnet lherzolite	41.34	0.41	19.46	5.09	20.79	4.84	0.19	7.39	99.51	0.83
343-19.1	coarse garnet lherzolite	41.67	0.40	19.58	5.24	20.87	4.82	0.19	7.44	100.21	0.83
343-19.2	coarse garnet lherzolite	41.63	0.42	19.54	5.17	20.98	4.88	0.18	7.42	100.22	0.83
343-19.3	coarse garnet lherzolite	41.40	0.41	19.41	5.20	20.83	4.85	0.21	7.42	99.73	0.83
347-5.1	transitional garnet lherzolite	41.40	0.59	20.02	3.93	20.04	4.98	0.23	9.17	100.37	0.80
347-5.2	transitional garnet lherzolite	41.17	0.63	19.95	3.91	20.01	4.96	0.26	9.30	100.19	0.79
347-5.3	transitional garnet lherzolite	41.34	0.59	19.99	3.97	20.10	4.98	0.26	9.03	100.26	0.80
347-22.1	transitional garnet lherzolite	41.57	0.46	20.20	4.12	20.43	4.98	0.24	8.85	100.85	0.80
347 22.2	transitional garnet lherzolite	41.16	0.46	20.12	4.25	20.19	4.94	0.23	8.88	100.23	0.80
347-22.3	transitional garnet lherzolite	41.25	0.48	20.34	4.11	20.04	4.93	0.24	8.86	100.25	0.80

Continued APPENDIX IV (garnet analyses)

Sample	Rock type	SiO2	TiO2	Al2O3	Cr2O3	MgO	CaO	MnO	FeO	Total	X Mg
347-23.1	transitional garnet lherzolite	41.31	0.36	20.37	4.36	20.35	4.99	0.23	8.48	100.45	0.81
347-23.2	transitional garnet lherzolite	41.31	0.39	20.27	4.32	20.34	5.01	0.20	8.57	100.41	0.81
347-23.3	transitional garnet lherzolite	41.43	0.37	20.29	4.27	20.25	5.03	0.21	8.50	100.35	0.81
347-10.1	transitional garnet lherzolite	41.42	0.49	20.40	4.04	20.38	4.91	0.23	8.21	100.08	0.82
347-10.2	transitional garnet lherzolite	41.32	0.52	20.20	4.11	20.59	4.97	0.24	8.26	100.21	0.82
347-10.3	transitional garnet lherzolite	41.24	0.54	20.26	4.15	20.51	4.88	0.20	8.20	99.97	0.82
347-17.1	transitional garnet lherzolite	41.28	0.37	20.40	4.32	20.79	5.06	0.20	7.91	100.34	0.82
347-17.2	transitional garnet lherzolite	41.38	0.40	20.32	4.31	20.53	5.10	0.19	7.95	100.18	0.82
347-17.3	transitional garnet lherzolite	41.37	0.39	20.18	4.25	20.79	5.02	0.22	7.98	100.20	0.82
347-32.1	transitional garnet lherzolite	41.15	0.26	21.07	4.43	20.62	4.99	0.22	8.09	100.83	0.82
347-32.3	transitional garnet lherzolite	41.40	0.30	21.03	4.43	20.65	4.93	0.23	8.01	100.98	0.82
359-7.1	coarse garnet lherzolite	41.14	0.35	19.24	6.12	20.71	5.44	0.21	6.97	100.18	0.84
359-7.2	coarse garnet lherzolite	41.13	0.36	19.17	6.09	20.64	5.38	0.18	6.97	99.92	0.84
359-7.3	coarse garnet lherzolite	41.15	0.36	19.41	6.15	20.58	5.37	0.20	6.97	100.19	0.84
359-9.1	coarse garnet lherzolite	41.45	0.48	19.15	6.00	20.88	5.36	0.19	7.08	100.59	0.84
359-9.2	coarse garnet lherzolite	41.16	0.50	19.25	6.02	20.73	5.35	0.24	6.94	100.19	0.84
359-9.3	coarse garnet lherzolite	41.35	0.49	19.05	6.02	20.92	5.40	0.20	7.05	100.49	0.84
359-10.1	coarse garnet lherzolite	41.23	0.65	19.12	5.71	20.71	5.58	0.19	7.06	100.25	0.84
359-10.2	coarse garnet lherzolite	41.24	0.68	19.12	5.69	20.77	5.57	0.21	7.09	100.37	0.84
359-10.3	coarse garnet lherzolite	41.06	0.75	19.30	5.53	20.89	5.43	0.16	7.08	100.20	0.84
372-16.1	coarse garnet lherzolite	41.02	0.31	18.21	7.44	20.29	5.78	0.14	7.03	100.21	0.84
372-16.2	coarse garnet lherzolite	40.98	0.35	18.57	7.44	20.28	5.76	0.15	6.98	100.49	0.84
372-16.3	coarse garnet lherzolite	41.14	0.37	18.31	7.35	20.16	5.84	0.18	6.97	100.33	0.84
372-12.1	coarse garnet lherzolite	41.11	0.37	18.03	7.31	20.23	5.77	0.13	7.02	99.96	0.84
372-12.2	coarse garnet lherzolite	41.17	0.42	18.02	7.44	20.20	5.71	0.13	7.08	100.17	0.84
372-12.3	coarse garnet lherzolite	40.80	0.37	18.15	7.26	20.28	5.74	0.14	7.06	99.80	0.84
372-16.1	coarse garnet lherzolite	41.00	0.35	18.16	7.48	20.28	5.81	0.14	7.05	100.27	0.84

Continued APPENDIX IV (garnet analyses)

Sample	Rock type	SiO2	TiO2	Al2O3	Cr2O3	MgO	CaO	MnO	FeO	Total	X Mg
372-16.2	coarse garnet lherzolite	40.98	0.35	18.57	7.44	20.28	5.76	0.15	6.98	100.49	0.84
372-16.3	coarse garnet lherzolite	41.14	0.37	18.31	7.35	20.16	5.84	0.18	6.97	100.33	0.84
372-12.1	coarse garnet lherzolite	41.11	0.37	18.03	7.31	20.23	5.77	0.13	7.02	99.96	0.84
372-12.2	coarse garnet lherzolite	41.17	0.42	18.02	7.44	20.20	5.71	0.13	7.08	100.17	0.84
372-12.3	coarse garnet lherzolite	40.80	0.37	18.15	7.26	20.28	5.74	0.14	7.06	99.80	0.84
372- 7.1	coarse garnet lherzolite	40.98	0.44	17.98	7.64	20.11	5.85	0.12	6.97	100.09	0.84
372-7.2	coarse garnet lherzolite	40.90	0.44	17.94	7.56	20.24	5.73	0.13	6.93	99.87	0.84
372-7.3	coarse garnet lherzolite	40.65	0.39	18.01	7.57	20.28	5.79	0.13	7.00	99.83	0.84
372-5.1	coarse garnet lherzolite	40.92	0.36	17.97	7.67	20.38	5.88	0.13	6.93	100.23	0.84
372-5.2	coarse garnet lherzolite	40.80	0.37	17.80	7.77	19.95	5.96	0.16	6.90	99.70	0.84
372-5.3	coarse garnet lherzolite	40.83	0.35	17.81	7.74	20.15	5.86	0.15	7.00	99.89	0.84
372-12.1	coarse garnet lherzolite	40.56	0.36	17.87	7.38	20.13	5.86	0.11	7.03	99.30	0.84
372-12.2	coarse garnet lherzolite	40.80	0.34	18.21	7.33	20.38	5.81	0.16	7.09	100.12	0.84
372-12.3	coarse garnet lherzolite	40.81	0.34	18.26	7.31	20.23	5.82	0.14	7.00	99.91	0.84
373-2.1	coarse garnet lherzolite	41.75	0.26	21.65	3.06	21.15	4.63	0.24	7.63	100.37	0.83
373-2.2	coarse garnet lherzolite	41.78	0.32	21.75	3.08	21.48	4.64	0.21	7.65	100.91	0.83
373-5.1	coarse garnet lherzolite	41.53	0.25	21.62	3.28	21.27	4.62	0.24	7.67	100.46	0.83
373-5.2	coarse garnet lherzolite	41.67	0.25	21.72	3.27	21.12	4.63	0.23	7.69	100.59	0.83
373-5.3	coarse garnet lherzolite	41.67	0.21	21.88	3.29	21.35	4.65	0.23	7.63	100.92	0.83
373-10.1	coarse garnet lherzolite	41.75	0.34	21.33	3.70	21.23	4.73	0.24	7.65	100.98	0.83
373-10.3	coarse garnet lherzolite	41.70	0.36	21.17	3.65	21.08	4.78	0.24	7.64	100.62	0.83
373-10.1	coarse garnet lherzolite	41.71	0.23	21.30	3.76	21.04	4.70	0.19	7.63	100.56	0.83
373-10.2	coarse garnet lherzolite	41.40	0.21	21.25	3.68	20.97	4.73	0.22	7.61	100.06	0.83
373-10.3	coarse garnet lherzolite	41.33	0.23	21.24	3.72	21.16	4.75	0.23	7.66	100.31	0.83
373-20.1	coarse garnet lherzolite	41.57	0.52	21.83	2.94	21.30	4.68	0.22	7.63	100.70	0.83
373-20.2	coarse garnet lherzolite	41.67	0.54	21.72	3.05	21.44	4.73	0.23	7.67	101.04	0.83
373-20.3	coarse garnet lherzolite	41.78	0.46	21.68	2.97	21.23	4.57	0.22	7.72	100.63	0.83

Continued APPENDIX IV (garnet analyses)

Sample	Rock type	SiO2	TiO2	Al2O3	Cr2O3	MgO	CaO	MnO	FeO	Total	X Mg
373-13.2	coarse garnet lherzolite	41.65	0.25	21.29	3.44	21.06	4.71	0.21	7.60	100.21	0.83
373-13.3	coarse garnet lherzolite	41.77	0.32	21.49	3.40	21.20	4.67	0.21	7.58	100.63	0.83
373-21.2	coarse garnet lherzolite	41.23	0.21	21.26	3.79	20.93	4.80	0.24	7.67	100.13	0.83
373-21.3	coarse garnet lherzolite	41.56	0.21	20.94	3.72	21.33	4.85	0.24	7.71	100.55	0.83
373-16.1	coarse garnet lherzolite	41.00	0.35	18.16	7.48	20.28	5.81	0.14	7.05	100.27	0.84
373-16.2	coarse garnet lherzolite	41.08	0.33	18.33	7.34	20.24	5.81	0.14	6.93	100.19	0.84
382-22.1	porphyroclastic garnet lherzolite	41.29	0.77	19.46	4.53	19.86	5.23	0.25	9.33	100.72	0.79
382-22.3	porphyroclastic garnet lherzolite	41.50	0.71	19.45	4.62	19.80	5.25	0.18	9.45	100.96	0.79
382-20.1	porphyroclastic garnet lherzolite	41.38	0.70	20.17	3.66	19.98	5.04	0.24	9.44	100.61	0.79
382-20.2	porphyroclastic garnet lherzolite	41.31	0.66	20.20	3.74	20.05	5.00	0.24	9.41	100.62	0.79
382-20.3	porphyroclastic garnet lherzolite	41.26	0.69	20.19	3.62	19.94	5.03	0.26	9.40	100.39	0.79
382-19.1	porphyroclastic garnet lherzolite	41.29	0.67	20.51	3.64	20.30	4.97	0.24	9.36	100.98	0.79
382-19.2	porphyroclastic garnet lherzolite	41.35	0.66	20.38	3.52	20.28	5.00	0.26	9.42	100.87	0.79
382-19.3	porphyroclastic garnet lherzolite	41.37	0.68	20.39	3.62	20.20	5.00	0.27	9.38	100.91	0.79
382-17.3	porphyroclastic garnet lherzolite	41.62	0.56	20.82	3.49	20.11	4.86	0.23	9.27	100.96	0.79
382-26.2	porphyroclastic garnet lherzolite	41.36	0.74	20.39	3.64	20.08	4.99	0.27	9.45	100.92	0.79
382-26.3	porphyroclastic garnet lherzolite	41.49	0.67	20.19	3.71	20.14	5.11	0.24	9.44	100.99	0.79
382-3.1	porphyroclastic garnet lherzolite	41.52	0.68	20.23	3.63	20.20	5.00	0.22	9.28	100.76	0.80
382-3.2	porphyroclastic garnet lherzolite	41.52	0.70	20.13	3.71	20.15	5.08	0.28	9.40	100.97	0.79
382-3.3	porphyroclastic garnet lherzolite	41.51	0.70	20.09	3.76	20.06	5.10	0.25	9.33	100.80	0.79
382-28.1	porphyroclastic garnet lherzolite	41.45	0.68	20.32	3.51	20.23	5.02	0.21	9.52	100.94	0.79
382-7.1	porphyroclastic garnet lherzolite	41.34	0.70	20.43	3.45	20.17	4.93	0.24	9.48	100.74	0.79
382-7.2	porphyroclastic garnet lherzolite	41.32	0.68	20.37	3.46	19.96	5.02	0.28	9.40	100.49	0.79
382-7.3	porphyroclastic garnet lherzolite	41.42	0.68	20.26	3.49	20.12	4.89	0.23	9.40	100.49	0.79
382-9.1	porphyroclastic garnet lherzolite	41.38	0.66	20.26	3.49	20.12	4.95	0.26	9.39	100.52	0.79
382-9.2	porphyroclastic garnet lherzolite	41.42	0.71	20.24	3.50	19.88	4.91	0.27	9.46	100.38	0.79
382-9.3	porphyroclastic garnet lherzolite	41.56	0.67	20.25	3.48	19.94	4.95	0.23	9.48	100.57	0.79
403-8.1	garnet harzburgite	40.30	0.28	17.23	8.63	19.91	6.09	0.15	7.05	99.64	0.83

Continued APPENDIX IV (garnet analyses)

Sample	Rock type	SiO2	TiO2	Al2O3	Cr2O3	MgO	CaO	MnO	FeO	Total	X Mg
403-8.2	garnet harzburgite	40.30	0.28	17.34	8.51	19.93	6.05	0.13	6.93	99.47	0.84
403-8.3	garnet harzburgite	40.35	0.28	17.51	8.49	19.91	6.02	0.19	6.95	99.70	0.84
403-7.1	garnet harzburgite	40.68	0.28	17.49	8.37	20.04	5.95	0.15	7.08	100.04	0.83
403-7.2	garnet harzburgite	40.81	0.31	17.44	8.37	19.95	6.02	0.16	7.10	100.16	0.83
403-7.3	garnet harzburgite	40.99	0.32	17.53	8.35	20.19	5.98	0.14	7.09	100.59	0.84
403-5.1	garnet harzburgite	40.85	0.22	17.56	8.38	20.01	5.91	0.20	7.01	100.14	0.84
403-5.2	garnet harzburgite	41.07	0.21	17.56	8.41	19.84	5.98	0.17	6.97	100.21	0.84
403-5.3	garnet harzburgite	41.02	0.21	17.67	8.37	19.69	6.00	0.13	6.97	100.06	0.83
403-15.1	garnet harzburgite	41.05	0.20	17.65	8.37	19.91	6.03	0.10	7.15	100.45	0.83
403-15.2	garnet harzburgite	41.14	0.24	17.28	8.42	19.83	6.06	0.09	7.15	100.20	0.83
403-15.3	garnet harzburgite	41.17	0.25	17.20	8.48	19.81	6.13	0.10	7.08	100.21	0.83
403-14.1	garnet harzburgite	40.90	0.22	17.46	8.19	19.95	6.08	0.18	7.20	100.17	0.83
403-14.2	garnet harzburgite	41.05	0.22	17.44	8.11	19.95	6.08	0.20	7.11	100.15	0.83
403-14.3	garnet harzburgite	41.09	0.20	17.33	8.31	20.14	6.08	0.10	7.04	100.29	0.84
403-11.1	garnet harzburgite	40.81	0.38	17.45	8.21	20.08	5.92	0.20	7.24	100.28	0.83
403-11.2	garnet harzburgite	41.14	0.35	17.31	8.17	19.85	6.03	0.11	7.19	100.15	0.83
403-11.3	garnet harzburgite	41.14	0.37	17.27	8.26	20.16	5.98	0.17	7.20	100.55	0.83
403-8.1	garnet harzburgite	40.76	0.28	17.11	8.63	19.84	6.10	0.11	7.13	99.96	0.83
403-8.2	garnet harzburgite	41.08	0.28	17.37	8.41	19.88	6.04	0.19	7.09	100.34	0.83
403-8.3	garnet harzburgite	40.99	0.29	17.34	8.49	19.98	6.01	0.15	7.00	100.25	0.84
403-7.1	garnet harzburgite	40.91	0.29	17.28	8.42	19.88	6.00	0.11	7.18	100.07	0.83
403-7.2	garnet harzburgite	40.77	0.28	17.48	8.35	19.92	6.05	0.14	7.13	100.12	0.83
403-7.3	garnet harzburgite	40.89	0.30	17.30	8.39	19.85	6.06	0.10	7.09	99.98	0.83
403-20.1	garnet harzburgite	41.14	0.35	17.30	7.89	20.27	5.81	0.11	7.23	100.10	0.83
403-20.2	garnet harzburgite	41.05	0.39	17.46	7.84	19.90	5.88	0.09	7.21	99.83	0.83
403-20.3	garnet harzburgite	41.06	0.36	17.58	7.93	20.28	5.80	0.10	7.21	100.32	0.83
403-18.1	garnet harzburgite	41.19	0.36	17.56	7.87	20.21	5.90	0.10	7.24	100.43	0.83

Continued APPENDIX IV (garnet analyses)

Sample	Rock type	SiO2	TiO2	Al2O3	Cr2O3	MgO	CaO	MnO	FeO	Total	X Mg
403-18.2	garnet harzburgite	41.19	0.38	17.65	7.88	20.23	5.90	0.13	7.11	100.46	0.84
403-18.3	garnet harzburgite	40.96	0.39	17.56	7.86	20.12	5.88	0.11	7.11	99.98	0.83
351-7.1	heterogeneous samples	41.37	0.03	21.46	3.66	20.01	5.27	0.41	8.62	100.83	0.81
351-7.2	heterogeneous samples	41.32	0.03	21.40	3.72	19.89	5.37	0.43	8.49	100.65	0.81
351-7.3	heterogeneous samples	41.34	0.06	20.71	4.65	19.49	5.75	0.40	8.57	100.96	0.80
351-10.1	heterogeneous samples	40.96	0.04	20.92	4.64	19.46	5.82	0.41	8.59	100.83	0.80
351-10.2	heterogeneous samples	40.46	0.03	21.64	4.52	19.42	5.61	0.43	8.44	100.55	0.80
351-10.3	heterogeneous samples	41.03	0.04	20.59	4.63	19.50	5.61	0.39	8.59	100.37	0.80
394 - 16.1	heterogeneous samples	40.78	0.04	20.65	5.45	20.07	4.99	0.32	8.12	100.42	0.81
394 - 16.2	heterogeneous samples	40.96	0.14	20.31	5.57	20.43	5.00	0.33	8.09	100.83	0.82
394 - 16.3	heterogeneous samples	41.10	0.14	20.35	5.70	20.29	4.87	0.29	8.26	101.00	0.81
368-19.1	spinel-garnet lherzolite	41.52	0.11	20.73	3.83	19.79	5.63	0.40	8.75	100.75	0.80
368-12.1	spinel-garnet lherzolite	41.83	0.09	21.14	3.59	19.80	5.37	0.38	8.78	100.99	0.80
368-12.2	spinel-garnet lherzolite	41.71	0.08	20.86	3.85	19.67	5.59	0.41	8.80	100.97	0.80
368-12.3	spinel-garnet lherzolite	41.47	0.09	21.15	3.62	19.78	5.42	0.42	8.87	100.82	0.80
368-22.3	spinel-garnet lherzolite	41.01	0.09	21.26	3.40	19.86	5.77	0.37	8.72	100.48	0.80
368-25.1	spinel-garnet lherzolite	41.38	0.07	21.93	2.49	19.98	4.96	0.39	8.73	99.92	0.80
368-1.1	spinel-garnet lherzolite	41.24	0.01	20.89	4.55	19.58	5.71	0.39	8.61	100.98	0.80
368-1.3	spinel-garnet lherzolite	41.17	0.03	20.72	4.49	19.55	5.67	0.39	8.58	100.60	0.80
368-4.1	spinel-garnet lherzolite	41.03	0.03	20.46	5.12	19.29	5.92	0.40	8.54	100.79	0.80
368-4.2	spinel-garnet lherzolite	41.17	0.04	20.32	5.09	19.21	5.89	0.44	8.54	100.70	0.80
368-4.3	spinel-garnet lherzolite	41.05	0.03	20.30	5.08	19.36	5.91	0.38	8.54	100.66	0.80
402-18.1	spinel-garnet lherzolite	41.27	0.02	20.79	4.32	19.16	5.91	0.36	8.57	100.40	0.80
402-18.2	spinel-garnet lherzolite	40.93	0.06	20.52	4.45	19.43	5.92	0.40	8.61	100.32	0.80
402-18.3	spinel-garnet lherzolite	41.02	0.08	20.67	4.31	19.32	5.87	0.36	8.75	100.38	0.80
402-17.1	spinel-garnet lherzolite	41.29	0.02	21.49	3.68	19.64	5.53	0.36	8.63	100.64	0.80
402-17.2	spinel-garnet lherzolite	41.10	0.05	21.37	3.75	19.63	5.58	0.38	8.59	100.45	0.80
402-17.3	spinel-garnet lherzolite	41.06	0.08	21.39	3.58	19.56	5.67	0.44	8.60	100.37	0.80

Continued APPENDIX I (garnet analyses)

Sample	Rock type	SiO2	TiO2	Al2O3	Cr2O3	MgO	CaO	MnO	FeO	Total	X Mg
402-13.1	spinel-garnet lherzolite	41.10	0.06	21.10	4.00	19.50	5.73	0.36	8.62	100.47	0.80
402-13.2	spinel-garnet lherzolite	40.93	0.07	21.00	4.05	19.58	5.68	0.43	8.60	100.34	0.80
402-13.3	spinel-garnet lherzolite	41.22	0.05	21.00	4.05	19.63	5.72	0.38	8.60	100.66	0.80
402-11.1	spinel-garnet lherzolite	41.18	0.05	21.23	3.69	19.52	5.67	0.44	8.49	100.27	0.80
402-11.2	spinel-garnet lherzolite	41.24	0.06	21.24	3.66	19.63	5.71	0.44	8.49	100.47	0.80
402-11.3	spinel-garnet lherzolite	41.13	0.05	21.14	3.70	19.39	5.60	0.39	8.56	99.96	0.80
402-6.1	spinel-garnet lherzolite	41.08	0.05	20.46	4.63	19.20	5.88	0.36	8.73	100.39	0.80
402-6.2	spinel-garnet lherzolite	41.20	0.06	20.52	4.59	19.16	5.91	0.37	8.67	100.48	0.80
402-6.3	spinel-garnet lherzolite	41.12	0.03	20.56	4.64	19.16	5.89	0.38	8.69	100.46	0.80
363-4.1	garnet wehrlite	41.05	0.69	17.42	8.06	19.97	6.14	0.11	7.40	100.84	0.83
363-4.2	garnet wehrlite	40.88	0.66	17.48	8.00	19.83	6.07	0.14	7.35	100.41	0.83
363-4.3	garnet wehrlite	41.08	0.65	17.45	7.89	19.96	6.10	0.12	7.34	100.59	0.83
363-10.1	garnet wehrlite	41.01	0.79	18.51	5.65	19.93	5.95	0.22	7.72	99.78	0.82
363-10.2	garnet wehrlite	41.52	0.80	18.80	5.73	20.01	6.03	0.22	7.62	100.74	0.82
363-10.3	garnet wehrlite	41.51	0.81	18.78	5.70	20.14	6.02	0.22	7.65	100.84	0.82
398-1.2	garnet wehrlite	41.34	0.37	19.80	5.18	20.83	4.97	0.19	7.83	100.50	0.83
398-1.3	garnet wehrlite	41.06	0.40	19.78	5.22	20.66	4.98	0.17	7.77	100.04	0.83
399-8.1	garnet wehrlite	41.26	0.29	19.67	5.21	20.41	4.92	0.18	8.23	100.16	0.82
399-8.2	garnet wehrlites	41.31	0.31	19.65	5.24	20.57	5.01	0.19	8.16	100.44	0.82
399-8.3	garnet wehrlite	41.64	0.28	19.84	5.16	20.44	4.86	0.22	8.17	100.60	0.82
399-9.1	garnet wehrlite	41.37	0.43	19.61	5.29	20.37	5.09	0.20	8.05	100.40	0.82
399-9.2	garnet wehrlite	41.44	0.39	19.48	5.27	20.45	5.06	0.16	8.06	100.31	0.82
399-9.3	garnet wehrlite	41.29	0.36	19.58	5.14	20.56	5.08	0.18	7.93	100.12	0.82
398-11.1	garnet wehrlite	41.39	0.40	19.75	5.09	20.51	5.04	0.18	8.31	100.67	0.81
398-11.2	garnet wehrlite	41.46	0.42	19.81	5.00	20.41	5.10	0.19	8.36	100.74	0.81
398-11.3	garnet wehrlite	41.38	0.39	19.69	5.06	20.48	4.99	0.16	8.33	100.48	0.81

APPENDIX V

Electron microprobe core analyses of spinels from the Voyageur peridotite xenoliths

Sample	Rock type	SiO2	TiO2	Al2O3	Cr2O3	Fe2O3	MgO	MnO	FeO	Total	Fe 3+	X Mg	XCr
375 - 1.1	spinel harzburgite	0.00	0.04	19.54	49.32	2.42	13.02	0.00	15.03	99.37	0.06	0.61	0.69
375 - 1.2	spinel harzburgite	0.00	0.08	19.49	49.11	2.47	12.91	0.00	15.18	99.24	0.06	0.60	0.69
375 - 1.3	spinel harzburgite	0.00	0.03	19.61	49.25	2.44	13.06	0.00	14.98	99.38	0.06	0.61	0.69
375 - 5.1	spinel harzburgite	0.00	0.03	19.20	49.60	2.97	13.12	0.00	14.98	99.90	0.07	0.61	0.69
375 - 5.2	spinel harzburgite	0.00	0.00	19.20	49.61	2.78	13.02	0.00	15.02	99.63	0.07	0.61	0.69
375 - 5.3	spinel harzburgite	0.01	0.00	19.25	49.56	2.78	12.94	0.00	15.20	99.74	0.07	0.60	0.69
375 - 13.3	spinel harzburgite	0.00	0.00	19.85	49.37	3.14	13.41	0.00	14.83	100.60	0.07	0.62	0.68
351-15.1	heterogeneous	0.02	0.27	13.12	52.38	6.86	11.99	0.00	16.25	100.88	0.17	0.57	0.72
351-15.2	heterogeneous	0.01	0.28	13.07	52.89	5.95	11.86	0.00	16.28	100.35	0.14	0.56	0.74
355-3.1	coarse spinel lherzolite	0.02	0.01	22.50	47.01	1.53	13.73	0.00	14.34	99.14	0.04	0.63	0.66
355-3.2	coarse spinel lherzolite	0.00	0.00	22.60	47.09	1.62	13.90	0.00	14.14	99.35	0.04	0.64	0.66
355-3.3	coarse spinel lherzolite	0.00	0.00	22.80	46.90	1.78	13.98	0.00	14.12	99.58	0.04	0.64	0.66
355-3.6	coarse spinel lherzolite	0.00	0.00	23.25	46.22	2.08	14.49	0.00	13.34	99.38	0.05	0.66	0.65
355-8.1	coarse spinel lherzolite	0.00	0.00	23.38	45.76	2.11	14.41	0.00	13.37	99.03	0.05	0.66	0.64
355-8.2	coarse spinel lherzolite	0.00	0.00	23.20	45.89	2.31	14.48	0.00	13.27	99.14	0.05	0.66	0.64
355-8.3	coarse spinel lherzolite	0.00	0.00	23.40	46.05	1.76	14.29	0.00	13.58	99.08	0.04	0.65	0.65
355-9.3	coarse spinel lherzolite	0.04	0.00	23.39	46.11	1.88	14.17	0.00	13.97	99.56	0.04	0.64	0.65
355-16.1	coarse spinel lherzolite	0.00	0.00	21.55	47.69	2.34	14.05	0.00	13.74	99.36	0.05	0.65	0.67
355-16.2	coarse spinel lherzolite	0.00	0.00	21.62	47.86	2.24	14.05	0.00	13.82	99.59	0.05	0.64	0.67
355-16.3	coarse spinel lherzolite	0.00	0.00	21.59	48.02	2.25	14.10	0.00	13.79	99.76	0.05	0.65	0.67
355-19.1	coarse spinel lherzolite	0.02	0.00	23.24	45.63	2.18	14.31	0.00	13.47	98.85	0.05	0.65	0.64
355-19.2	coarse spinel lherzolite	0.00	0.00	23.01	46.31	2.36	14.42	0.00	13.46	99.56	0.05	0.66	0.65
355-19.3	coarse spinel lherzolite	0.00	0.02	22.70	46.56	2.14	14.23	0.00	13.63	99.27	0.05	0.65	0.65
356-5.1	coarse spinel lherzolite	0.02	0.00	21.29	47.93	1.44	12.26	0.00	16.49	99.42	0.03	0.57	0.68
356-5.2	coarse spinel lherzolite	0.00	0.00	20.99	48.06	1.31	12.37	0.00	16.05	98.77	0.03	0.58	0.68

Continued APPENDIX V

Sample	Rock type	SiO2	TiO2	Al2O3	Cr2O3	Fe2O3	MgO	MnO	FeO	Total	Fe 3+	X Mg	XCr
356-5.3	coarse spinel lherzolite	0.00	0.00	21.30	47.87	1.97	12.90	0.00	15.53	99.57	0.05	0.60	0.67
356-8.3	coarse spinel lherzolite	0.00	0.00	21.39	47.85	1.92	12.66	0.00	15.99	99.81	0.04	0.59	0.67
356-10.1	coarse spinel lherzolite	0.00	0.00	20.61	48.09	1.85	12.47	0.00	15.86	98.89	0.04	0.58	0.68
356-10.2	coarse spinel lherzolite	0.00	0.00	20.38	48.59	1.86	12.44	0.00	15.99	99.26	0.04	0.58	0.69
356-10.3	coarse spinel lherzolite	0.00	0.00	20.66	48.43	1.91	12.59	0.00	15.87	99.46	0.04	0.59	0.68
356-14.1	coarse spinel lherzolite	0.00	0.00	21.26	47.51	1.62	12.32	0.00	16.20	98.91	0.04	0.58	0.67
356-14.2	coarse spinel lherzolite	0.05	0.00	21.11	47.86	1.93	12.63	0.00	15.96	99.54	0.05	0.59	0.68
356-14.3	coarse spinel lherzolite	0.00	0.00	21.20	47.62	1.93	12.59	0.00	15.87	99.21	0.05	0.59	0.67
369 - 1.1	coarse spinel lherzolite	0.00	0.09	23.65	44.63	2.94	14.60	0.00	13.22	99.12	0.07	0.66	0.63
369 - 1.2	coarse spinel lherzolite	0.02	0.10	23.24	45.08	2.91	14.50	0.00	13.38	99.23	0.07	0.66	0.63
369 - 1.3	coarse spinel lherzolite	0.00	0.09	23.56	44.67	3.06	14.63	0.00	13.18	99.19	0.07	0.66	0.63
369 - 6.1	coarse spinel lherzolite	0.00	0.09	19.18	49.70	3.10	14.18	0.00	13.29	99.54	0.07	0.66	0.69
369 - 6.2	coarse spinel lherzolite	0.00	0.03	21.57	46.76	3.14	14.30	0.00	13.28	99.09	0.07	0.66	0.65
369 - 6.3	coarse spinel lherzolite	0.00	0.08	23.67	44.50	2.98	14.56	0.00	13.25	99.05	0.07	0.66	0.63
369 - 18.1	coarse spinel lherzolite	0.00	0.09	23.50	44.75	2.79	14.37	0.00	13.51	99.01	0.06	0.65	0.63
369 - 16.1	coarse spinel lherzolite	0.00	0.10	23.10	45.32	2.66	14.33	0.00	13.52	99.03	0.06	0.65	0.64
369 - 16.2	coarse spinel lherzolite	0.00	0.03	23.76	44.55	2.87	14.58	0.00	13.15	98.94	0.07	0.66	0.63
369 - 16.3	coarse spinel lherzolite	0.00	0.09	23.87	44.64	3.05	14.71	0.00	13.23	99.58	0.07	0.66	0.62
369 - 10.1	coarse spinel lherzolite	0.06	0.09	23.13	45.16	2.59	14.43	0.00	13.39	98.85	0.06	0.66	0.64
369 - 10.2	coarse spinel lherzolite	0.02	0.07	24.29	44.05	3.01	14.72	0.00	13.21	99.36	0.07	0.67	0.62
369 - 10.3	coarse spinel lherzolite	0.01	0.10	23.56	45.18	2.64	14.43	0.00	13.63	99.54	0.06	0.65	0.63
371 - 1.2	coarse spinel lherzolite	0.02	0.01	21.75	47.34	1.90	13.72	0.00	14.16	98.90	0.04	0.63	0.67
371 - 1.3	coarse spinel lherzolite	0.01	0.02	21.55	47.73	2.19	14.03	0.00	13.80	99.33	0.05	0.64	0.67
371 - 4.1	coarse spinel lherzolite	0.00	0.03	20.24	48.93	2.37	13.85	0.00	13.83	99.25	0.06	0.64	0.68
371 - 4.2	coarse spinel lherzolite	0.00	0.02	20.33	49.11	2.03	13.84	0.00	13.81	99.14	0.05	0.64	0.69
371 - 4.3	coarse spinel lherzolite	0.00	0.00	20.27	48.87	2.48	13.86	0.00	13.79	99.28	0.06	0.64	0.68
371 - 10.3	coarse spinel lherzolite	0.00	0.00	20.18	48.91	2.76	13.90	0.00	13.80	99.56	0.06	0.64	0.68
411 - 6.1	coarse spinel lherzolite	0.00	0.00	22.87	46.43	2.31	14.37	0.00	13.48	99.46	0.05	0.66	0.65

Continued APPENDIX V

Sample	Rock type	SiO2	TiO2	Al2O3	Cr2O3	Fe2O3	MgO	MnO	FeO	Total	Fe 3+	X Mg	XCr
411 - 6.2	coarse spinel lherzolite	0.03	0.00	22.80	46.60	2.16	14.34	0.00	13.58	99.51	0.05	0.65	0.65
411 - 6.3	coarse spinel lherzolite	0.00	0.01	22.87	46.09	2.68	14.51	0.00	13.26	99.42	0.06	0.66	0.64
411 - 6.6	coarse spinel lherzolite	0.00	0.00	23.01	46.68	2.36	14.46	0.00	13.57	100.08	0.05	0.66	0.65
411 - 12.1	coarse spinel lherzolite	0.02	0.00	21.60	48.12	2.05	14.12	0.00	13.76	99.67	0.05	0.65	0.67
411 - 12.2	coarse spinel lherzolite	0.01	0.00	21.71	47.72	2.52	14.30	0.00	13.52	99.78	0.06	0.65	0.66
411 - 12.3	coarse spinel lherzolite	0.00	0.02	21.56	47.88	2.25	14.13	0.00	13.68	99.51	0.05	0.65	0.67
411 - 8.3	coarse spinel lherzolite	0.01	0.00	21.68	48.17	2.60	14.36	0.00	13.65	100.47	0.06	0.65	0.66
411 - 14.1	coarse spinel lherzolite	0.06	0.00	23.38	45.73	2.42	14.68	0.00	13.16	99.43	0.06	0.67	0.64
411 - 14.2	coarse spinel lherzolite	0.00	0.00	23.24	45.89	2.58	14.84	0.00	12.78	99.33	0.06	0.67	0.64
411 - 14.3	coarse spinel lherzolite	0.00	0.00	23.35	45.66	2.86	14.70	0.00	13.12	99.69	0.07	0.67	0.64
368 2.1	sp-grt lherzolite	0.05	1.38	8.38	51.02	10.97	11.43	0.17	17.00	100.39	0.27	0.54	0.73
368 2.2	sp-grt lherzolite	0.04	1.35	8.33	51.09	11.20	11.26	0.18	17.34	100.79	0.28	0.53	0.72
368 2.3	sp-grt lherzolite	0.05	1.32	8.45	51.00	10.95	11.04	0.19	17.62	100.61	0.27	0.53	0.72
368 3.1	sp-grt lherzolite	0.03	1.35	9.06	49.88	11.16	11.30	0.15	17.19	100.11	0.28	0.54	0.71
368 3.2	sp-grt lherzolite	0.08	1.37	9.03	49.59	11.18	11.34	0.15	17.13	99.87	0.28	0.54	0.71
368 3.3	sp-grt lherzolite	0.02	1.36	9.04	49.19	11.39	11.36	0.17	16.82	99.35	0.28	0.54	0.71
368 4.1	sp-grt lherzolite	0.14	0.94	27.47	33.75	8.69	15.00	0.26	14.24	100.50	0.19	0.65	0.48
368 4.2	sp-grt lherzolite	0.24	1.04	20.37	41.60	8.18	13.82	0.26	15.24	100.74	0.19	0.61	0.59
368 4.3	sp-grt lherzolite	0.09	0.60	34.44	27.07	8.43	16.01	0.21	13.40	100.23	0.18	0.68	0.39
402 1.3	sp-grt lherzolite	0.05	0.52	9.30	54.07	8.63	11.28	0.17	16.77	100.80	0.21	0.54	0.75
402 2.1	sp-grt lherzolite	0.03	0.51	9.37	54.05	8.27	11.22	0.16	16.71	100.33	0.20	0.54	0.75
402 2.2	sp-grt lherzolite	0.03	0.51	9.26	54.21	8.30	11.10	0.14	16.94	100.49	0.21	0.54	0.76
402 3.3	sp-grt lherzolite	0.04	0.52	9.22	53.69	8.99	11.35	0.17	16.54	100.52	0.22	0.55	0.75
402 4.1	sp-grt lherzolite	0.03	0.52	9.28	53.73	8.74	11.23	0.18	16.69	100.39	0.22	0.54	0.75
402 4.2	sp-grt lherzolite	0.05	0.51	9.28	53.70	8.63	11.12	0.16	16.87	100.33	0.21	0.54	0.75
402 4.3	sp-grt lherzolite	0.01	0.51	9.24	53.62	8.85	11.19	0.18	16.65	100.25	0.22	0.54	0.75
402 5.1	sp-grt lherzolite	0.04	0.52	9.29	54.22	8.61	11.51	0.16	16.40	100.74	0.21	0.55	0.75

APPENDIX VI

Laser-ablation ICPMS averaged analyses of lherzolitic garnets from the Voyageur peridotite xenoliths

Sample		347-1	347-2	343-1	343-2	359-2	359-1	373-3	373-2	373-1	372-1	372-2	372-3	382-1	382-2	382-3
Sc	ppm	146.40	146.60	146.30	136.00	139.60	135.60	121.60	119.30	124.00	126.90	125.30	130.80	171.90	173.40	179.20
Ti	ppm	814.80	625.30	742.90	818.70	448.40	429.00	524.90	398.40	403.20	518.80	666.90	381.80	1368.00	1317.00	1352.00
V	ppm	268.30	258.90	240.30	274.40	293.40	303.70	278.70	273.20	271.80	238.30	209.60	275.30	383.00	360.50	356.30
Ni	ppm	61.22	57.58	63.86	68.25	50.65	53.54	71.93	63.60	65.81	51.01	50.27	45.48	80.86	82.34	77.75
Ga	ppm	8.55	9.01	8.52	10.23	10.11	10.36	12.54	12.25	12.43	5.15	5.39	4.80	17.94	18.13	17.04
Sr	ppm	1.47	0.95	0.55	0.60	0.58	0.47	0.44	0.48	0.46	0.59	0.70	0.92	2.12	3.22	1.05
Y	ppm	12.93	5.88	9.21	14.40	13.84	13.31	20.02	19.49	19.84	5.64	12.58	4.13	38.88	40.16	41.98
Zr	ppm	61.47	42.61	51.38	55.42	36.00	35.74	44.31	32.46	28.61	44.78	58.56	42.77	100.60	104.40	107.50
Nb	ppm	1.48	1.45	1.55	1.57	1.62	1.72	1.28	1.25	1.23	1.87	1.95	1.92	1.53	1.54	1.43
La	ppm	0.02	0.04	0.02	0.01	0.02	0.03	0.03	0.02	0.04	0.03	0.03	0.03	0.08	0.06	0.04
Ce	ppm	0.29	0.28	0.32	0.32	0.32	0.39	0.29	0.29	0.32	0.37	0.39	0.38	0.73	0.55	0.53
Pr	ppm	0.12	0.12	0.11	0.10	0.14	0.13	0.16	0.13	0.12	0.14	0.16	0.14	0.53	0.21	0.20
Nd	ppm	1.24	1.28	1.10	1.17	1.65	1.45	1.32	1.33	1.18	1.66	1.55	1.41	2.05	1.98	2.13
Sm	ppm	1.06	1.27	1.05	1.06	1.11	1.21	1.04	0.98	0.63	1.23	1.33	1.49	1.75	1.63	1.57
Eu	ppm	0.54	0.52	0.48	0.58	0.50	0.55	0.56	0.41	0.43	0.62	0.62	0.64	0.84	0.82	0.86
Gd	ppm	1.95	1.72	1.71	1.77	1.65	1.73	1.90	1.70	1.57	1.79	2.03	1.67	3.14	3.35	3.63
Tb	ppm	0.43	0.27	0.32	0.40	0.31	0.32	0.40	0.42	0.30	0.27	0.48	0.24	0.82	0.81	0.92
Dy	ppm	2.56	1.46	1.98	2.84	2.43	2.15	3.70	3.22	3.07	1.44	2.73	1.17	6.02	6.35	7.16
Ho	ppm	0.53	0.25	0.36	0.53	0.48	0.48	0.75	0.70	0.77	0.20	0.46	0.15	1.49	1.45	1.53
Er	ppm	1.26	0.69	0.84	1.46	1.68	1.52	2.26	2.27	2.20	0.53	1.02	0.38	4.40	4.63	4.75
Tm	ppm	0.16	0.12	0.15	0.21	0.26	0.23	0.34	0.34	0.31	0.04	0.12	0.06	0.76	0.72	0.82
Yb	ppm	1.32	0.93	1.14	1.61	1.80	1.95	2.55	2.49	2.39	0.56	0.78	0.46	5.03	5.18	5.43

Continued APPENDIX VI

Sample		347-1	347-2	343-1	343-2	359-2	359-1	373-3	373-2	373-1	372-1	372-2	372-3	382-1	382-2	382-3
Lu	ppm	0.21	0.14	0.22	0.25	0.32	0.30	0.39	0.32	0.38	0.10	0.11	0.10	0.77	0.81	0.81
Hf	ppm	1.24	0.88	1.10	1.24	0.77	0.70	0.71	0.64	0.72	0.71	1.20	0.95	2.39	2.58	2.63
Th	ppm	0.03	0.62	0.01	0.04	0.08	0.70	0.12	5.22	0.02	0.14	0.02	0.25	1.14	1.87	1.24
U	ppm	0.01	0.01	0.02	0.01	0.01	0.01	0.23	0.01	0.02	0.02	0.01	0.01	0.18	0.22	0.03

APPENDIX VII

Laser-ablation ICPMS averaged analyses of lherzolitic clinopyroxenes from the Voyageur peridotite xenoliths

Sample		359-1	359-2	359-3	343-1	343-2	373-2	373-1	382-2	382-1	372-1	372-2	372-3	347-2	347-1
Sc	ppm	20.75	28.22	23.60	22.94	21.99	18.28	22.83	23.18	23.49	25.03	24.78	23.76	23.50	24.37
Ti	ppm	257.00	260.80	272.40	260.50	253.30	218.70	267.90	253.50	257.30	274.00	261.00	250.30	268.30	284.70
V	ppm	158.30	204.00	220.80	207.30	203.50	209.30	226.80	203.10	211.90	204.80	218.20	212.40	254.60	250.70
Ni	ppm	224.40	292.90	313.60	298.20	297.40	293.90	334.90	278.10	304.40	321.60	336.50	320.00	277.50	282.30
Ga	ppm	3.75	4.67	4.82	4.41	4.42	5.45	5.00	4.96	5.48	3.49	3.47	3.32	5.71	6.77
Sr	ppm	134.30	131.70	146.10	126.20	127.70	345.20	160.40	134.70	139.50	144.20	149.20	151.10	132.30	152.50
Y	ppm	2.15	2.16	2.16	1.94	2.08	2.19	2.62	2.86	2.82	2.36	1.94	1.85	2.38	2.52
Zr	ppm	9.79	9.35	9.63	9.13	9.05	10.83	12.77	9.19	9.16	11.72	11.04	10.77	10.17	11.17
Nb	ppm	0.59	0.51	0.61	0.42	0.44	2.90	0.50	1.55	1.06	0.69	0.54	0.63	0.42	3.08
La	ppm	2.25	2.12	2.78	2.19	2.18	6.29	2.81	3.46	3.11	2.40	2.48	2.55	2.37	4.60
Ce	ppm	7.32	8.48	9.01	7.64	7.61	13.37	10.52	10.74	10.36	8.53	8.87	8.85	9.20	13.01
Pr	ppm	1.43	1.43	1.44	1.37	1.37	1.81	1.85	1.79	1.61	1.57	1.57	1.59	1.56	1.89
Nd	ppm	6.03	6.30	6.65	5.92	5.86	7.73	7.84	7.33	7.25	6.95	7.23	7.09	6.57	7.83
Sm	ppm	1.52	1.54	1.44	1.35	1.48	1.82	1.86	1.69	1.86	1.60	1.77	1.66	1.56	1.51
Eu	ppm	0.51	0.56	0.42	0.42	0.41	0.50	0.66	0.52	0.50	0.58	0.44	0.57	0.59	0.52
Gd	ppm	1.00	1.12	1.19	1.02	1.19	1.44	1.59	1.42	1.45	1.37	1.31	1.45	1.37	1.36
Tb	ppm	0.15	0.15	0.14	0.13	0.14	0.13	0.27	0.26	0.29	0.25	0.14	0.14	0.14	0.15
Dy	ppm	0.63	0.70	0.79	0.67	0.62	0.64	0.87	0.85	0.81	0.79	0.62	0.54	0.73	0.81
Ho	ppm	0.11	0.19	0.10	0.19	0.19	0.18	0.12	0.12	0.12	0.10	0.19	0.17	0.10	0.11
Er	ppm	0.20	0.21	0.27	0.21	0.29	0.27	0.29	0.23	0.24	0.20	0.26	0.12	0.22	0.22
Tm	ppm	0.03	0.02	0.02	0.02	0.02	0.02	0.03	0.03	0.03	0.02	0.02	0.01	0.02	0.03
Yb	ppm	0.10	0.18	0.10	0.19	0.17	0.12	0.10	0.14	0.26	0.12	0.17	0.16	0.19	0.12
Lu	ppm	0.02	0.02	0.01	0.02	0.01	0.01	0.01	0.02	0.02	0.00	0.01	0.01	0.01	0.01
Hf	ppm	0.62	0.72	0.75	0.60	0.78	0.53	0.82	0.62	0.63	0.83	0.77	0.64	0.73	0.70
Th	ppm	0.12	0.15	0.04	0.03	0.02	0.17	0.16	0.13	0.14	0.01	0.03	0.02	0.16	0.33
U	ppm	0.48	0.46	0.04	0.01	0.00	0.15	0.01	0.02	0.02	0.00	0.02	0.01	0.01	0.05